

The series of environmental radioactivity measuring methods
No.33

In-situ Measurement Using Germanium Detector

Amendment of March 2017
Radiation Monitoring Division
Radiation Monitoring Department
Nuclear Regulation Authority

Table of Contents

Chapter 1 Introduction.....	1
Chapter 2 Definitions of terminology.....	2
Chapter 3 Measurement equipment.....	4
3.1 Requirements for the equipment.....	4
3.2 Composition of the equipment	4
3.3 Example of the equipment specifications	4
3.4 Equipment calibration.....	7
3.5 Measures against equipment contamination.....	12
3.6 Other preparations	14
Chapter 4 Measurement methods and spectral analysis	15
4.1 Selection of the measurement site	15
4.2 Measurement	15
4.3 Recording	17
4.4 Spectral analysis	19
Chapter 5 Calculation of radioactivity concentration and ambient dose rate.....	21
5.1 Conditions for analysis.....	21
5.2 Calculation of radioactivity concentration.....	22
5.3 Calculation of ambient dose rate	32
Chapter 6 Interpretation of measured results.....	36
6.1 Implications of discrepancies between analytical and actual measurement conditions	36
6.2 Management of accuracy in measured result.....	38
Explanation	
Explanation A Calculation of peak efficiency by simulated calculation	41
Explanation B Measurable ranges and measuring times for in-situ measurement	45
Explanation C Example of spectrum by in-situ measurement	52
Explanation D Energy calibration in a nuclear disaster	56
Explanation E Vertical profile of radioactive materials in the ground.....	58
Explanation F Implications of discrepancies between analytical and actual measurement conditions	76
Explanation G Directional characteristics of detector (angular dependence of peak efficiency) ..	87
Explanation H Example of actual measurement.....	89
Explanation I Intercomparison measurement.....	97

Appendix

Appendix 1	Relationship between radionuclide activity and gamma-ray fluence rate 1 m above ground	103
Appendix 2	Relationship between dose rate and gamma-ray fluence rate 1 m above ground ..	115
Appendix 3	Relationship between radionuclide activity and dose rate 1 m above ground	137
Appendix 4	References	149

Chapter 1 Introduction

In situations where radioactive materials are released into the environment, such as accidents occurring at nuclear facilities (hereafter, “nuclear accidents”), conducting an in-situ measurement^{*1} using a germanium (hereafter, “Ge”) semiconductor detector, which has excellent energy resolution, enables the identification of the radioactive materials deposited on the ground. Further the radioactivity concentration and ambient dose rate attributable to the deposition can be obtained. As an in-situ measurement entails the measurement of the ground surface in the field, it requires approximately one-tenth of the time needed to conduct a measurement of a soil sample in a laboratory. While it is difficult to obtain representative readings from a soil sample if the deposition of radioactive materials is uneven over the ground owing to weather conditions, an in-situ measurement can facilitate obtaining the result that indicates the average readings of the area measured. Therefore, it is particularly useful when developing a distribution map of radioactive deposition over a wide area following a release of radioactive materials into the environment. It was also employed in the effort to grasp the distribution of radioactive deposition following the nuclear accident that occurred at the Fukushima Dai-ichi Nuclear Power Plant of Tokyo Electric Power Company Holdings (hereafter, “Fukushima Dai-ichi Nuclear Accident”), which was triggered by the major earthquake that hit eastern Japan in March 2011.^{*2} The ability to identify the radioactive materials enables the estimation of the state of emissions and furthermore, based on the half-lives of the identified radioactive materials, the prediction of the future ambient dose rate fluctuations to contribute toward accurate dose evaluation. This document describes the calibration of a Ge detector for in-situ measurement and methods of measurement and analysis based on the gamma rays of radioactive materials deposited on the ground. It also includes points of caution in terms of in-situ measurement following a nuclear accident, which differ from measurement during normal times, drawing on the post-Fukushima-Dai-ichi-Nuclear-Disaster measurement examples.

The analytical method is based on the HASL^{*3} method (H. L. Beck, et al.; HASL-258 (1972)) and has drawn on the research published in ICRU^{*4} Rep. 53 (1994), and other studies. The HASL method is based on certain assumptions in the analysis in terms of the vertical in-soil profile of radioactive materials, topography of the surrounding areas, installation height of the detector, etc.; thus, it is necessary to understand the impact on the analysis results if the actual conditions differ from these assumptions. In this manual, this impact is clarified and further described in terms of the correction method.

The detectability level is approximately 0.03 kBq/m² of ground-deposited radionuclides through a 1-h measurement, and approximately 0.1 nGy/h of ambient radiation dose rate from those nuclides (see Explanation B).

Because the in-situ measurement can serve to obtain the radioactivity concentrations in the ground and ambient dose rates of naturally occurring radionuclides such as uranium series, thorium series, and potassium-40, the methods to perform these are also explained.

*1 “in-situ” means the field where things are taking place. In this document, “in-situ measurement” refers to an “in-situ measurement conducted using a Ge detector.”

*2 “FY 2014 Commissioned Investigation of Radioactive Materials (collection of data on the distribution of radioactive materials in relation to the accident at Tokyo Electric Power Company’s Fukushima Dai-ichi Nuclear Power Plant and the development of transition models) Outcome Report, Area Research of Radioactive Cesium Deposition Amounts” by Satoshi Mikami and Kimiaki Saito (2015)

*3 Acronym for the Health and Safety Laboratory. Subsequently, it underwent changes to the Environmental Measurements Laboratory (EML) and is presently known as the National Urban Security Technology Laboratory (NUSTL).

*4 Acronym for the International Commission on Radiation Units and Measurements.

Chapter 2 Definitions of terminology

Terms, in particular, those specific to in-situ measurement, are defined below. For the basic terms used in relation to the Ge detector, refer to the Radioactivity Measurement Series No. 7 “Gamma-ray Spectrometry Using Germanium Detectors.”

In-situ measurement

A measurement taken on-site, out in the field. In Latin, “in-situ” literally means “in place.”

Response

The ratio of an indicated value to the amount to be measured. It is the inverse of a calibration constant.

Angular dependence

The property that the response to gamma rays that enter the Ge crystal of the detector depends on the angle of incidence.

Deposition amount

The amount of radioactive material that is deposited on, or penetrates, the ground of unit area (Bq/cm^2).

Mass depth

The depth measured from the ground surface by per-unit-area mass of the soil (g/cm^2).

β

Weight buffer depth (g/cm^2). A parameter to indicate the vertical profile of radioactive materials in the ground, which equals the mass depth at which the radioactivity concentration is 37% of the ground surface ($= 1/e$). This expresses the degree of penetration, where greater values indicate deeper penetration.

Scraper plate

A device to sample segments of soil vertically at any intervals, consisting of a metal frame to install on the ground and a metal plate for scraping the soil within the frame. By attaching a metal bar to the metal plate, the depth is adjusted for sampling.

Infinite plane

A plain flat open ground that spreads wide with no obstacles.

Vertical profile

The distribution of radioactive material in the ground in the direction of depth.

Ground surface distribution

The state of radioactive materials distributed over an area of ground.

Exponential distribution

The state in which radioactive materials in the ground are distributed in such a manner that they diminish exponentially in the direction of depth.

Homogeneous distribution

The state of radioactive materials distributed equally in the ground.

HASL

Acronym for the Health and Safety Laboratory. Subsequently, it underwent changes to the Environmental Measurements Laboratory (EML) and is presently known as the National Urban Security Technology Laboratory (NUSTL).

ICRU

Acronym of the International Commission on Radiation Units and Measurements.

Chapter 3 Measurement equipment

3.1 Requirements for the equipment

The Ge detector used in the in-situ measurement is essentially the same as the ordinary gamma-ray spectrometer used to measure environmental samples in a laboratory. For the details about the detector and other measurement equipment, refer to the Radioactivity Measurement Series No. 7 “Gamma-ray Spectrometry Using Germanium Detectors” and the IEC^{*1} Standards.

However, note that the following conditions must be met for conducting the measurements outdoors, in addition to the requirements for ordinary spectrometers.

- (1) The equipment must be easily portable and installable.
- (2) It must be able to operate reliably in outdoor weather conditions.^{*2}
- (3) It must be able to operate on batteries.
- (4) The dewar bottle must be functional, light, robust, and of the smallest possible size so as not to provide a shielding effect to the detector.

3.2 Composition of the equipment

The equipment compositions are shown in Figures 3.1 and 3.2, illustrating the liquid nitrogen cooling system and electric cooling system, respectively.

- (1) Ge detector
- (2) Portable dewar bottle (for the liquid nitrogen cooling system only)
- (3) Multichannel analyzer (MCA)
- (4) Detector support rack
- (5) Personal computer (PC) (for the use of MCA control and data analysis)
- (6) Software
- (7) Other auxiliary devices

The electric cooling type is available in an all-in-one portable system including the detection unit, cooling system, MCA, and control unit.

3.3 Example of the equipment specifications

An example of the specifications for in-situ measurement equipment is presented below. Note that the example is indicative of typical specifications and not intended to limit the use of other equipment.

- (1) Ge detector
 - Coaxial high-purity Ge detector^{*3}

^{*1} Acronym for the International Electrotechnical Commission.

^{*2} In particular, measures to protect the equipment from direct sunlight on extremely hot days are essential.

^{*3} Ideally, the diameter and length of the germanium crystal are equal (which minimizes the gamma-ray incidence angular dependence of peak efficiency). The n-type detector is used for measuring low-energy gamma/X rays, but those with an injection window made of beryllium, etc. are vulnerable and not suitable for outdoor use. It is better to use a detector with an aluminum end cap.

- Relative efficiency at 25 cm approximately 25%^{*4}
 - Energy resolution half-width (FWHM) 2.3 keV or lower^{*5} against cobalt-60 1333 keV
 - Peak-to-Compton ratio 30–60:1^{*6}
 - Measurable energy range 50–2000 keV^{*7 *8}
 - Battery operation time (with the electric cooling system only) up to 8 h of consecutive operation

 - Crystal cooling time at least 4 h^{*9}
 - The detector can be installed in the downward-facing position.^{*10}
- (2) Portable dewar bottle (for the liquid nitrogen cooling system only)
- The bottle capacity up to 7 L^{*11}
- (3) Multichannel analyzer (MCA)^{*12}
- High-voltage power source with built-in amplifier
 - Amplifier gain approximately 2 to 2000^{*13}
 - HV ±10 to 5000 V
 - Detector over voltage protection
- Must be installed with a feature to automatically shut down the high-voltage power before the detector overheats.
- Spectral memory 4–8 kch^{*14}
 - Integral nonlinearity 0.025% or lower
 - Differential nonlinearity 1% or lower
 - It can be run on batteries (portable type).
 - If it has no display panel on the main part and is used with a PC to display the spectrum and control the measurement, ensure that it can operate even when the PC is turned off.
- (4) Detector support rack
- It must be able to support with stability the detector and dewar bottle facing downward 1 m above the ground surface.

^{*4} Electric cooling system detectors with the relative efficiency of 10–20% are commercially available. For measurements in places with high ambient dose rates, detectors with low relative efficiencies may prove advantageous as they are more unlikely to overload the signal processing.

^{*5} Unlike a liquid nitrogen cooling system, a Ge detector with an electric cooling system tends to increase the half-widths owing to the device's mechanical noise.

^{*6} As the peak-to-Compton ratio is calculated based on the spectrum measured inside the shields, this serves only as a guide for in-situ measurements.

^{*7} Set this to roughly 30–2000 keV when measuring low-energy X/gamma rays.

^{*8} When measuring gamma rays of more than 2000 keV of natural radionuclides (thallium-208 of 2615 keV) etc., set the upper limit of the measurable energy range to 4000 keV.

^{*9} This depends on the size of the crystal and the performance of the freezing device. Thus, the cooling time above is a reference guide.

^{*10} This is necessary to ensure that the liquid nitrogen does not leak, irrespective of the orientation in which the detector is installed.

^{*11} Considering the ease of handling as well as the possibility that the dewar shields the rays, it is normally 3–5 L.

^{*12} Some detectors come with a built-in electric cooling system.

^{*13} The amplifier gain should be adjustable between 2000 and 4000 keV within the range of the spectral memory.

^{*14} The energy per channel is normally at 0.5 keV/ch, and the channels to use are determined according to the energy range of the target to be measured (2000 keV: 4 kch, 4000 keV: 8 kch). When measuring gamma rays of energy 2000 keV or more of natural radionuclides (thallium-208 of 2615 keV) etc., use 8 kch.

- Structurally, it should not pose obstacles between the detector and ground surface.
- (5) Personal computer (PC) (for the use of MCA control and data analysis)^{*15}
- It must be compatible with MCA to perform measurements.
 - It must be able to operate on batteries.
 - It must have a display screen that is viewable in the daylight.^{*16}
- (6) Software
- MCA control software
 - Analysis software
- It must be compatible with HASL-258 and ICRU Rep. 53 (more details are given in Chapter 5.)
- (7) Other auxiliary devices
- Carrying cases for the detector, MCA, and PC
 - Cables (MCA-detector, MCA-PC connection cables, power cable, etc.)
 - DC/AC converter (from 24/12 V DC to 100 V AC) (optional)
 - Spare batteries for the detector, MCA, and PC
 - A dewar bottle to refill liquid nitrogen (20–30 L capacity) (for the liquid nitrogen cooling system only)
 - Other utensils required for the refilling of liquid nitrogen (for the liquid nitrogen cooling system only)
 - Gamma-ray radiation source for calibration
 - Jigs to set up the gamma-ray radiation source
 - Items to prevent contamination (plastic bags, etc.)

^{*15}The PC is preferably water-proofed as it is used outdoors.

^{*16}As a PC's LCD panel is often difficult to view in the bright daylight outside, it is advisable that a simple light shade or similar be provided to improve the visibility.

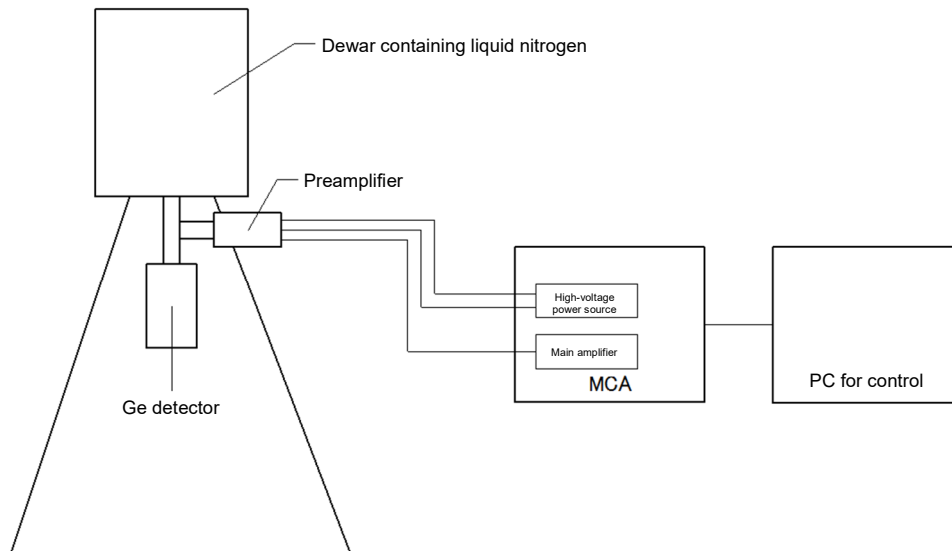


Figure 3.1 Configuration example of devices for in-situ measurement (liquid nitrogen cooling system)

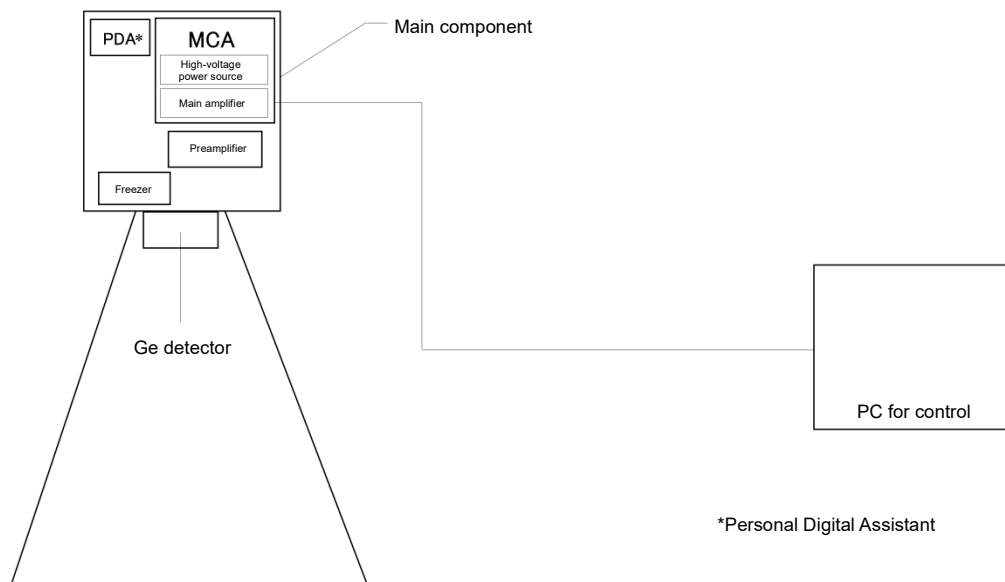


Figure 3.2 Configuration example of devices for in-situ measurement (electric cooling system)
(All-in-one portable system including the detection unit, cooling system, MCA, and control unit)

3.4 Equipment calibration

The in-situ measurement involves a Ge detector installed 1 m above the ground, facing downward. In this position, the gamma rays emitted by the radioactive materials deposited on the ground surface reach the detector directly at angles between 0° and 90° , given that the detector axis of symmetry is 0° . For this reason, it is necessary to consider the detector's gamma-ray angular dependence of peak efficiency. See Chapter 5 for the details about how to calibrate for angular dependence. In this Chapter, the angular dependence calibration is described in terms of the detector's peak efficiency, which is necessary for the calibration, and the procedures of the calibration.

3.4.1 Energy calibration

Measure any given gamma-ray radiation source (ideally, use cobalt-57, cobalt-60, etc.) and adjust the amplifier gain and analog-to-digital converter (ADC) zero level such that the total absorption peak is aligned with the target channel.

Use the software to prepare a relational function of the gamma-ray energy and channel and save the calibration formula thus obtained in a file.*¹⁷

3.4.2 Peak efficiency calibration

It is desirable that the peak efficiency calibration*¹⁸ be conducted regularly using a standard point radiation source, etc. to obtain the efficiency curve. It is also recommended that resolution be calculated and used to check that these values do not change significantly over time.

3.4.2.1 Calibration using standard point radiation source

3.4.2.1.1 Necessary devices

(1) Ge detector and a measurement circuit

(2) Standard point radiation source

The nuclide should be selected such that it covers the gamma-ray energy range of the measurement target.

Table 3.1 illustrates an example of nuclides used for calibration and their gamma-ray energies.

The magnitude of the radiation source should be approximately 100 kBq. At this level of radioactivity, it can be used with a simple registration with the authorities as an approved device with a certification label. It is required that an “application for Approved Devices with Certification Labels” be submitted to the Nuclear Regulatory Commission within 30 days of starting to use it.

The application form of “Approved Devices with Certification Labels” can be obtained from the vendor of the radiation source. Alternatively, it can be downloaded from the Nuclear Regulatory Commission website.

http://www.nsr.go.jp/activity/ri_kisei/shinsei/shinsei1-1.html

*¹⁷Most MCAs can save an energy calibration result taken in advance and use it to display the horizontal axis of the spectrum in gamma-ray energies.

*¹⁸It is also possible to obtain the peak efficiency by simulation computing (see Explanation A).

Table 3.1 Example of nuclides used for calibration and their gamma-ray energies

Nuclides	Gamma-ray energy (keV)	Emission ratio	Half-life
²⁴¹ Am	59.5	0.359	432.6 yrs.
¹³³ Ba	81.0	0.355*	10.55 yrs.
⁵⁷ Co	122.1	0.856	271.7 days
¹³⁹ Ce	165.9	0.799	137.6 days
¹³³ Ba	356.0	0.621	10.55 yrs.
¹³⁷ Cs	661.7	0.851	30.08 yrs.
⁵⁴ Mn	834.8	1.000	312.2 days
⁸⁸ Y	898.0	0.937	106.6 days
⁶⁰ Co	1173.2	0.999	5.27 yrs.
²² Na	1274.5	0.999	2.60 yrs.
⁶⁰ Co	1332.5	1.000	5.27 yrs.
⁸⁸ Y	1836.1	0.992	106.6 days

*Because the peaks of ¹³³Ba of 79.6 keV (emission ratio: 0.026) overlap, the total of the emission ratio is shown here (cited from the Evaluated Nuclear Structure Data File (ENSDF) (March 2016)).

(3) Jigs to fix the detector and radiation source

The jig must be able to hold the Ge detector and radiation source at a set distance (1 m or more) and to alter the angle between the line formed by the radiation source and detector and the detector axis of symmetry (changeable by 10° – 15°).

Figure 3.3 illustrates an example of the jig used in a measurement.

When installing the radiation source, pay attention to its orientation such that it does not render itself as a shield. The revolution axis of the jig should be aligned with the center of the detector.

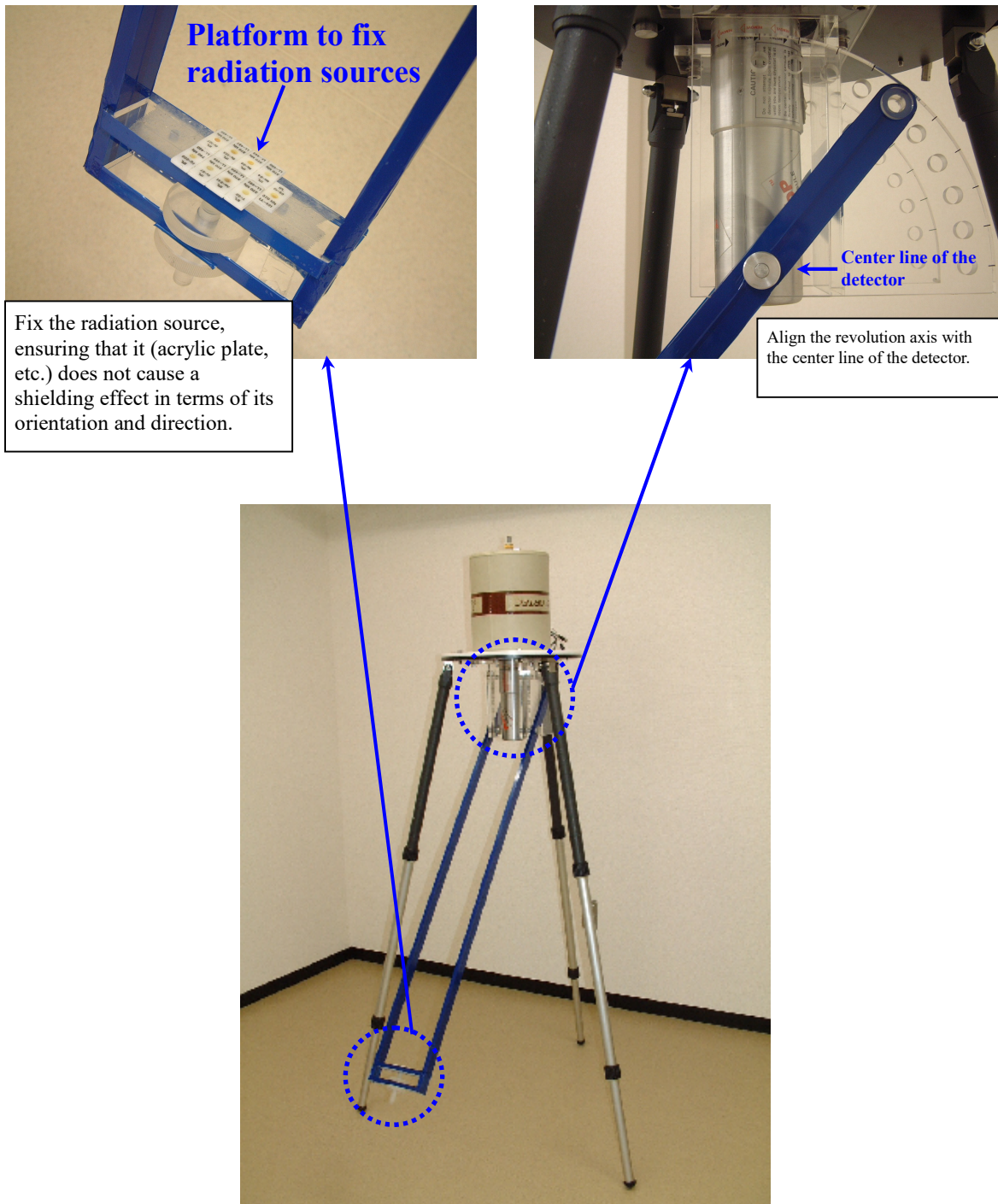


Figure 3.3 Example of a jig

To correct the angular dependence, measure the detector's angular dependence of peak efficiency $N(\theta)/N_0$.^{*19} The angular dependence of peak efficiency fluctuates with the gamma-ray energies. Thus, it is necessary to measure the dependence with a number of gamma-ray energies.

3.4.2.1.2 Measurement procedures^{*20}

- (1) Fix the point radiation source on the jig and run a measurement until the net peak count reaches approximately 10000 (multiple point radiation sources may be measured simultaneously).
- (2) Repeat the measurement by varying the angle (between 0° and 90°).
- (3) From the measured results, obtain the net peak count rate (s^{-1}) of the target nuclide.
- (4) Calculate the gamma-ray fluence rate ($cm^{-2}s^{-1}$) at the detector's location based on the number of gamma rays per second emitted from the standard radiation source used and the distance between the detector and the radiation source (see 5.2.1 (1)).
- (5) Obtain the peak efficiency per unit fluence rate by dividing the net peak count rate (3) by the fluence rate (4).
- (6) Express the peak efficiency for each gamma-ray energy by the function of the angle θ (standardize by giving $\theta = 0^\circ$ the value of 1.0 and apply the least square).
- (7) Using the function thus obtained, calculate the angular dependence correction term N_{θ}/N_0 for each gamma-ray energy through Equation (5.6) in Chapter 5.

3.4.2.1.3 Angular dependence

If the ratio between the length (L) and the diameter (D) of the Ge crystal close to 1, the detector is less angle-dependent in terms of the peak efficiency outside the low-energy area (> 200 keV), and the angular dependence correction term becomes close to 1 (see Figures 3.4 and 3.5).

If the detector has an L/D ratio between 0.9 and 1.1 and the low-energy gamma/X rays below 200 keV are excluded from the measurement, then the angular dependence correction term N_{θ}/N_0 will probably be within the range of 0.9 to 1.1. In this case, the angular dependence calibration is not mandatory, and it can be calibrated solely with the irradiation from the 90° direction.

^{*19} See Chapter 5, Equation (5.6)

^{*20} Procedures (3) to (7) may be automatically performed using the device vendor's software.

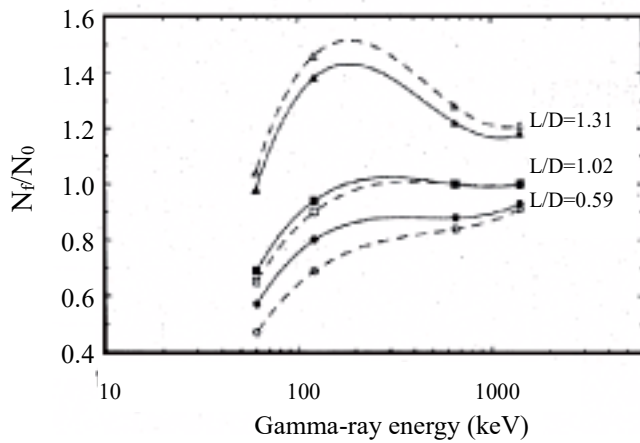


Figure 3.4 Relationship between gamma-ray energy and angular dependence correction term (N_f/N_0) (cited from ICRU Rep. 53)

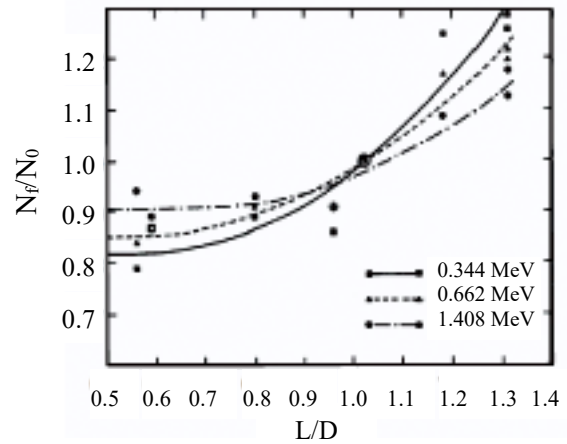


Figure 3.5 Relationship between the L/D ratio and angular dependence correction term (N_f/N_0) of a Ge detector (cited from HASL-300)

3.5 Measures against equipment contamination

3.5.1 Anti-contamination measures

If an in-situ measurement is conducted with contaminated equipment, the measured results may not be reliable. If the measurement will be conducted at a place with radioactive contamination, or contamination is not verified in that place, then anti-contamination measures should be taken in advance. As preventive measures, it is effective to cover the equipment with plastic bags, etc. (see Figure 3.6). To prevent the equipment from being contaminated during transfer, it is recommended to double the plastic layers for transportation, as long as this does not interfere with the measuring performance, use the detector's cover, etc. It is also important to cover the interior of the transit vehicle and change the plastic protections frequently to avoid introducing contamination into the vehicle.



Figure 3.6 Example of protecting the equipment

(1) Protection on the detector

Cut out a large sheet of vinyl plastic to the shape of the detector and cover it, using sealants as necessary, so that the main component of the detector is not contaminated (see Figure 3.7). It is important to remember that necessary arrangements are made to enable the handling of the device for transportation, cable connection, and inlet of liquid nitrogen (only for devices with the liquid nitrogen cooling system). If the main component has air intake/ventilation openings, these should be fitted with filters to prevent dust from entering the device.

In summer, the in-situ measurement may be under strong sunlight, in which case the temperature inside the plastic bag will increase and affect the detector itself. Therefore, provide a sun shade, etc. as necessary.



Liquid nitrogen cooling type)

(Electric cooling type)

Figure 3.7 Protection example on the detector

(2) Protection of MCA, etc. (except where MCA is mounted inside the main detector)

Using plastic bags, etc. that are larger than the MCA and the PC, protect these devices, with sealant if necessary, to prevent contamination. The protection must be able to accommodate certain arrangements with the MCA, as it must be connected to the detector and the PC for control with cables, as well as attaching a power cable. As the MCA releases heat during operation, the protection must not be hermetic, but must have some ventilation possibilities. Similar to the detector, it requires some protection against sun light.

(3) Protection of the cables

For applying protection to the cables, long plastic tubes are useful. Cables are most susceptible to damage while being handled; therefore, the protection must be as robust as the system with two layers, etc. to prevent breakage and tearing. Pay attention not to allow the protection to place loads on the connections.

(4) Protection of the detector support rack

For protecting the legs of the detector support rack, long plastic tubes are useful as in the case of the cables. Because these legs will be in constant contact with the ground during an in-situ measurement, extra measures must be taken such as doubling the plastic layers, using thick plastic bags, etc.

3.5.2 Decontamination methods

If the equipment becomes contaminated during an in-situ measurement, etc., decontamination is necessary. If the contaminated location/parts are identified, wipe off the contaminant. If wiping is not effective, consider the possibilities of replacing contaminated parts.

To verify the equipment contamination, perform regular background measurements under the same conditions and ascertain the background levels.

3.6 Other preparations

- Start cooling the detector in advance, considering the time needed for cooling it before starting the measurement. It is desirable, where it is operationally possible, to keep it cool at all times to prevent the degradation of the Ge crystal. If it is stored at the ambient temperature for a long period, it is necessary to check its efficiency regularly.
- Ensure that the batteries are fully charged (for the detector, portable MCA, and PC). In summer, the batteries may run out significantly more quickly. Spare batteries will help to extend the measurement duration in the field.
- If the equipment includes devices that cannot be run on batteries, a mobile generator may be used as a power supply. However, in this case, verify in advance that the noise does not interfere with the measurement.
- If using automotive batteries to supply power, it is necessary to verify in advance the batteries' stability as a power source and the device specifications.

4.1 Selection of the measurement site^{*1}

When calculating the radioactivity concentration, the conditions of the place where the measurement is taken has a significant bearing on the analysis results. Thus, it is necessary to consider the following points when selecting the measurement site.

- For the measurement, it is desirable that the conditions of the measurement site should be similar to that of the analysis (infinite plane), that is, a flat and wide area (area, ideally a 30-m radius, and at least 10 m radius).
- The radioactivity concentration measured by the in-situ measurement is the amount deposited on the ground. When comparing with the amount of fallout, etc. the site should be a grassland or bare ground where radioactive materials are considered to be held and where human interventions have not been made, instead of covered surfaces such as tarmacked ground.
- To avoid making the transit vehicles become gamma-ray shields, they should be parked away from the measurement site.

However, note that the site does not have to be an infinite plane if the measurement is for the identification of nuclides or calculation of the ambient dose rates.

It is practically difficult to find an ideal location that satisfies all the points raised above in the real environment for selecting the measurement site. The in-situ measurement is based on certain assumptions in the analysis in terms of the topography of the surrounding areas, vertical profile of radioactive materials in the ground, installation height of the detector, etc.; thus, it is necessary to understand the impact on the analysis results if the actual conditions differ from these assumptions (see Chapter 6).

4.2 Measurement

4.2.1 Installation of the equipment

- (1) Set up the Ge detector in the center of the selected measurement site, positioning the device on a rack facing downward, such that the distance between the ground surface and the crystal's geometric center is 1 m, and having studied the ground surface contour, adjust the legs of the rack to make the detector parallel to the ground surface.
- (2) Place the portable MCA and PC at least 3 m away from the detector^{*2} and connect these with cables. If a table is used for the MCA and PC, it should be of the minimum size to minimize the shielding effect on the gamma rays that arise from the ground.
- (3) Take measures to stabilize the equipment temperature within the range of guaranteed operation if the weather conditions necessitate it, to prevent the gain fluctuation due to extreme temperatures.^{*3}
- (4) If necessary, the rack legs can be fixed to the ground to prevent a fall.

4.2.2 Detector startup and measurement procedures

- (1) Turn on the MCA and PC, and apply a high voltage to the Ge detector. Leave the setup for a while to warm up. The time required for the warm-up depends on the devices involved. Know the timing specific to the devices used in advance.

^{*1} See Explanation F

^{*2} When taking a measurement at a site that is possibly contaminated, apply anti-contamination measures (see 3.5.1).

^{*3} Provide sun shades in summer, and thermal insulation covers in winter.

- (2) Perform a measurement to run equipment adjustments. Normally, a measurement picks up peaks deriving from natural radionuclides such as potassium-40 (1461 keV), which are used to adjust gains. In situations following a nuclear accident, however, it is necessary to consider using artificial radionuclides for the gain adjustments (see Explanation D). During the measurement, it is recommended that the detector and MCA be operated on batteries to ensure electric stability.
- (3) Preset the measuring time and start measuring. The measuring time should be approximately 30 min to 1 h, which must be judged by visually checking the measured spectrum (see Explanation B).
- (4) Check the dead time.
- (5) Once the measurement commences, do not approach the detector (to avoid shielding of the gamma rays rising from the ground).

4.2.3 Verifications to be conducted during the measurement

Normally, the gamma-ray spectrum obtained through an in-situ measurement contains peaks of natural radionuclides. Therefore, the spectrum can be checked during the measurement using these. Confirm the peak of potassium-40 (1461 keV) to verify its position (center channel) and FWHM in the spectrum. If the peak center is off the true center by two channels or more, or the FWHM is significantly changed, an insufficient warm-up or equipment faults are suspected. Take a second measurement or run an equipment inspection.

4.2.4 Procedures for finishing the measurement

- (1) Check if the measuring time has reached the preset value.
 - (2) Verifying that the data collection has been terminated, save the spectrum in a data file and note the file name.
 - (3) Take an overview of the spectrum. If unexpected peaks, noises, etc. are found, investigate their causes and arrange necessary measures, such as taking a second measurement.
 - (4) If an analysis is conducted on the in-situ measurement site, refer to “4.4 Spectral analysis.”
- Steps (5) to (7) below can be omitted if it is difficult to secure the time for warm-up before the measurement at a subsequent measurement site, provided that no problems are caused in transferring the equipment.
- (5) Shut down the high-voltage power source and turn off the MCA.
 - (6) Close the PC and turn off the power.
 - (7) Disconnect the MCA, detector, and PC and remove the respective connecting cables.
 - (8) Dismantle the detector from the support rack carefully and place it into a carrying case.
 - (9) Move to the next measurement site.

4.3 Recording

Take records of the following items in terms of the measurement sites and measurements. Table 4.1 illustrates an example of such a recording format.

4.3.1 Records of the measurement site

- (1) Take notes about the descriptions of the surrounding areas.^{*4}
 - (1) Topography (level ground, slanted, etc.)
 - (2) Land use (sports ground, part of precincts of temple, cultivated area, noncultivated area, etc.)
 - (3) Surface conditions (grassed, bare ground, turfed, sand dunes, vegetable farm, orchard, tarmacked, etc.)
 - (4) Type of the soil (sandy, loamy, clay, etc.)^{*5}
 - (5) Breadth of grasslands, etc.
 - (6) Condition of the soil
 - (7) Structures in the surrounding areas (distances between the measurement point and the buildings, size of the building, materials (timber, concrete, etc.))
- (2) Take photographs of the surrounding areas.
- (3) Measure the dose rate near the measurement site with a survey meter and record the readings.
^{*6}
- (4) If a GPS^{*7} is available, record the coordinates of the measurement site.
- (5) Weather conditions (take detailed notes about precipitation, and if possible, record the wind direction, velocity and ambient temperature)

4.3.2 Records about the measurement

- (1) Date and start time of the measurement
- (2) Name of the person who conducted the measurement
- (3) Detector and measurement equipment (model, serial number, etc.)
- (4) Data file name of the spectral data measured
- (5) Center channels, etc. of the main peak^{*8}
- (6) Characteristics of the spectrum (note if there are irregular forms or increase in FWHM, etc.)

^{*4} The descriptions are about the area of approximately 30 m radius around the measurement site.

^{*5} The soil classification is described in the Radioactivity Measurement Series No. 16 "Methods of environmental sampling." Take notes of the details if the soil is of a special kind (humic soil, etc.).

^{*6} This is for the purpose of ensuring that the measurement point is not on a locally high/low-dose-rate spot.

^{*7} Global positioning system

^{*8} See Table 4.3 for the radionuclides usually detected and their gamma-ray energies.

Table 4.1 Example of recording format

1. Records of the measurement site

(Describe the required details or put a circle on applicable items. If more space is needed, write in the Remarks section.)

(1) Measurement site			(2) Measurement point		
(3) Coordinates	N: ° ' '' E: ° ' ''	(4) Weather conditions (precipitations in particular)		(5) Snow cover (cm)	
(6) Topography	• Flat ground / slanted ground • Other ()	(7) Land use	• Sports ground • Precincts of a temple, etc. • Cultivated land • Non-cultivated land • Other ()	(8) Type of the soil	•Sandy -Loamy •Clay •Other ()
(9) Ground surface conditions	• Grassland • Bare ground • Turfed land • Sandy land • Farmland • Orchard • Tarmacked surface • Other ()	(10) Breadth of grasslands, etc.		(11) Condition of the soil	•Wet •Dry •Other ()
(12) Structures in the surrounding areas	•Yes / No (within 30 m)	(13) Dose rate measurement		(14) Photograph taken	•Yes / No
	• Distance from the buildings: m • Type of the buildings: Timber; Concrete; Other () • Number of stories:				
(15) Remarks					

2. Records of the measurement

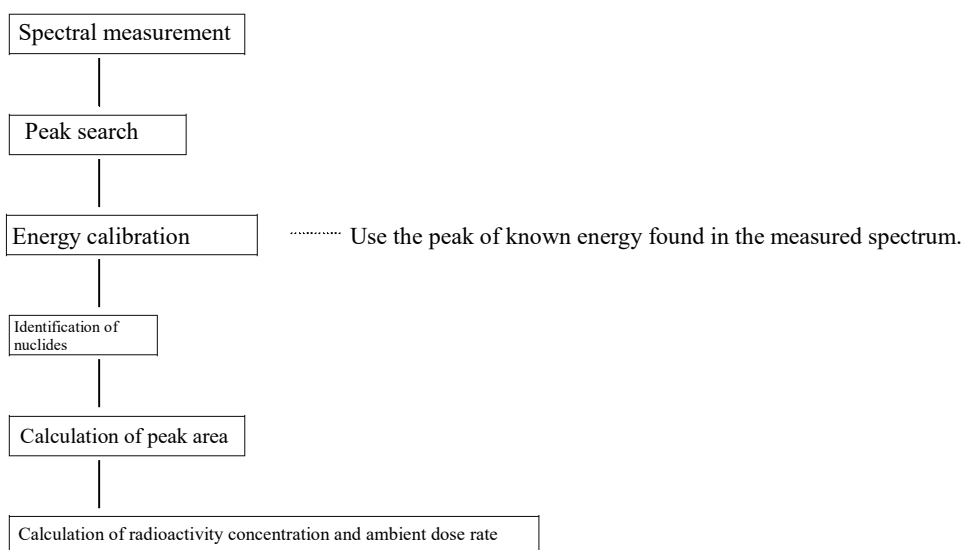
(Describe the required details or put a circle on applicable items. If more space is needed, write in the Remarks section.)

(1) Measurement start date	[month]/[date]/[year]	(2) Measurement start time	[hour]:[minute]	(3) Measuring time	seconds	
(4) Name of the person who conducted the measurement			(5) Detector/equipment No.	Detector No. Measurement equipment No.		
(6) File name of the spectral data measured			(7) Irregularities in the spectrum	• None • Yes ()		
(8) Main peak center channel (For other nuclides, describe in the Remarks section)	Peak (ch)					FWHM (keV) ⁴⁰ K
	²¹² Pb (239 keV)	²¹⁴ Pb (352 keV)	²¹⁴ Bi (609 keV)	²²⁸ Ac (911 keV)	⁴⁰ K (1461 keV)	
(9) Detected artificial radionuclides						
(10) Remarks						

4.4 Spectral analysis

The analysis of the spectrum obtained by a Ge detector will focus on the total absorption peak based on the monochromatic photons found in the spectrum. Although it is possible to perform automatic analysis using the software provided by the measurement equipment manufacturer, it is necessary to verify the software’s analytical conditions before putting it to use. To avoid errors in quantification due to changes made in the analytical conditions, it is important to ensure that the same analytical conditions are applied both to the equipment calibration and in-situ measurements. When altering certain analytical conditions, it is recommended that the impact of the condition difference on analytical results be understood in advance.

4.4.1 Analytical procedures



4.4.2 Peak search, identification of nuclides, and calculation of peak area

The peak search, identification of nuclides, and calculation of peak area are performed in the same manner as in the case of the general gamma-ray spectrometry. Refer to the Radioactivity Measurement Series No. 7 “Gamma-ray Spectrometry Using Germanium Detectors” for operation procedures.

Table 4.2 lists the radionuclides generally detected under normal circumstances.

Table 4.2 Radionuclides normally detected through in-situ measurements

Naturally occurring radionuclides			Artificial radionuclides
Uranium series	Thorium series	Other	
^{214}Pb ^{214}Bi	^{208}Tl ^{212}Pb ^{212}Bi ^{228}Ac	^{40}K ^7Be	^{137}Cs

As many peaks of artificial radionuclides are expected to be detected in a nuclear accident, data analyses for nuclide identifications and peak area calculations must be conducted carefully.

An example of an in-situ measurement spectrum is shown in Explanation C.

4.4.3 Energy calibration

Energy calibration needs special precautions for in-situ measurements, as it is conducted outdoors, which means that it is exposed to temperature fluctuations and the measurement must be commenced relatively quickly after turning on the power of the equipment. There is a risk that peaks may move owing to the variation in gains caused by changes in temperatures subsequent to the lab-based energy calibration using gamma-ray radiation sources. Therefore, conduct the calibration again in the field using the known peak detected in the spectrum obtained through an in-situ measurement. In the in-situ measurement, it is often the case that certain naturally occurring radionuclides are detected in the spectrum. Use the peak of such a nuclide to carry out the energy calibration. Table 4.3 illustrates an example of these nuclides and their gamma-ray energies. When a nuclear accident occurs, the background radiation level rises and some radionuclides in Table 4.3, especially those in the low-energy region, become unsuitable for calibrations. In such a case, it may be necessary to perform the energy calibration using gamma-ray energy of the artificial radionuclides emitted through the accident, as seen in Table 4.4 (see Explanation D).

Table 4.3 Naturally occurring radionuclides usable for energy calibration and their gamma-ray energies

Nuclides	Gamma-ray energy (keV)	Emission ratio *
²¹² Pb	239	0.434
²¹⁴ Pb	352	0.369
²⁰⁸ Tl	583	0.306
²¹⁴ Bi	609	0.469
²²⁸ Ac	911	0.290
⁴⁰ K	1461	0.107
²⁰⁸ Tl	2615	0.359

* ²³⁸U and ²³²Th series show the per-decay emission rates of the parent nuclides

(cited from ICRU Rep. 53, Table 3.4)

Table 4.4 Artificial radionuclides usable for energy calibration in a nuclear accident and their gamma-ray energies

Nuclides	Gamma-ray energy (keV)	Emission ratio
¹³⁴ Cs	605	0.975
¹³⁷ Cs	662	0.849
¹³⁴ Cs	796	0.851
^{110m} Ag	885	0.729
^{110m} Ag	1384	0.243
^{110m} Ag	1505	0.131

(cited from ICRU Rep. 53, Table A.1)

Chapter 5 Calculation of radioactivity concentration and ambient dose rate

5.1 Conditions for analysis

The in-situ measurement enables calculation of the radioactivity concentration (radiation per unit area: Bq/cm²) of the radioactive materials deposited on the ground and ambient dose rate. The HASL analytical method developed by Beck et al. (hereafter, the “HASL method”) has been used worldwide for the evaluation of such data, and it is employed by the ICRU. Therefore, this manual also adopts the HASL method for conducting analyses.

The HASL method uses certain assumptions to calculate the radioactivity concentration and ambient radiation dose rate, such as the topography, vertical profile of radioactive materials in the ground, and the detector installation height. Table 5.1 lists these assumptions.

Table 5.1 Assumptions used in in-situ measurement

Condition	Description
Topography of the surrounding areas	A flat and wide, infinitely open area (infinite plane)
Vertical profile of radioactive materials in the ground	The distribution expressed by Equation (5.1)
Height of the detector	1 m from the ground surface

The radioactivity concentration $A(Z)$ at mass depth Z in the ground is expressed as follows:

$$A(Z) = A_0 \cdot \exp\left(-\frac{Z}{\beta}\right) \quad (5.1)$$

$A(Z)$: Radioactivity concentration (Bq/g) at mass depth Z

Z : Mass depth (g/cm²)

The depth measured from the ground surface by per-unit-area mass of the soil.

A_0 : Radioactivity concentration (Bq/g) at the ground surface

β : Weight buffer depth (g/cm²)

A parameter to indicate the vertical profile of radioactive materials in the ground. It expresses the degree of penetration, where greater values indicate deeper penetration.

The value of β is the mass depth at which the radioactivity concentration is 37% of that at the ground surface (= 1/e); it is almost zero for ground surface distribution and infinite for an underground homogeneous distribution in the ground. The exponential model is simply an approximation, but it suggests relatively realistic values after a certain time has elapsed since the radioactive deposition.

As time passes, the distribution may present peaks at certain depths owing to the transition or diffusion of the radioactive materials, or the distribution may cease to be exponential as the land is subjected to use, erosion, or decontamination. However, even in such cases, a practically valid β can be employed to associate the measured results on the ground with the radiation sources in the ground (see Explanation E).

The radiation (deposition amount) per unit area A_a is expressed as follows:

$$A_a = \beta \cdot A_0 \quad (5.2)$$

A_a : Radioactivity per unit area (Bq/cm²)

5.2 Calculation of radioactivity concentration

5.2.1 Analysis of radioactive materials deposited on the ground

For evaluating the radioactive materials deposited on the ground, the radioactivity concentration A_a (radiation per unit area: Bq/cm²) can be calculated by the following equation.

$$A_a = \frac{N_f}{N_f/A_a} \quad (5.3)$$

A_a : Radioactivity per unit area (Bq/cm²)

N_f : Peak count rate of energy E (s⁻¹) in in-situ measurement

N_f/A_a : Efficiency in in-situ measurement

N_f/A_a is calculated by the following equation:

$$\frac{N_f}{A_a} = \frac{N_0}{\phi} \cdot \frac{N_f}{N_0} \cdot \frac{\phi}{A_a} \quad (5.4)$$

N_0 : Peak count rate (s⁻¹) of the gamma ray of energy E that enters the detector at the angle (0°) to the detector axis of symmetry

ϕ : Fluence rate (cm⁻²s⁻¹)

(1) N_0/ϕ

N_0/ϕ indicates the peak count rate (s⁻¹) at the fluence rate (cm⁻²s⁻¹) at the angle of the detector axis of symmetry (0°). This value is dependent on the detector and calculated by the gamma-ray radiation source measured for each detector.

- Install several radiation sources with varying energies at distances of 1 m or more along the detector axis of symmetry.
- Perform the measurement and calculate N_0 .
- ϕ is calculated by the following equation:

$$\varphi = \frac{S \cdot a}{4 \cdot \pi \cdot r^2} e^{-\mu_a x} e^{-\mu_h y} \quad (5.5)$$

S : Radioactivity of the gamma-ray radiation source (Bq)

A : Gamma-ray emission ratio

μ_a : Attenuation coefficient in air for gamma rays (cm^{-1})

x : Distance from the radiation source to the detector front cap (cm)

μ_h : Attenuation coefficient of gamma rays in radiation source holder (in the ground) (cm^{-1})

y : Distance through radiation source holder that gamma rays (in the ground) pass on the way to detector (cm)

r^{*1} : Distance from the radiation source to the detector's effective crystal center (cm)

- 1) If the gamma-ray energy is over 1 MeV, the detector's effective crystal center is the geometric center of the Ge crystal.
- 2) If the gamma-ray energy is less than 0.1 MeV, the detector's effective crystal center is the Ge crystal face.
- 3) Where the energy is in the range between 1) and 2) above, use the following equation to obtain r .

$$r = \frac{1}{\mu} \cdot \frac{1 - e^{-\mu d} (\mu d + 1)}{1 - e^{-\mu d}} + d_{0+x}$$

μ : Attenuation coefficient in Ge crystal for gamma rays (cm^{-1})

d : Ge crystal thickness (cm)

d_0 : Distance from detector cap to crystal face (cm)

An example of the calculation to obtain distance (r) from the radiation source to the detector's effective crystal center is illustrated in Table 5.2.1.

Table 5.2.2 illustrates an example calculation of attenuation ($e^{-\mu_a x}$) by air.

Tables 5.2.3 and 5.2.4 illustrate the coefficients in the radiation source holder (in the ground) for gamma rays (μ_h) and the soil compositions used in this calculation, respectively.

Calculate N_0/φ as a function of energy. An example is shown in Figure 5.1.

*1 When determining the distance between the source and the detector, it is useful to introduce the notion of the "effective center" of the detector, as the detectors have finite dimensions. There are several ways to obtain the effective center. Here, the method from the IAEA's TECDOC-1092 (1999) is introduced.

Table 5.2.1 Calculation to obtain distance (r) from the radiation source to the detector's effective crystal center

Unit: (cm)

Gamma-ray energy (MeV)	μ (cm^{-1})	Ge crystal thickness d (cm)				
		4	5	6	7	8
0.1	2.94	100.8	100.8	100.8	100.8	100.8
0.15	1.32	101.2	101.3	101.3	101.3	101.3
0.2	0.883	101.5	101.6	101.6	101.6	101.6
0.3	0.601	101.8	101.9	102.0	102.1	102.1
0.4	0.496	101.9	102.1	102.2	102.3	102.4
0.5	0.437	101.9	102.2	102.3	102.4	102.5
0.6	0.397	102.0	102.2	102.4	102.6	102.7
0.8	0.342	102.1	102.3	102.5	102.7	102.9
1	0.305	102.1	102.4	102.6	102.8	103.0

- x: Distance from the radiation source to the detector front cap = 100 cm
- μ : Attenuation coefficient in Ge crystal for gamma rays (cm^{-1})
- d_0 : Distance from detector cap to Ge crystal face (cm) = 0.5 cm

Table 5.2.2 Calculation of attenuation ($e^{-\mu_a x}$) by air

Gamma-ray energy (MeV)	Linear attenuation coefficient at 20 °C* ($\times 10^{-4} \text{ cm}^{-1}$)	Attenuation by air at a distance of 1 m
0.06	2.159	0.979
0.08	1.945	0.981
0.1	1.820	0.982
0.15	1.616	0.984
0.2	1.476	0.985
0.3	1.281	0.987
0.4	1.148	0.989
0.5	1.048	0.990
0.6	0.9689	0.990
0.8	0.8513	0.992
1	0.7649	0.992
1.5	0.6227	0.994
2	0.5351	0.995

*PHOTX database

Table 5.2.3 Attenuation coefficient for gamma rays in radiation source holder (in the ground)

Gamma-ray energy (keV)	(μ_h)	
	Mass attenuation coefficient of soil* (cm^2/g)	Linear attenuation coefficient of soil** (cm^{-1})
20	2.78	4.45
25	1.52	2.43
30	0.938	1.50
35	0.644	1.03
40	0.471	0.754
45	0.381	0.610
50	0.314	0.502
55	0.277	0.443
60	0.248	0.397
65	0.230	0.368
70	0.214	0.342
75	0.202	0.323
80	0.190	0.304
85	0.185	0.296
90	0.178	0.285
95	0.173	0.277
100	0.167	0.267
150	0.139	0.222
200	0.125	0.200
250	0.115	0.184
300	0.108	0.173
350	0.101	0.162
400	0.0963	0.154
450	0.0919	0.147
500	0.0875	0.140
550	0.0844	0.135
600	0.0813	0.130
650	0.0788	0.126
700	0.0756	0.121
750	0.0731	0.117
800	0.0713	0.114
850	0.0694	0.111
900	0.0675	0.108
950	0.0650	0.104
1000	0.0638	0.102
1500	0.0521	0.0834
2000	0.0449	0.0718
2500	0.0401	0.0642
3000	0.0364	0.0582

*Cited from HASL-258

**The soil density is given at 1.6 g/cm^3 for the calculation

Table 5.2.4 Soil composition

Component	Composition
Al ₂ O ₃	13.5 wt%
Fe ₂ O ₃	4.5 wt%
SiO ₂	67.5 wt%
CO ₂	4.5 wt%
H ₂ O	10 wt%
ρ (density)	1.6 g/cm ³

(Cited from HASL-258)

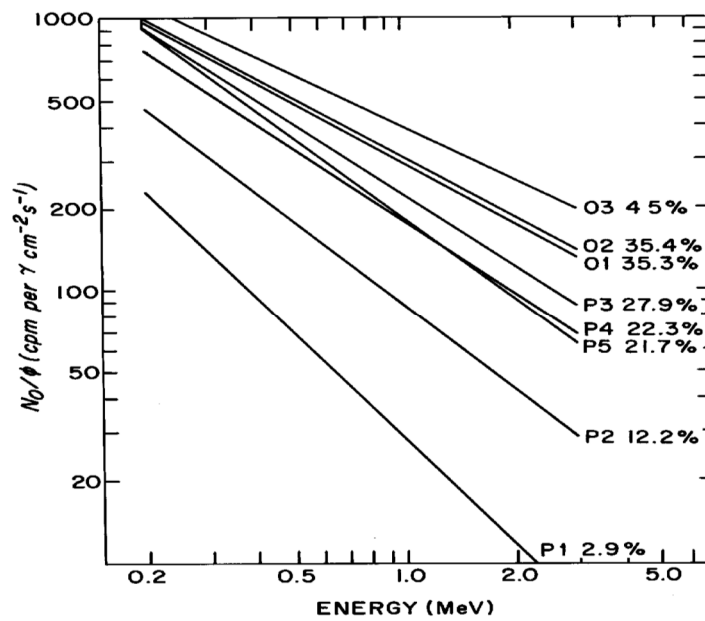


Figure 5.1 Fluctuation by energy of count rate per fluence rate (N_0/ϕ) in several detectors of different relative efficiencies

P1 to P5 and O1 to O3 are different types of detectors, and the values to the right indicate the relative efficiencies.

(Cited from HASL-300)

(2) N_f/N_0

N_f/N_0 is a component of the directional dependence correction of a detector, and it is calculated by the following equation, considering the direction of incidence of environmental gamma rays and the detector's directional dependence:

$$\frac{N_f}{N_0} = \int_0^{\frac{\pi}{2}} \frac{\phi(\theta)}{\phi} \frac{N(\theta)}{N_0} d\theta \quad (5.6)$$

$\phi(\theta)/\phi$: The proportion in which an environmental gamma ray of energy E enters the detector at angle θ in a given geometry. To illustrate, some calculations of cesium-137 (662 keV) in several geometries are shown in Figure 5.2. Note that this value does not vary significantly depending on the gamma-ray energy.

$N(\theta)/N_0$: The relative sensitivity (to a baseline of 0°) of a gamma ray of energy E with respect to the angle of incidence θ . The calculation is repeated several times using different gamma-ray radiation sources of varying energy and by changing the angle of incidence.

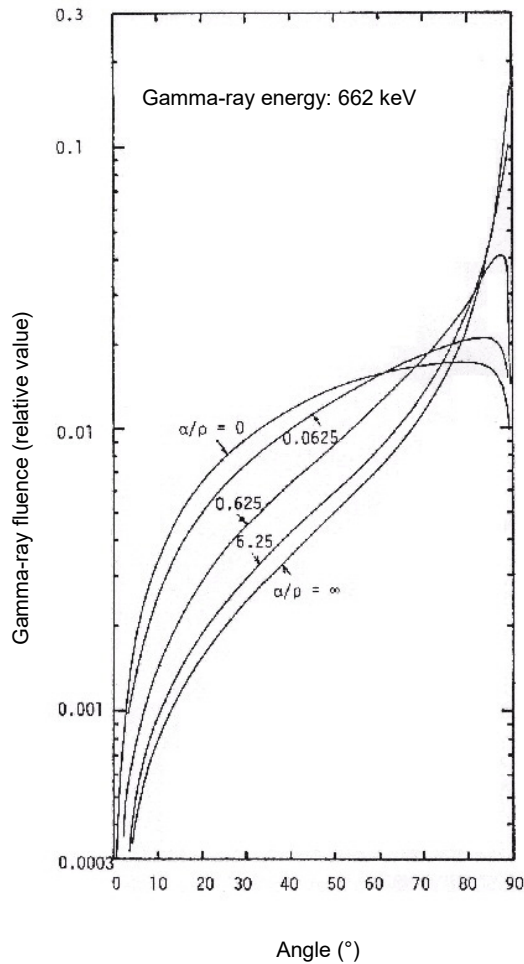


Figure 5.2 Distribution of gamma-ray incidence direction 1 m above ground level
 α/ρ in the figure is an inverse of β in Expression (5.1)
 (Cited from JAERI-M 6498)

For detectors with Ge crystals of approximately equal dimensions (length (L) and diameter (D)), their sensitivity to angular dependence is small; thus, the correction term N_f/N_0 is close to 1. In the in-situ measurement, many gamma rays enter the detector at almost horizontal angles. For these reasons, it is possible to calibrate the equipment with the irradiation only in this direction. In this case, Equation (5.4) takes a simple form as follows:

$$\frac{N_f}{A_a} = \frac{N_{90}}{\phi} \cdot \frac{\phi}{A_a} \quad (5.7)$$

N_{90} : Peak count rate (s^{-1}) of the gamma ray of energy E incident at right angle (90°) to the detector axis of symmetry.

In the in-situ measurement, the detector is usually set in a downward-facing position, and many environmental gamma rays are injected horizontally. Therefore, $N_{90} = N_f$ can be assumed.

(3) ϕ/A_a

ϕ/A_a indicates the relationship between the radioactivity concentration in the ground (A_a) and the detection position (at a height of 1 m) in terms of the gamma-ray fluence rate, the value of which varies depending on the radiation source distribution. Table-1 illustrates the ϕ/A_a values of major nuclides by the vertical profile in the ground of radioactive materials (β).

Ideally, β is obtained through measurements, but this is usually very difficult to do.

Alternatively, therefore, the values indicated in Table 5.3 can be in principle applied, according to the time elapsed since the radioactive deposition and the amount of precipitation as a guide. If the ground surface is nonpermeable (rooftop, asphalt, and concrete), it is appropriate to assume β to be 0.1 g/cm². The values in Table 5.3 can only be used if the soil is not of a special kind (humic soil, etc.) and not disturbed by human activities. Moreover, the accuracy of the analysis of in-situ measured results can be enhanced by sampling the soil at the measurement site by soil layers and evaluating the radioactive distribution by depth.

Note that details are given in Explanation E, because the accurate understanding of the vertical profile of radioactive materials in the ground is the most effective way to improve the reliability of in-situ measurements.

Table 5.3 Recommended values for vertical profile of radioactive materials in the ground

Time elapsed since deposition (years)	Precipitation after deposition (mm)	Vertical profile parameter β (g/cm ²)
0~1	<3	0.1
0~1	≥ 3	1.0
1~5	-	3.0
5~20	-	10

(Cited from ICRU Rep.53)

5.2.2 Analysis of radioactive materials evenly distributed in the ground

The same calculation method can be applied to the naturally occurring radioactive materials that are considered to be distributed evenly in the ground, such as the uranium series, thorium series, and potassium-40. However, radioactivity concentration is expressed by activity per unit mass A_m , where the unit is Bq/g. Table 5.4 lists the ϕ/A_m calculated assuming a homogeneous distribution. In most natural environments, it is valid to assume that naturally occurring radioactive materials are distributed evenly in the ground. However, artificial structures standing nearby also contain naturally occurring radioactive materials; thus, their influence must be considered.

Note that, when analyzing nuclides of the uranium series, the radioactive equilibrium must be considered. As radon-222 dissipates from the soil, its product nuclides such as lead-214 and bismuth-214 may indicate low values. While the dissipation rate of radon-222 is generally approximately 15%, the extent of underestimation cannot be generalized owing to the influence of airborne disintegration products. Similarly, precipitation collects radon-222 and its disintegration products onto the ground surface. Therefore, measurements taken in rain or within several hours after precipitation are not suitable for analyses of uranium-series nuclides in the ground.

Radium-226 of the uranium series releases a gamma-ray of energy 186 keV, which is identical to that of radium-235 (186 keV), and thus is not usable for quantification.

Table 5.4 Relationship between radionuclide activity in the ground and gamma-ray fluence rate 1 m above ground (ϕ/A_m)

(Assuming a homogeneous distribution of radioactive materials in the ground)

Series	Nuclides	Energy (MeV)	Emission ratio*	ϕ/A_m ($\text{cm}^{-2}\text{s}^{-1}$)/(Bq/g)
²³⁸ U	²¹⁴ Pb	0.295	0.192	0.828
	Same as above	0.352	0.369	1.71
	²¹⁴ Bi	0.609	0.469	2.75
	Same as above	0.665	0.0158	0.0965
	Same as above	0.768	0.0497	0.325
	Same as above	0.934	0.0319	0.229
	^{234m} Pa	1.001	0.00845	0.0629
	²¹⁴ Bi	1.120	0.155	1.22
	Same as above	1.238	0.0610	0.507
	Same as above	1.378	0.0410	0.361
	Same as above	1.408	0.0250	0.223
	Same as above	1.509	0.0220	0.203
	Same as above	1.730	0.0300	0.298
	Same as above	1.765	0.162	1.62
	Same as above	1.847	0.0216	0.222
	Same as above	2.119	0.0125	0.138
	Same as above	2.204	0.0525	0.592
	Same as above	2.448	0.0162	0.193
	²³² Th	²¹² Pb	0.239	0.434
²²⁴ Ra		0.241	0.0397	0.158
²²⁸ Ac		0.338	0.120	0.547
Same as above		0.463	0.0464	0.241
²⁰⁸ Tl		0.511	0.0809	0.438
Same as above		0.583	0.306	1.76
²¹² Bi		0.727	0.0675	0.430
²²⁸ Ac		0.795	0.0484	0.322
²⁰⁸ Tl		0.861	0.0453	0.313
²²⁸ Ac		0.911	0.290	2.060
Same as above		0.965	0.0545	0.398
Same as above		0.969	0.175	1.282
Same as above		1.588	0.0371	0.352
²¹² Bi		1.621	0.0149	0.143
²²⁸ Ac		1.630	0.0195	0.187
²⁰⁸ Tl	2.615	0.359	4.418	
⁴⁰ K	⁴⁰ K	1.461	0.107	0.971

*²³⁸U and ²³²Th series show the per-decay emission rates of the parent nuclides
(Cited from ICRU Rep. 53)

5.3 Calculation of ambient dose rate

For the radioactive materials deposited on the ground surface or distributed evenly in the ground, the ambient dose rate measured 1 m above ground level (“dose rate”) is calculated by the following equation:

$$I = N_f / \frac{N_f}{I} \quad (5.8)$$

I : dose rate (ambient absorbed dose rate: $\mu\text{Gy/h}$, or peripheral dose equivalent rate: $\mu\text{Sv/h}$)

N_f : peak count rate of energy E (s^{-1}) in in-situ measurement

N_f/I is calculated by the following equation:

$$\frac{N_f}{I} = \frac{N_0}{\phi} \cdot \frac{N_f}{N_0} \cdot \frac{\phi}{I} \quad (5.9)$$

N_0 : peak count rate (s^{-1}) of gamma-ray incident from the detector axis of symmetry direction (0°)

ϕ : fluence rate ($\text{cm}^{-2}\text{s}^{-1}$)

Equation (5.9) is the same as Equation (5.4), except that the radioactivity concentration A is replaced with the dose rate I . ϕ/I is a coefficient that expresses the relationship in a given geometry between the gamma-ray fluence rate of the gamma ray of energy E emitted by a radioactive material and the total dose rate of this radioactive material. The dose rate I must include not only the primary gamma ray of energy E , but also contributions by scattered rays and all other gamma rays of the radioactive material. For the scattered ray evaluation, it is necessary to use either the Monte Carlo method or Lattice Boltzmann transport equation. Values for ϕ/I of radioactive materials exponentially distributed in the ground are listed in Table-2-1 (air absorbed dose rate: $\mu\text{Gy/h}$ unit) and Table-2-2 (peripheral dose equivalent rate: $\mu\text{Sv/h}$ unit). Table 5.5 lists ϕ/I in the case of homogeneous distribution in the ground (naturally occurring radioactive materials). ϕ/I for uranium- and thorium-series nuclides indicates the relationship between the fluence rate of a given gamma ray released by a given nuclide within the series and the dose rate of gamma rays from all nuclides within the series. It follows that the dose rate of a given gamma ray of a given nuclide is the same as the dose rate of all the nuclides within that series.*¹ When analyzing either the gamma rays emitted by several nuclides of the same series (e.g., ^{214}Pb and ^{214}Bi of the uranium series) or several gamma rays emitted by a single nuclide (^{214}Bi : 609 keV, 1765 keV, etc.), the average dose rate of those gamma rays*² is used as the series dose rate.

The dose rate can also be calculated from radioactivity concentration. Conversion factors in the case of exponential distribution are listed in Table-3-1 (air absorbed dose rate: $\mu\text{Gy/h}$ unit) and

*¹ This enables obtaining the results equivalent to those by measuring up to 3 MeV using a NaI(Tl) scintillation detector, for the dose rate calculated through the analysis of gamma rays of less than 2 MeV includes contributions by gamma rays of more than 2 MeV emitted by other nuclides of the same series, even though the energy range for in-situ measurement is limited to a maximum of 2 MeV.

*² Take weighted average using a counting error.

Table-3-2 (peripheral dose equivalent rate: $\mu\text{Sv/h}$ unit). Table 5.6 indicates the conversion factors (air absorbed dose rate: $\mu\text{Gy/h}$ unit) in the case of homogeneous distribution (naturally occurring radioactive materials). The total values for the uranium series and thorium series in Table 5.6 are calculated assuming that the series nuclides are in radioactive equilibrium.*³

*³ Although the uranium series includes gaseous radon, which suggests a possibility that radioactive equilibrium is not established, this does not usually pose a problem as the in-situ measurement measures the post-radon-222 products of lead-214 and bismuth-214, and also because dose contributions are attributed mainly to these decay products.

Table 5.5 Relationship between dose rate of radioactive materials evenly distributed in the ground measured 1 m above ground and gamma-ray fluence rate (ϕ/I)

Series	Nuclides	Energy (MeV)	ϕ/I ($\text{cm}^{-2}\text{s}^{-1}$)/($\mu\text{Gy/h}$)
²³⁸ U	²¹⁴ Pb	0.295	1.79
	Same as above	0.352	3.70
	²¹⁴ Bi	0.609	5.95
	Same as above	0.665	0.209
	Same as above	0.768	0.703
	Same as above	0.934	0.496
	^{234m} Pa	1.001	0.136
	²¹⁴ Bi	1.120	2.64
	Same as above	1.238	1.10
	Same as above	1.378	0.781
	Same as above	1.408	0.483
	Same as above	1.509	0.439
	Same as above	1.730	0.645
	Same as above	1.765	3.51
	Same as above	1.847	0.481
	Same as above	2.119	0.299
	Same as above	2.204	1.28
	²³² Th	²¹² Pb	0.239
²²⁴ Ra		0.241	0.262
²²⁸ Ac		0.338	0.906
Same as above		0.463	0.399
²⁰⁸ Tl		0.511	0.725
Same as above		0.583	2.91
²¹² Bi		0.727	0.712
²²⁸ Ac		0.795	0.533
²⁰⁸ Tl		0.861	0.518
²²⁸ Ac		0.911	3.41
Same as above		0.965	0.659
Same as above		0.969	2.12
Same as above		1.588	0.583
²¹² Bi		1.621	0.237
²²⁸ Ac		1.630	0.310
²⁰⁸ Tl	2.615	7.31	
⁴⁰ K	⁴⁰ K	1.461	23.3

Dose rate (I) is regarded to be of all the nuclides within the series, assuming the establishment of radioactive equilibrium among them.

Table 5.6 Relationship between radioactivity concentration in the ground measured 1 m above ground and dose rate (I/A_m)*
(Assuming a homogeneous distribution of radioactive materials in the ground)

Nuclides	Kerma rate per radioactivity concentration ($\mu\text{Gy/h}/(\text{Bq/g})$)
²³⁸ U series	
²³⁸ U	$4.33/10^{-5}$
²³⁴ U	$5.14/10^{-5}$
²³⁴ Th	$9.47/10^{-4}$
^{234m} Pa	$3.00/10^{-3}$
²³⁴ Pa	$4.49/10^{-4}$
²³⁰ Th	$6.90/10^{-5}$
²²⁶ Ra	$1.25/10^{-3}$
²²² Rn	$8.78/10^{-5}$
²¹⁴ Pb	$5.46/10^{-2}$
²¹⁴ Bi	$4.01/10^{-1}$
²¹⁰ Tl	$1.15/10^{-4}$
²¹⁰ Pb	$2.07/10^{-4}$
Total	$4.62/10^{-1}$
²³² Th series	
²³² Th	$4.78/10^{-5}$
²²⁸ Ra	$5.45/10^{-5}$
²²⁸ Ac	$2.21/10^{-1}$
²²⁸ Th	$3.44/10^{-4}$
²²⁴ Ra	$2.14/10^{-3}$
²²⁰ Rn	$1.73/10^{-4}$
²¹² Pb	$2.77/10^{-2}$
²¹² Bi	$2.72/10^{-2}$
²⁰⁸ Tl	$3.26/10^{-1}$
Total	$6.04/10^{-1}$
⁴⁰ K	$4.17/10^{-2}$

*The values assume the establishment of radioactive equilibrium.

(Cited from ICRU Rep.53)

Chapter 6 Interpretation of measured results

The in-situ measurement is based on certain assumptions in the analysis in terms of the topography of the surrounding areas, installation height of the detector, etc.; thus, it is necessary to understand the impact on the analysis results if the actual conditions differ from these assumptions.

6.1 Implications of discrepancies between analytical and actual measurement conditions

6.1.1 Breadth of surrounding areas

The coefficients required for the calculation of radioactivity concentration from an in-situ measurement (ϕ/A in Equation 5.4 and the values in Table-1 and Table 5.4) assume an infinitely open and flat landscape (infinite plane) with no obstacles that attenuate gamma rays. In reality, however, it is impossible to expect such a perfect infinite plane; therefore, the analysis of radioactivity concentration based on this assumption of an infinite plane will result in underestimation. Figure 6.1 illustrates the peripheral contribution ratio in the gamma-ray fluence rate 1 m above the ground with an assumption that cesium-137 is exponentially distributed in the ground (β : 4.8 g/cm²). The contributions from the area of 10 m radius from the detector are equal to 85% of the total contribution in an infinite plane. The extent to which the fluence rate is underestimated because the measured area is not an infinite plane depends on the vertical profile of radioactive materials in the ground. To be more precise, it also depends on the gamma-ray energies. Details are given in Explanation F.1.

The underestimation may be corrected by the correction coefficients given in Table 6.1, provided that the area of radioactive deposition can be identified. However, in typical cases, the extent of the underestimation would be within some tens of percent, even if the correction is not applied. However, note that if β is 0.1 g/cm² and the deposition is confined within a small area of 10 m radius, correction must be considered as the result would be significantly underestimated.

To do this, measure the radioactive deposition area (an average radius) centering on the detector, using a tape measure, etc. and multiply the measured value of the concentration by the correction coefficient from Table 6.1. The correction coefficients included in Table 6.1 are applicable to gamma rays of 600 keV, and they can be used for gamma rays of other energies as the difference in the correction coefficients with respect to energy variation is not considerable. In cases where artificial radioactive materials as have been deposited as fallout for some time, and it is more likely to be on grasslands or bare grounds than tarmacked surfaces or buildings, then correction must be performed based on the area over grasslands, bare grounds, etc. When a deposition area cannot be identified, such as during the early stages of a nuclear accident, correction is difficult to achieve. Thus, it must be performed after the deposition has taken place.

However, note that correction is not obligatory if the in-situ measurement is for the purpose of fixed-point fluctuation surveillance.

Similarly, dose rate values need not be corrected as the differences in the breadth of surrounding areas have a little impact on dose rates.

6.1.2 Height of detector installation

The detector is normally installed at a height of 1 m; thus, correction is not necessary. The impact of the installation height of the detector on the measured value of radioactivity concentration is described in Explanation F.2.

6.1.3 Moisture in the ground

Moisture in the ground does not need correction, as it is included in the effects of the vertical distribution of radioactive materials in the ground (see Explanation E). The impact of the in-soil moisture on the measured value of radioactivity concentration is described in Explanation F.3.

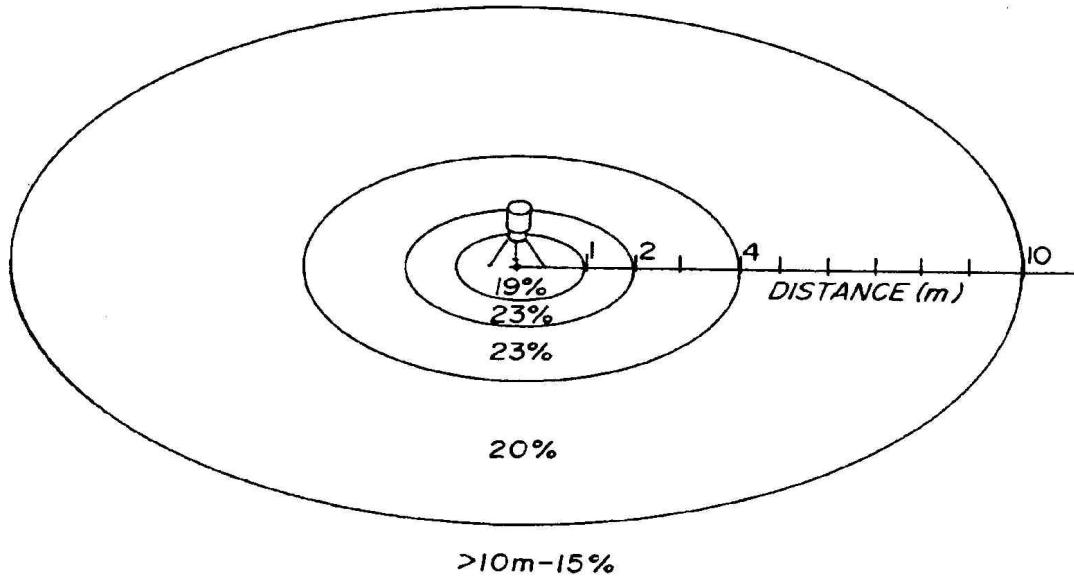


Figure 6.1 Peripheral contribution ratio in the gamma-ray fluence 1 m above ground with an assumption that cesium-137 is exponentially distributed in the ground (β : 4.8 g/cm²) (cited from HASL-300)

Table 6.1 Correction coefficients for the breadth of surrounding areas

Vertical profile parameter β (g/cm ²)	Area of radioactive deposition (radius: m)			
	10	15	20	25
0.100	1.6	1.4	1.3	1.2
1.00	1.3	1.2	1.1	1.1
3.00	1.2	1.1	1.1	1.1
10.0	1.1	1.1	1.0	1.0
4.8	1.2	1.1	1.1	1.0
∞ (homogeneous distribution)	1.1	1.0	1.0	1.0

6.2 Management of accuracy in measured result

6.2.1 Routine and periodical inspections

To achieve reliable measurement readings from in-situ measurement, it is desired that the following routine and periodical inspections are performed.

Daily inspection

- If the detector is cooled at all times, check the device temperature (if monitoring of the temperature is possible) and liquid nitrogen consumption (for liquid nitrogen cooling system only).
- Verify the energy resolution using a radiation source such as cobalt-60.

Periodical inspection

- Verify the peak efficiency (see 3.4.2).
- Take the detector in for a manufacturer servicing, etc.

6.2.2 Intercomparison measurement

As part of the measurement accuracy management to improve the reliability of in-situ measurement readings, the intercomparison measurement of measurement equipment is an effective method (see Explanation I). Urgent in-situ measurement in a nuclear disaster is well anticipated, and it is important to ascertain the equipment conditions regularly and routinely. If multiple devices of measuring equipment are employed in surveying a wide area for radioactive deposition distribution, it is advantageous to verify in advance that all pieces of equipment are equal in terms of measurement accuracy.

Explanation

Explanation A Calculation of peak efficiency by simulated calculation

Explanation A.1 Outline

It is possible to obtain the peak efficiency by simulation computing without using a standard point radiation source. For the computation, peak efficiency simulation software is often used, employing the MCNP Monte Carlo code, etc. By modeling the detector in preparation in terms of the relationship between the gamma-ray energy and geometrical conditions (distance, angle of incidence, etc.), it is possible to quickly prepare a peak efficiency that is compatible with a given energy, shape, and size of the sample.

However, it is different from the peak efficiency calibration using a traceability-ensured standard point radiation source, and it is desirable that the reliability of the simulation-computed peak efficiency be verified regularly by comparing it with the peak efficiency prepared based on a standard point radiation source.

For its use, give thorough consideration to the computing requirements, including the detector information, and verify the validity of the computing result thoroughly before using it with caution.

The simulation requires modeled data of the detector; thus, it is important to manage the detector such that its attributes are not altered. Specifically, it is desirable that a Ge detector be cooled at all times and managed such that its dead layer is not altered.

Explanation A.2 Comparison with the peak efficiency from a standard point radiation source

Table A.1 shows a comparison between the peak efficiency prepared using a standard point radiation source measured with a Ge detector of relative efficiency 30.1% (hereafter, “radiation source efficiency”) and peak efficiency based on simulation^{*1 *2} (hereafter, “simulation efficiency”).

Table A.1 Comparison between radiation source efficiency and simulation efficiency

(^1^)\Nuclides	(^2^)\Energy (keV)	(^3^)\Radiation source efficiency (A)	(^4^)\Simulation efficiency (B)	(^5^)\Ratio (B) / (A)
(^6^)\Am-241	59.5	1.729E-04	1.613E-04	0.933
(^9^)\Ba-133	81.0	1.676E-04	1.666E-04	0.994
(^10^)\Ba-133	356.0	8.353E-05	8.201E-05	0.982
(^13^)\Cs-137	661.7	5.119E-05	4.925E-05	0.962
(^14^)\Co-60	1173.2	3.060E-05	3.108E-05	1.016
(^15^)\Co-60	1332.5	2.715E-05	2.832E-05	1.043

In the energy range approximately between 60 and 1300 keV, the difference between the radiation source efficiency and simulation efficiency was approximately within 5%.

Using the spectrum from the in-situ measurement, the radioactivity concentration and dose rate were analyzed in terms of the uranium series, thorium series, ⁴⁰K, ¹³⁴Cs, and ¹³⁷Cs using their respective peak efficiencies. The comparison results are presented in Tables A.2 to A.6. Note that the nuclides analyzed of the uranium and thorium series are ²¹⁴Bi and ²¹⁴Pb for the former, and ²⁰⁸Tl and ²²⁸Ac for the latter.

Table A.2 Comparison of in-situ measurement spectrum analytical results (grassland 1 - β: 1.4 g/cm²)

(^23^)\Weight buffer depth β	1.4									
	(^24^)\Radiation source efficiency			(^25^)\Simulation efficiency				(^26^)\Ratio		
	(^27^)\(A)			(^28^)\(B)				(^29^)\(B) / (A)		
	(^30^)\Radioactivity concentration	(^31^)\Dose rate	(^32^)\Proportions of component nuclides	(^33^)\Radioactivity concentration	(^34^)\Dose rate	(^35^)\Proportions of component nuclides	(^36^)\Radio activity concentration	(^37^)\Dose rate	(^38^)\Proportions of component nuclides	
	(^39^)\nGy/h	(^40^)\%		(^41^)\nGy/h		(^42^)\%				
(^43^)\U series	(^44^)\-	3.7	7.2	(^45^)\-	3.3	6.3	(^46^)\-	0.89	0.87	
(^47^)\Th series	(^48^)\-	5.8	11.3	(^49^)\-	6.2	11.6	(^50^)\-	1.05	1.03	
(^51^)\K-40	1.99E-01 (^52^)\Bq/g	8.3	16.1	1.85E-01 (^53^)\Bq/g	7.7	14.5	0.93	0.93	0.90	
(^54^)\Cs-134	2.98E+09 (^55^)\Bq/k	12.4	24.0	3.18E+09 (^56^)\Bq/k	13.2	24.9	1.07	1.07	1.04	
(^57^)\Cs-137	1.32E+10 (^58^)\Bq/k	21.3	41.3	1.40E+10 (^59^)\Bq/k	22.6	42.7	1.06	1.06	1.03	

*1 For the simulation, peak efficiency simulation software (calculation code: MCNP Monte Carlo code^{*2}) was used.

*2 Briesmeister, J. F., “MCNP-A General Monte Carlo N-particle Transport Code Version 4C”, Los Alamos National Laboratory Report LA-13709-M (2000)

Table A.3 Comparison of in-situ measurement spectrum analytical results (gravel - β : 1.4 g/cm²)

	(^85^A)Radiation source efficiency			(^86^A)Simulation efficiency			(^87^A)Ratio		
	(^88^A)(A)			(^89^A)(B)			(^90^A)(B) / (A)		
	(^91^A)Radioactivity concentration	(^92^A)Dose rate	(^93^A)Proportions of component nuclides	(^94^A)Radioactivity concentration	(^95^A)Dose rate	(^96^A)Proportions of component nuclides	(^97^A)Radioactivity concentration	(^98^A)Dose rate	(^99^A)Proportions of component nuclides
	(^100^A) nGy/h	(^101^A) %		(^102^A) nGy/h	(^103^A) %				
(^104^A)U series	(^105^A)-	37.1	36.4	(^106^A)-	36.6	34.8	(^107^A)-	0.99	0.96
(^108^A)Th series	(^109^A)-	34.8	34.1	(^110^A)-	37.1	35.3	(^111^A)-	1.07	1.03
(^112^A)K-40	1.09E-01 (^113^A)Bq/g	4.5	4.4	1.01E-01 (^114^A)Bq/g	4.2	4.0	0.93	0.93	0.90
(^115^A)Cs-134	2.22E+09 (^116^A)Bq/km ²	9.2	9.0	2.37E+09 (^117^A)Bq/km ²	9.8	9.4	1.07	1.07	1.03
(^118^A)Cs-137	1.01E+10 (^119^A)Bq/km ²	16.3	16.0	1.07E+10 (^120^A)Bq/km ²	17.4	16.5	1.06	1.06	1.03
(^121^A)Total	(^122^A)-	102.0	(^123^A)-	(^124^A)-	105.1	(^125^A)-	(^126^A)-	(^127^A)-	(^128^A)-

Table A.4 Comparison of in-situ measurement spectrum analytical results (tarmacked - β : 1.4 g/cm²)

	(^146^A)Radiation source efficiency			(^147^A)Simulation efficiency			(^148^A)Ratio		
	(^149^A)(A)			(^150^A)(B)			(^151^A)(B) / (A)		
	(^152^A)Radioactivity concentration	(^153^A)Dose rate	(^154^A)Proportions of component nuclides	(^155^A)Radioactivity concentration	(^157^A)Proportions of component nuclides	(^158^A)Radioactivity concentration	(^159^A)Dose rate	(^160^A)Proportions of component nuclides	
	(^161^A)nGy/h	(^162^A) %		(^163^A)nGy/h	(^164^A) %				
(^165^A)U series	(^166^A)-	10.1	20.7	(^167^A)-	9.7	20.0	(^168^A)-	0.96	0.96
(^169^A)Th series	(^170^A)-	10.9	22.3	(^171^A)-	11.6	23.8	(^172^A)-	1.06	1.06
(^173^A)K-40	4.00E-01 (^174^A)Bq/g	16.7	34.0	3.71E-01 (^175^A)Bq/g	15.5	31.7	0.93	0.93	0.93
(^176^A)Cs-134	9.85E+08 (^177^A)Bq/km ²	4.1	8.4	1.05E+09 (^178^A)Bq/km ²	4.4	8.9	1.07	1.07	1.07
(^179^A)Cs-137	4.43E+09 (^180^A)Bq/km ²	7.2	14.6	4.72E+09 (^181^A)Bq/km ²	7.6	15.6	1.06	1.06	1.07
(^182^A)Total	(^183^A)-	49.0	(^184^A)-	(^185^A)-	48.8	(^186^A)-	(^187^A)-	(^188^A)-	(^189^A)-

Table A.5 Comparison of in-situ measurement spectrum analytical results (grassland 2 - β : 1.4 g/cm²)

	(^207^A)Radiation source efficiency			(^208^A)Simulation efficiency			(^209^A)Ratio		
	(^210^A)(A)			(^211^A)(B)			(^212^A)(B) / (A)		
	(^213^A)Radioactivity concentration	(^214^A)Dose rate	(^215^A)Proportions of component nuclides	(^216^A)Radioactivity concentration	(^217^A)Dose rate	(^218^A)Proportions of component nuclides	(^219^A)Radioactivity concentration	(^220^A)Dose rate	(^221^A)Proportions of component nuclides
	(^222^A)nGy/h	(^223^A) %		(^224^A)nGy/h	(^225^A) %				
(^226^A)U series	(^227^A)-	8.3	17.9	(^228^A)-	7.8	16.6	(^229^A)-	0.94	0.93
(^230^A)Th series	(^231^A)-	8.2	17.7	(^232^A)-	8.7	18.4	(^233^A)-	1.06	1.04
(^234^A)K-40	1.99E-01 (^235^A)Bq/g	8.3	17.8	1.84E-01 (^236^A)Bq/g	7.7	16.3	0.93	0.93	0.91
(^237^A)Cs-134	1.88E+09 (^238^A)Bq/km ²	7.8	16.8	2.00E+09 (^239^A)Bq/km ²	8.3	17.6	1.07	1.07	1.05
(^240^A)Cs-137	8.53E+09 (^241^A)Bq/km ²	13.8	29.7	9.07E+09 (^242^A)Bq/km ²	14.7	31.1	1.06	1.06	1.05
(^243^A)Total	(^244^A)-	46.4	(^245^A)-	(^246^A)-	47.2	(^247^A)-	(^248^A)-	(^249^A)-	(^250^A)-

Table A.6 Comparison of in-situ measurement spectrum analytical results (concrete (basement inside a building) - β : 1.4 g/cm²)

	(^268^)^Radiation source efficiency			(^269^)^Simulation efficiency			(^270^)^Ratio		
	(^271^)^(A)			(^272^)^(B)			(^273^)^(B) / (A)		
	(^274^)^Radioactivity concentration	(^275^)^Dose rate	(^276^)^Proportions of component nuclides	(^277^)^Radioactivity concentration	(^278^)^Dose rate	(^279^)^Proportions of component nuclides	(^280^)^Radioactivity concentration	(^281^)^Dose rate	(^282^)^Proportions of component nuclides
	(^283^)^mGy.h	(^284^)^%		(^285^)^mGy.h	(^286^)^%				
(^287^)^U series	(^288^)^-	19.8	25.7	(^289^)^-	19.8	25.9	(^290^)^-	1.00	1.01
(^291^)^Th series	(^292^)^-	25.6	33.3	(^293^)^-	27.3	35.7	(^294^)^-	1.06	1.07
(^295^)^K-40	7.57E-01 (^296^)^Bq/g	31.6	41.0	7.03E-01 (^297^)^Bq/g	29.3	38.4	0.93	0.93	0.94
(^298^)^Cs-134	(^299^)^- (^300^)^Bq/km2	(^301^)^-	(^302^)^-	(^303^)^- (^304^)^Bq/km2	(^305^)^-	(^306^)^-	(^307^)^-	(^308^)^-	(^309^)^-
(^310^)^Cs-137	(^311^)^- (^312^)^Bq/km2	(^313^)^-	(^314^)^-	(^315^)^- (^316^)^Bq/km2	(^317^)^-	(^318^)^-	(^319^)^-	(^320^)^-	(^321^)^-
(^322^)^Total	(^323^)^-	76.9	(^324^)^-	(^325^)^-	76.3	(^326^)^-	(^327^)^-	(^328^)^-	(^329^)^-

In each analysis, the discrepancies in the radioactivity concentration and dose rate are approximately within 10%. It is important that the employment of simulation efficiency is regularly accompanied by the verification of analytical results based on radiation source efficiency.

Explanation B Measurable ranges and measuring times for in-situ measurement

Explanation B.1 Detectable levels (minimum) and measuring time

Assuming the detectable level to three times the counting error, the detectable levels under the following conditions are listed in Table B.1.

- Cesium-137 is distributed on the ground (infinite plane)
- Ge detector with 25% relative efficiency is employed
- Background reading is equal to the average level in Japan (dose rate: 50 nGy/h)

Table B.1 Examples of detectable levels

Measuring time (min)	Detectable levels for ¹³⁷ Cs	
	Radioactivity concentration (kBq/m ²)	Dose rate (nGy/h)
1	0.34	0.87
5	0.13	0.32
10	0.09	0.22
20	0.06	0.15
30	0.05	0.12
60	0.03	0.08

The detectable levels of cesium-137 fluctuate depending on the contributions of other radionuclides. The values indicated here are for reference purposes only.

Note that the detectable level (radioactivity) for measuring in-situ for 60 min is almost equivalent to the level of measuring for 10 h using a Marinelli beaker in a laboratory. The detectable level (dose rate) is approximately 1/1000 of 1 mSv/year (equivalent to approximately 140 nGy/h).

Explanation B.2 Upper limit in measurement

Measuring in places of high dose rates is expected to have the risk of underestimation of radioactivity concentration because of increased photon injections, resulting in increased dead time and leading to counting losses and/or pulse pile-ups. Additionally, from the viewpoint of personnel exposure to radiation, it is necessary to set an upper limit to determine whether to pursue the in-situ measurement. Based on general MCA performance, when the number of incident photons (Input Count Rate) increases to a certain level, the number of photons detected (Throughput Count Rate) decreases (Figure B.1), the resolution increases (Figure B.2), and the dead time also increases (Figure B.3). If the dead time grows in proportion (100 – % Live time), the error in measuring the peak area also increases (Figure B.4).

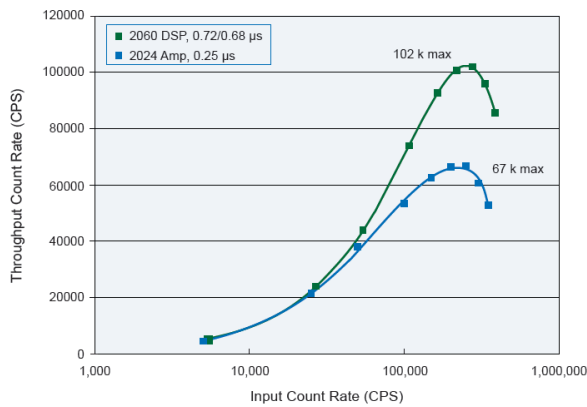


Figure B.1 Relationship between Input Count Rate and Throughput Count Rate^{*1}

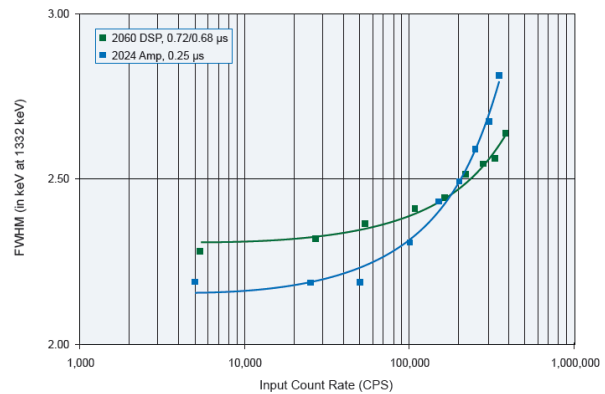


Figure B.2 Relationship between Input Count Rate and FWHM^{*1}

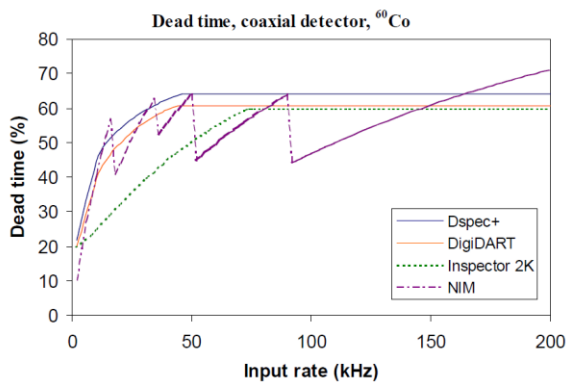


Figure B.3 Relationship between Input Rate and dead time^{*2}

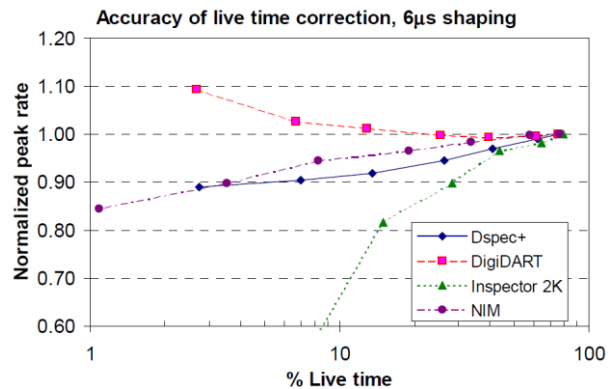


Figure B.4 Relationship between % live time and peak area^{*2} (dead time = 100 – % live time)

It is difficult to determine the feasibility of in-situ measurement by the input count rate on site; it is better in practice if the judgment reference is provided before conducting the in-situ measurements. Given this, we considered setting an upper limit using the dose rate previously measured on the same

^{*1} “Performance of Digital Signal Processors for Gamma Spectrometry,” Canberra Industries, Inc., Application Note (2008)

^{*2} “Comparisons of the Portable Digital Spectrometer Systems,” Duc T. Vo, Phyllis A. Russo, LA-13895-MS, Los Alamos NATIONAL LABORATORY (2002)

site with a survey meter. Figure B.5 illustrates the relationship between the dose rate measured with the survey meter and the in-situ Ge dead time based on readings taken in Fukushima prefecture (date of measurement: August to September 2012; taken in-situ by one Ge detector of the same model).

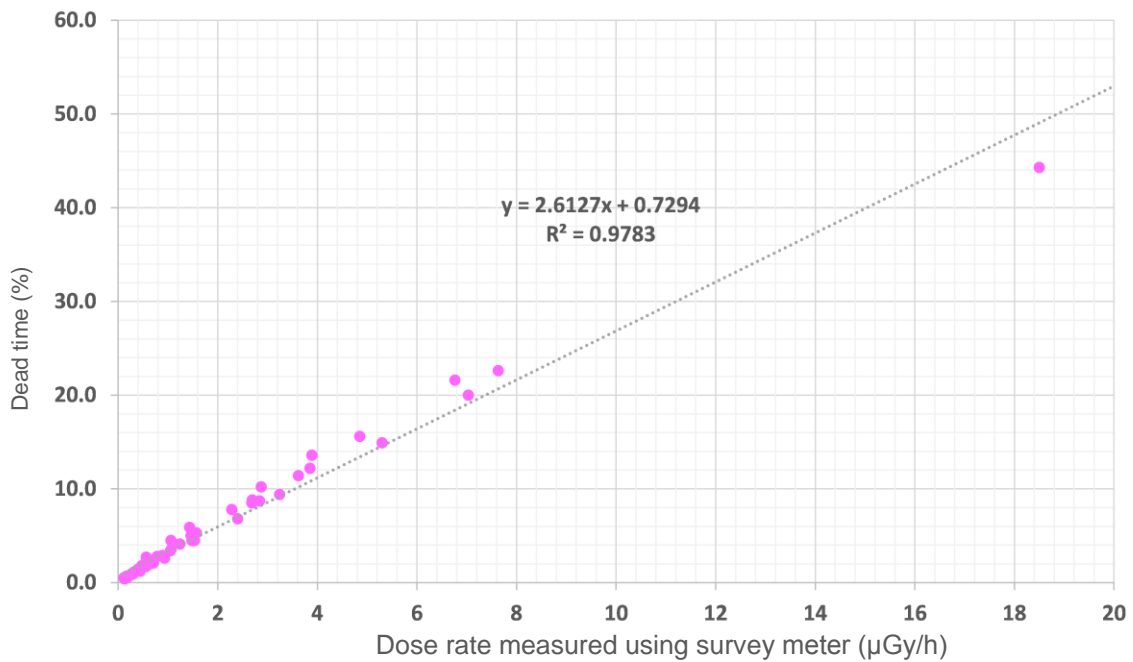


Figure B.5 Relationship between dose rate by survey meter and in-situ Ge detector dead time

Based on the results shown in Figure B.5 and the following conditions, the relationships between the dose rates measured with a survey meter, dead time, and measuring time are organized in Table B.2.

- Measuring time: 30 min
- Ge detector with 20.6% relative efficiency is employed

Table B.2 Relationships between dose rate by survey meter, dead time, and measuring time

Dose rate measured using survey meter (μGy/h)	Dead time (%)	Measuring time (min)
1	3	31
5	14	35
10	27	41
15	40	50
20	53	64

According to Table B.2, the dead time is expected to reach approximately 50% if the survey-meter dose rate is 20 $\mu\text{Gy/h}$. A dead time of 50% means that the required measurement time doubles. From the viewpoints of work efficiency and personnel exposure, it is not realistic to pursue a measurement in places where the dead time exceeds this level; thus, the upper limit was set at 20 $\mu\text{Gy/h}$. The processing time varies between detector models. Thus, the upper limit indicated here is only provided as a guide.

As stated above, measurements at locations of high dose rates are likely to suffer from increased dead time due to counting losses and pulse pile-ups, resulting in fewer photons detected (Throughput Count Rate) with respect to the number of incident photons (Input Count Rate).

Meanwhile, the peak counts of target artificial radionuclides will increase, which makes it possible that a relatively short measuring time may ensure sufficiently accurate readings if they are the sole target for measuring. Therefore, based on the comprehensive consideration of the nuclides to measure, measurement accuracy, and personnel safety, it is important to set limits to the maximum dose rate and the measuring time. As for the relationship between the measuring time and measurement accuracy in locations of high dose rates, it is described in Explanation B.3.

Explanation B.3 Relationship between measuring time and measurement accuracy in locations of high dose rates

Measurements taken at locations of high dose rates are expected to have sufficient accuracy with short measuring time, owing to increased numbers of peak counts for target artificial radionuclides.

We considered the following data measured in Fukushima prefecture. Figure B.6 shows an in-situ measurement spectrum, and Figure B.7 illustrates the relative counting errors of the detected artificial radionuclides.

Data measured in Fukushima prefecture (measured on December 27, 2011)

Real time: 4478.5 s. Live time: 3600 s. DT: 32.7%

Dose rate: 6 μ SV/h

^{134}Cs : $8.0 \times 10^5 \text{ Bq/m}^2$, ^{137}Cs : $9.3 \times 10^5 \text{ Bq/m}^2$, $^{110\text{m}}\text{Ag}$: $3.5 \times 10^3 \text{ Bq/m}^2$

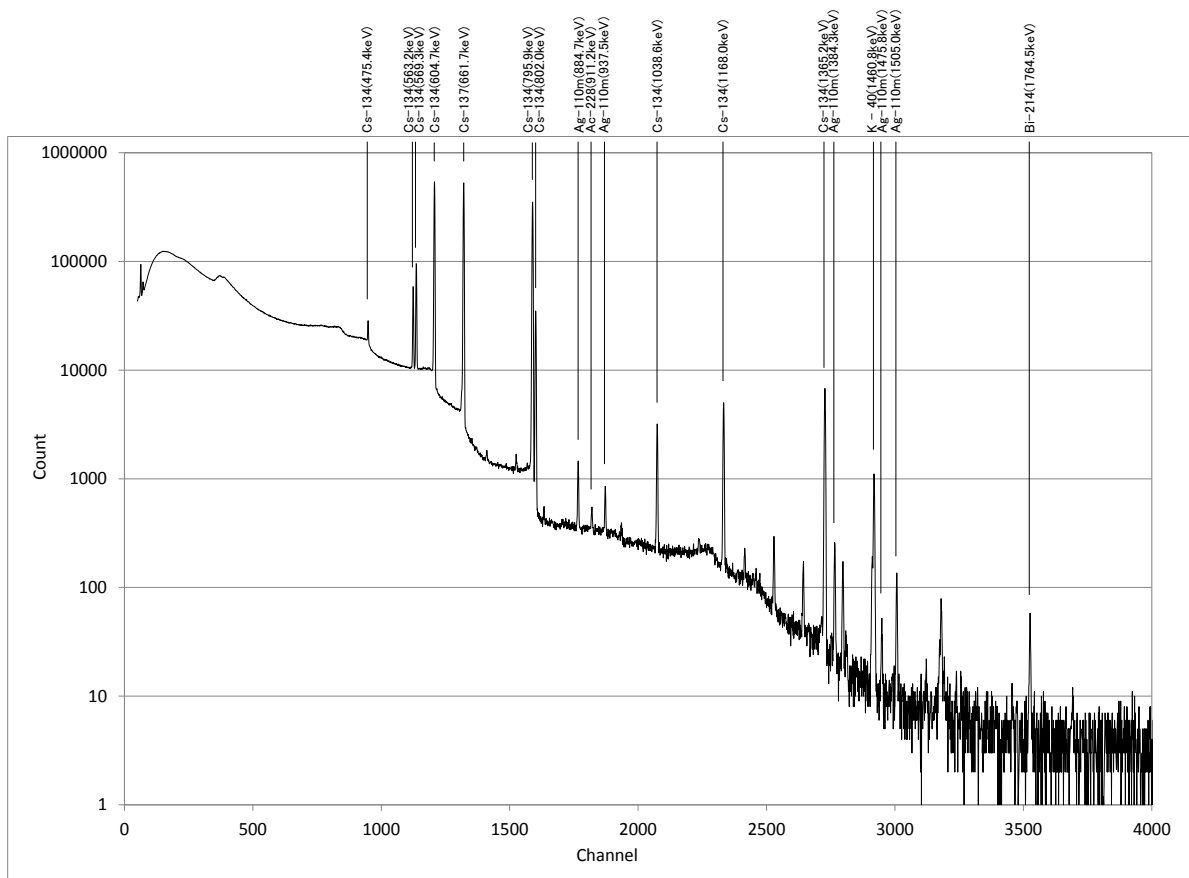
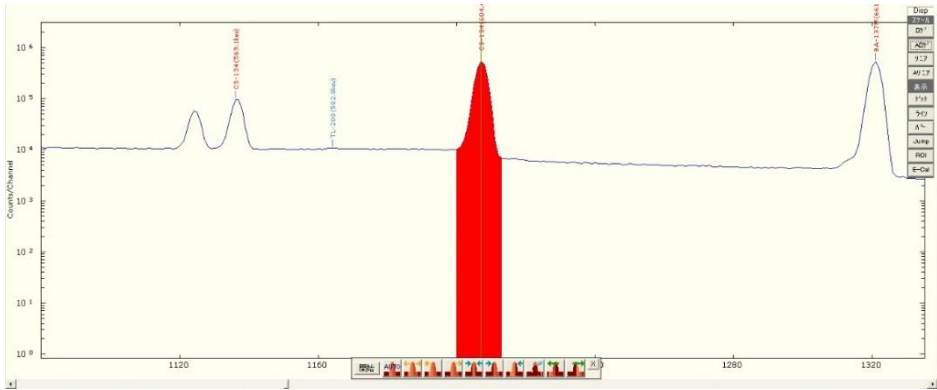


Figure B.6 Example of spectrum acquired by in-situ measurement

○ ^{134}Cs (605 keV) (measured for 1 h)

Total count: 2023934 Net count: 1906609 Base count: 117325

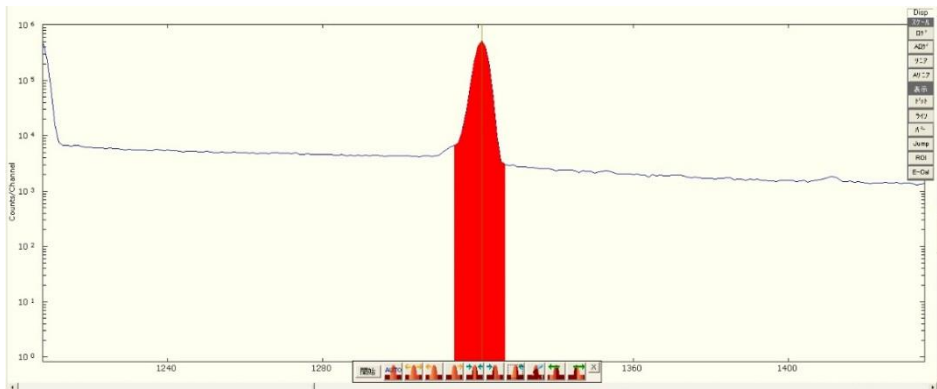
Counting error: 1463.3 Relative counting error: 0.077%



○ ^{137}Cs (662 keV) (measured for 1 h)

Total count: 1971520 Net count: 1906912 Base count: 64608

Counting error: 1426.9 Relative counting error: 0.075%



○ $^{110\text{m}}\text{Ag}$ (885 keV) (measured for 1 h)

Total count: 9098 Net count: 4714 Base count: 4384

Counting error: 116.1 Relative counting error: 2.5%

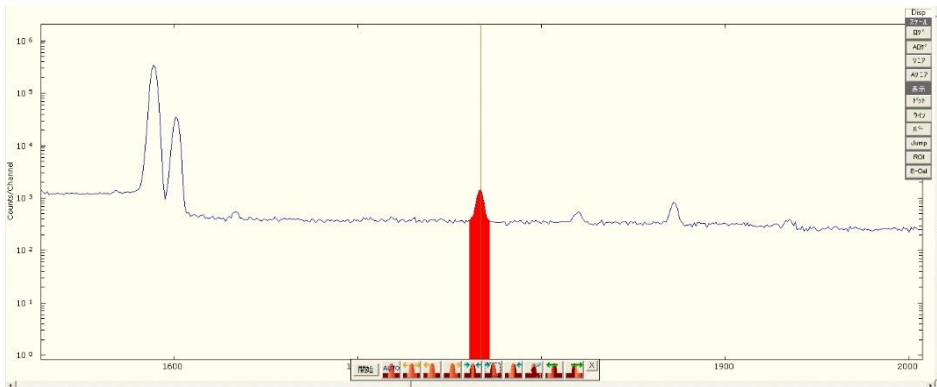


Figure B.7 Relative counting errors of detected artificial radionuclides

As seen in Figure B.7, the relative counting error of ^{137}Cs measured at a location with a dose rate of $6\ \mu\text{Gy/h}$ for 1 h is 0.075%, which is more than sufficient in terms of statistical accuracy. Based on this measurement data, we evaluated the fluctuation of the measurement accuracy by varying the measuring time, which is illustrated in Figure B.8.

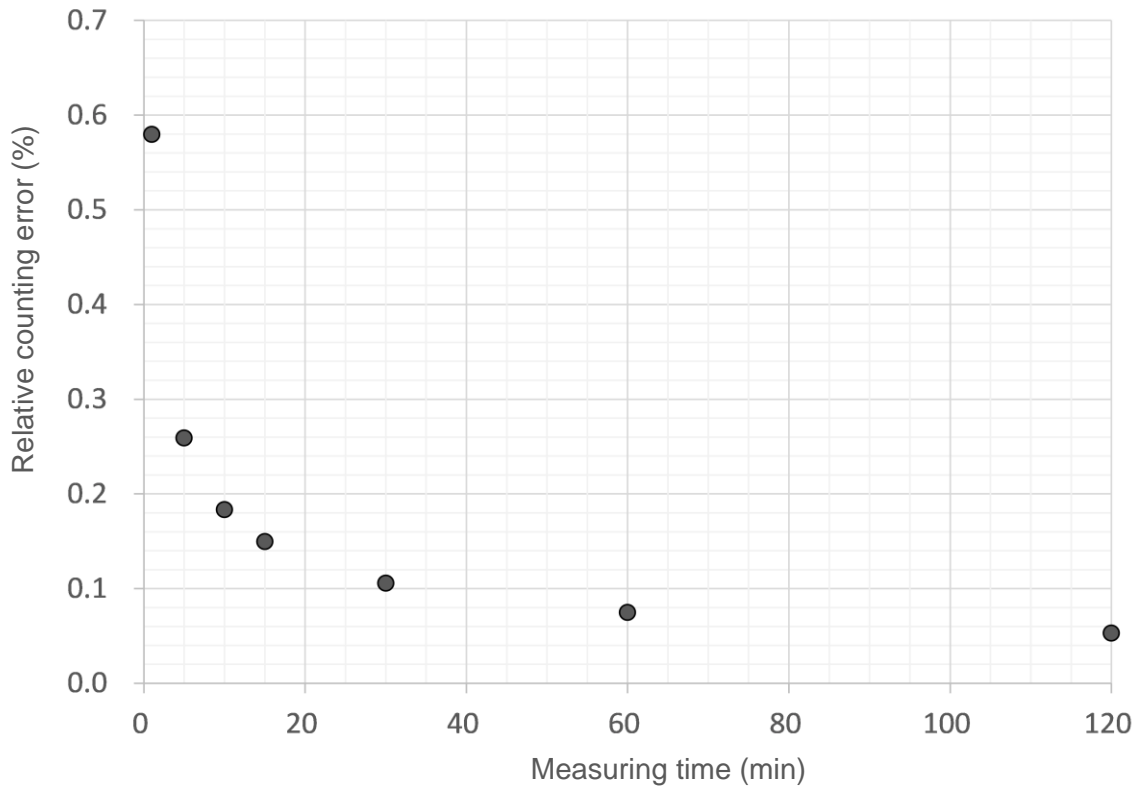
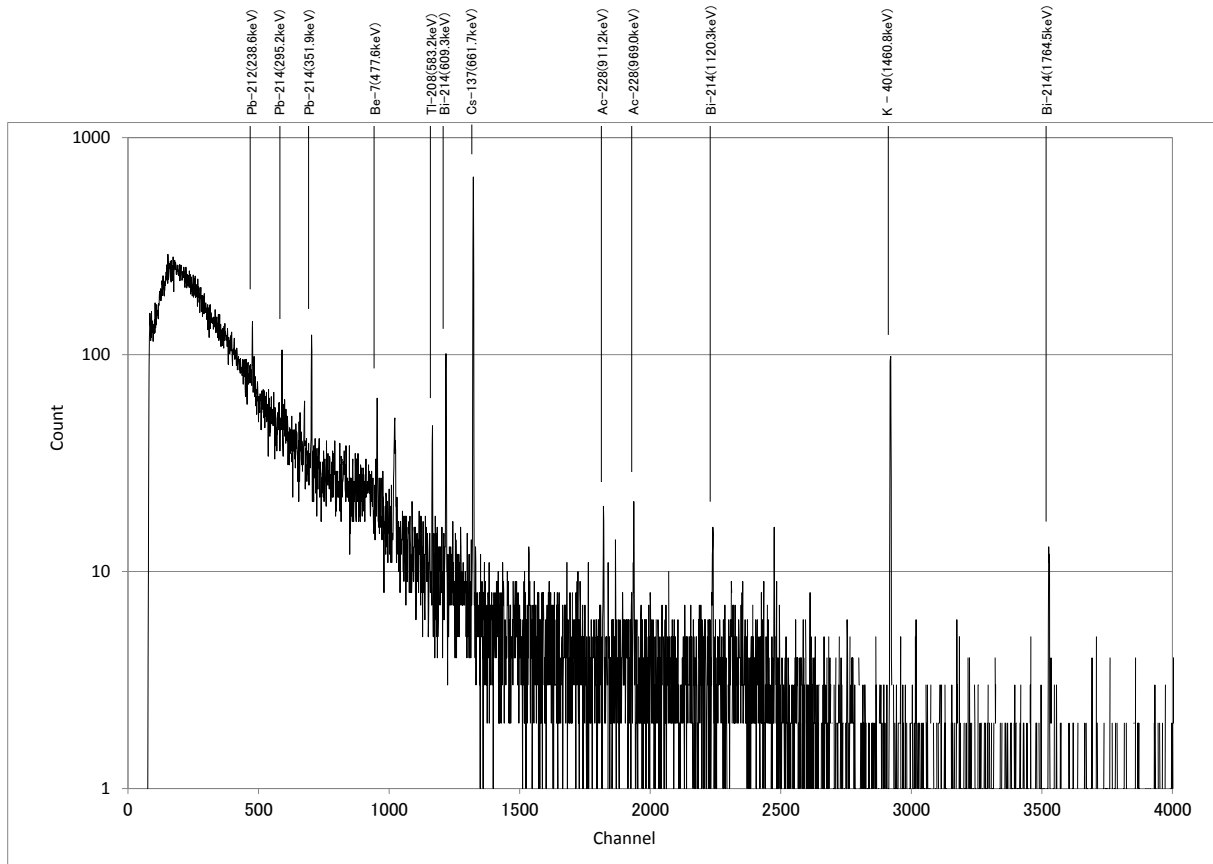


Figure B.8 Relationship between measuring time and relative counting error of ^{137}Cs

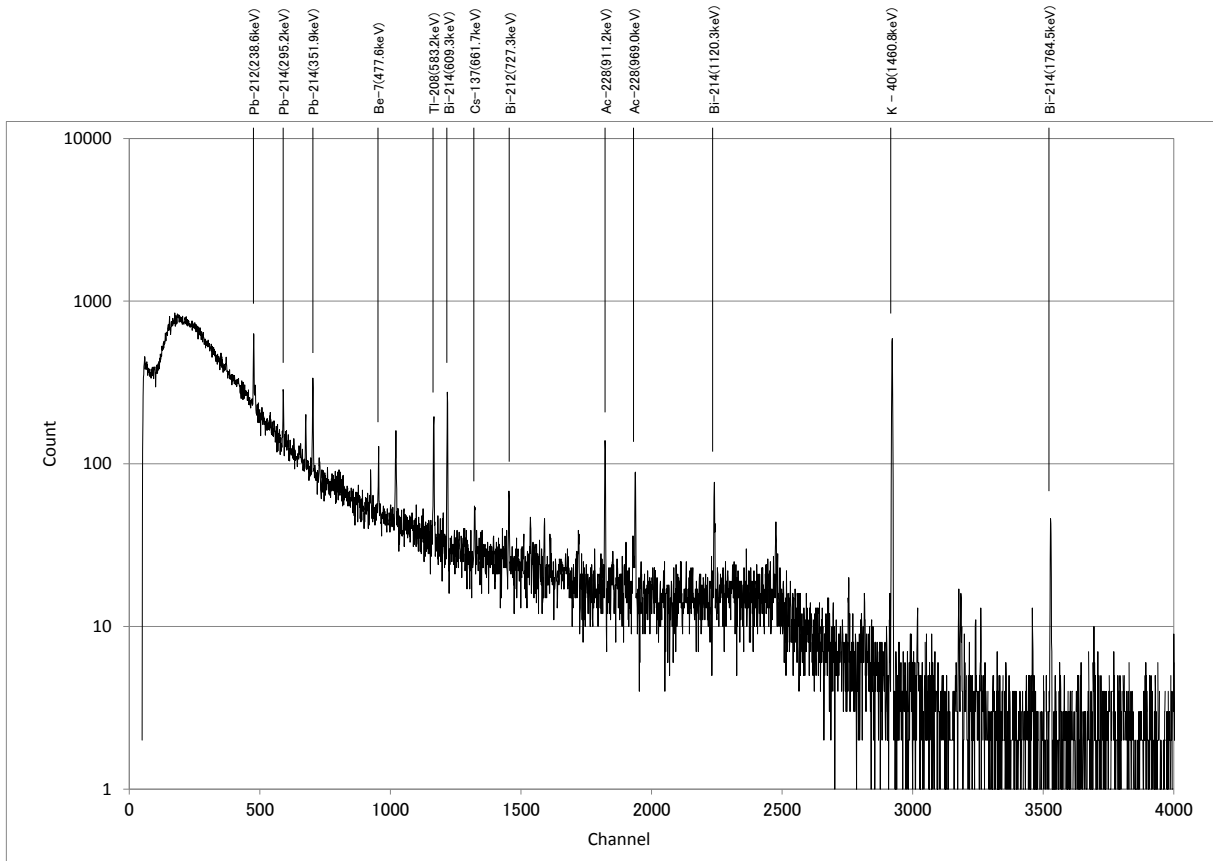
Based on Figure B.8, in locations where the dose rate is as high as $6\ \mu\text{Gy/h}$, a measurement of a few minutes yields a reading with a relative counting error of 1% or lower, which is considered sufficient to ensure statistical accuracy. As longer measuring time to increase the accuracy of the measurement necessarily increases the personnel exposure, it is important to switch to short-period measurements, in contrast to nonemergency situations.

Explanation C Example of spectrum by in-situ measurement

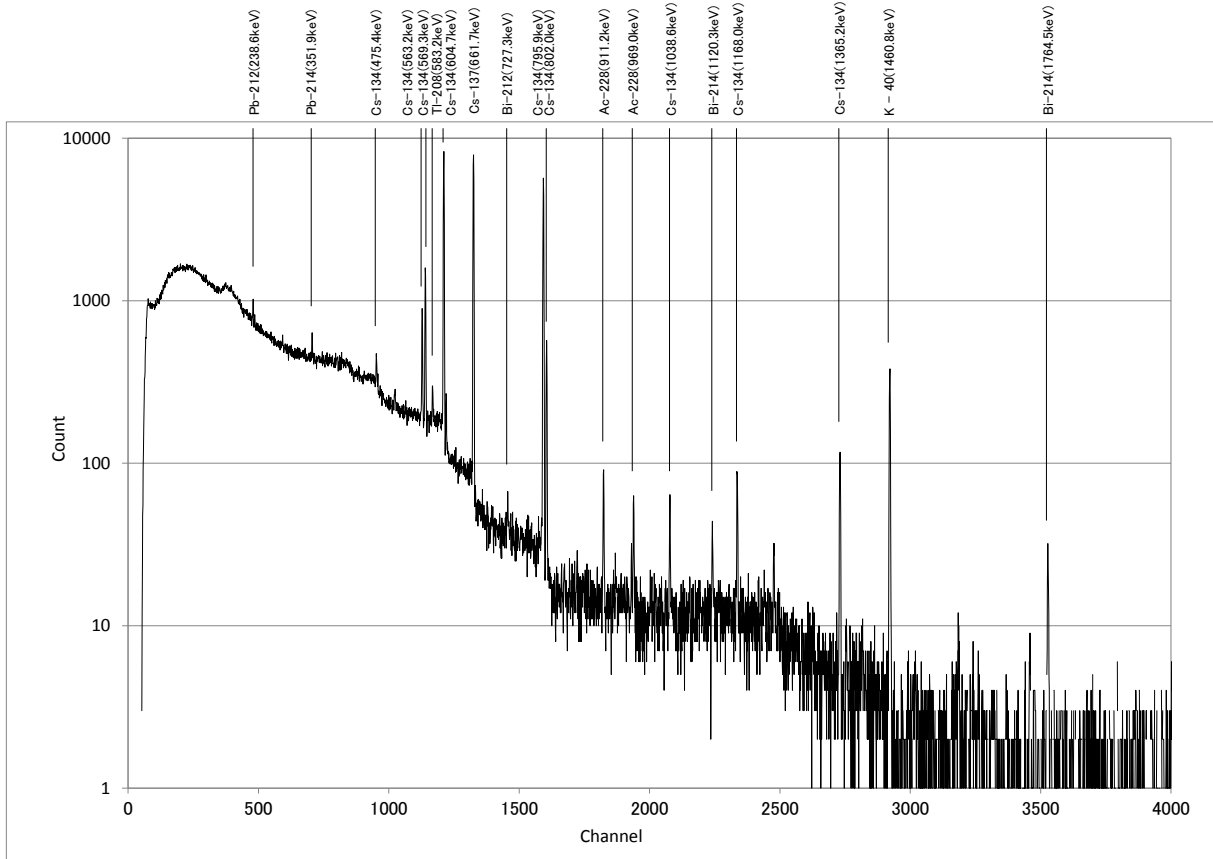
Spectrum measured in the vicinity of Mt. Fuji (March 7, 2001)



Spectrum measured in Chiba prefecture before the Fukushima Dai-ichi Nuclear Accident (December 2, 2010)

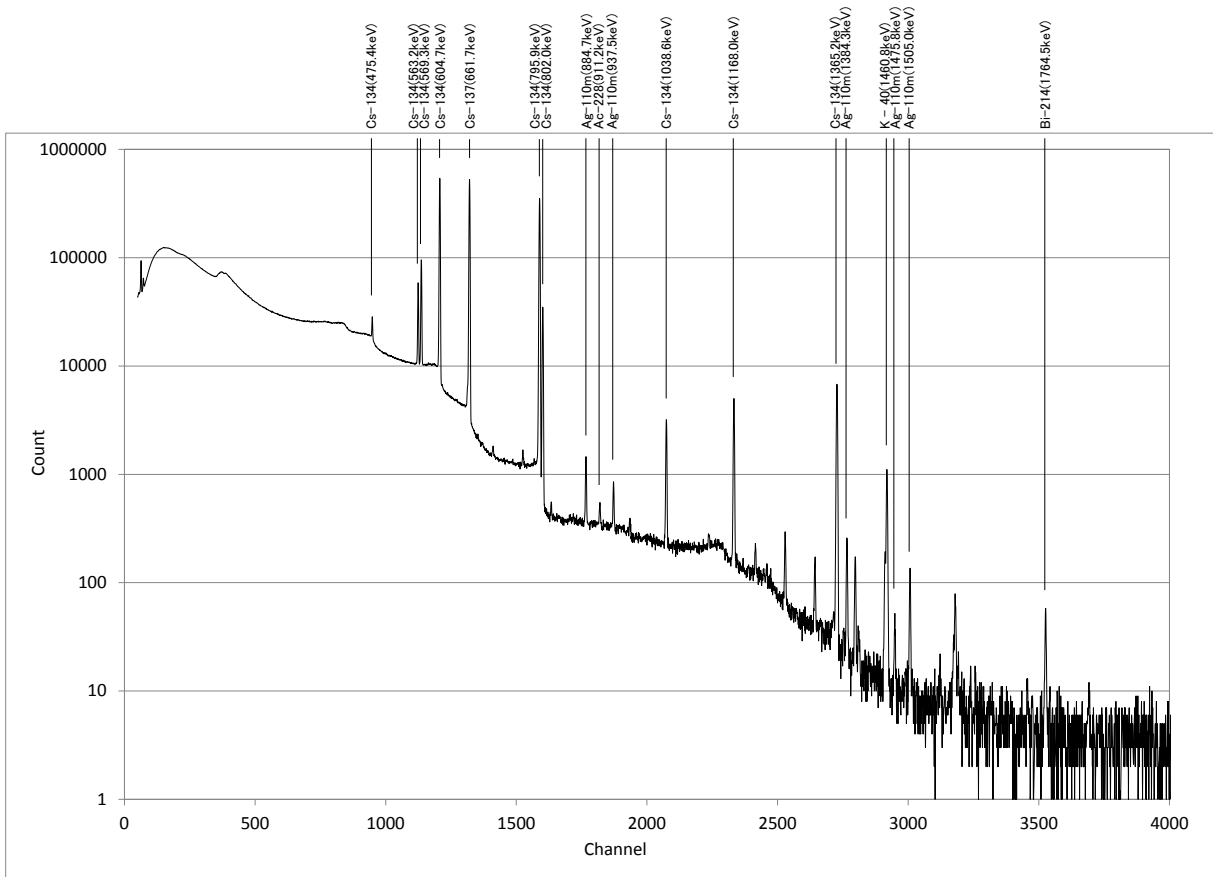


Spectrum measured in Chiba prefecture nine months after the Fukushima Dai-ichi Nuclear Accident (December 7, 2011)

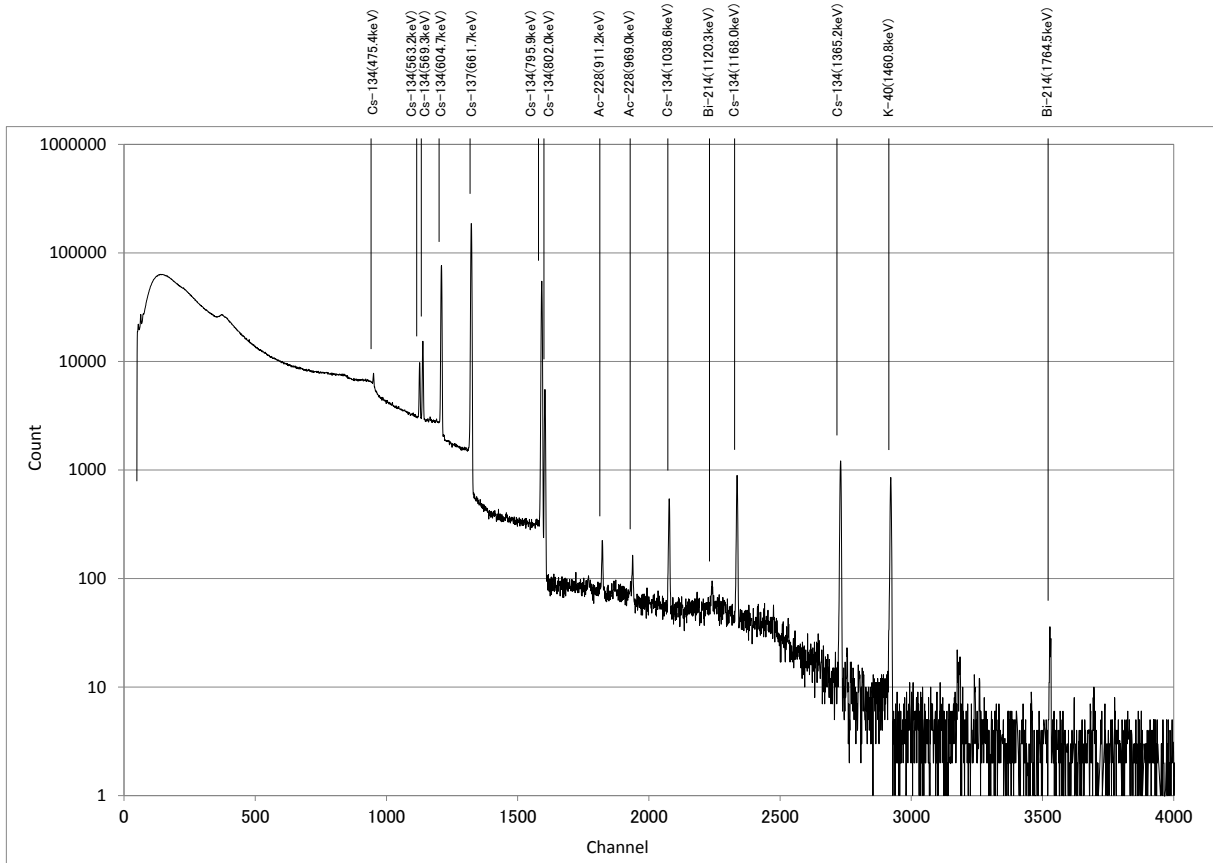


Spectrum measured in Fukushima prefecture nine months after the Fukushima Dai-ichi Nuclear

Accident (December 27, 2011)

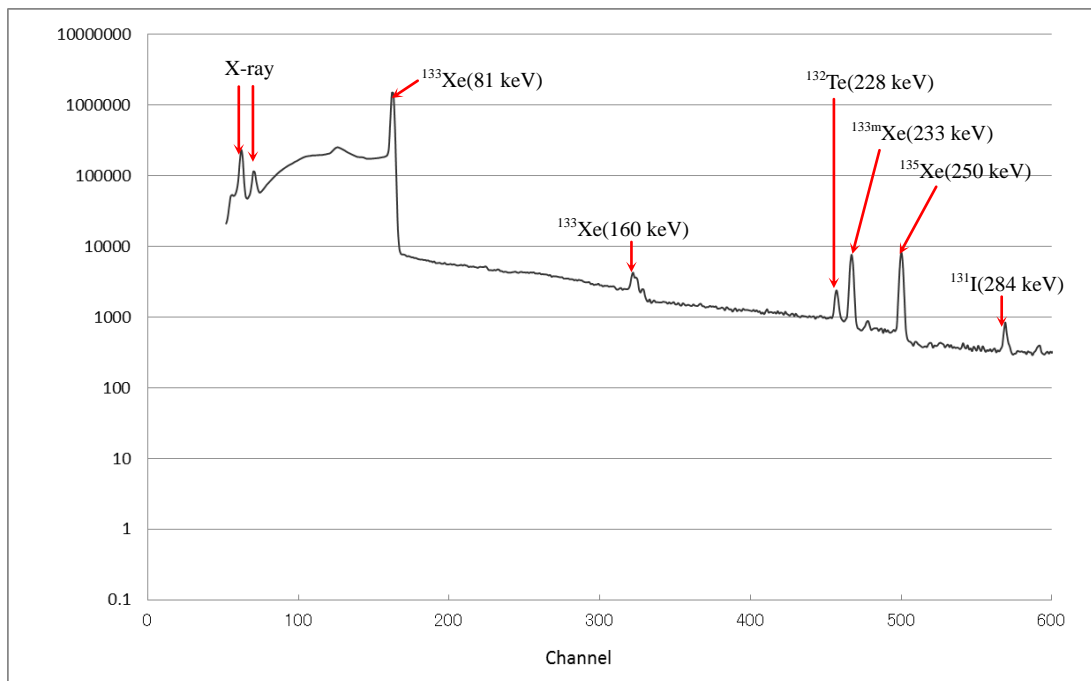
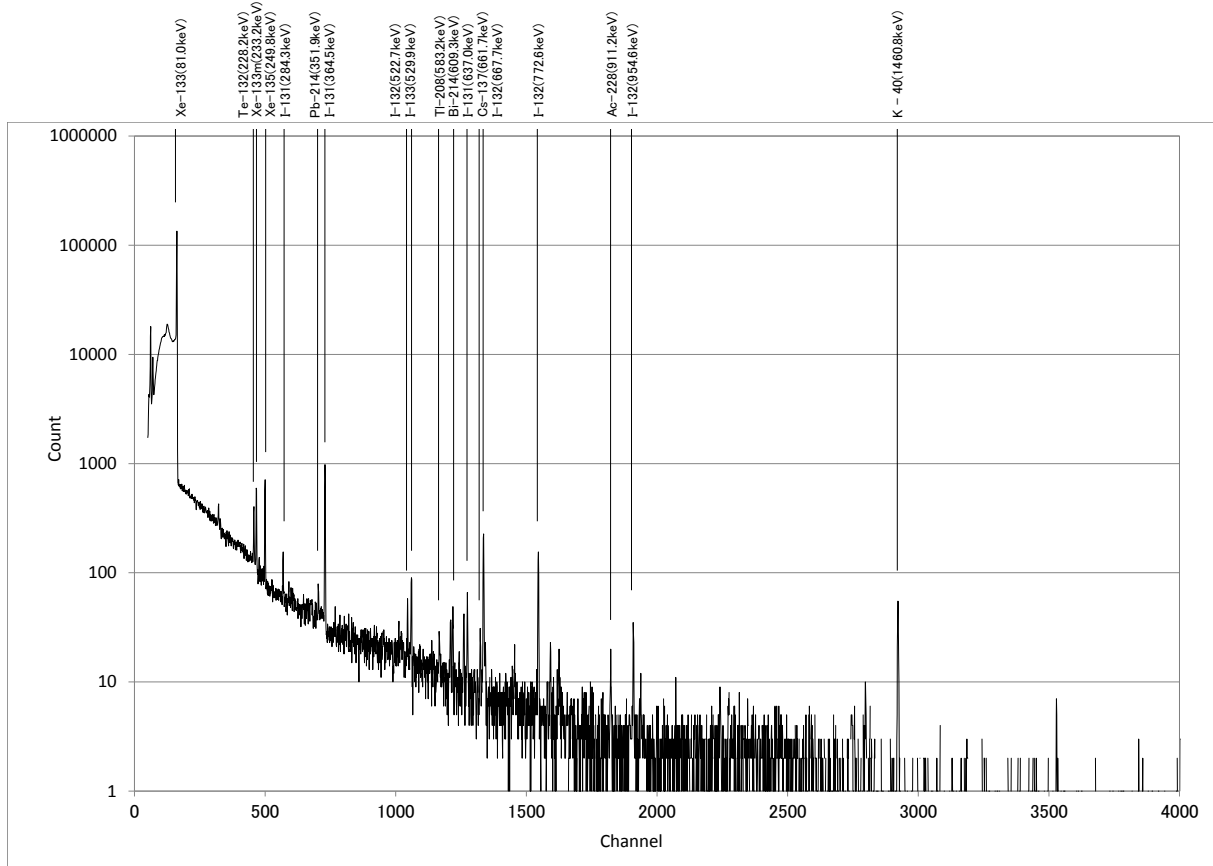


Spectrum measured in Fukushima prefecture three years and eight months after the Fukushima Dai-ichi Nuclear Accident (November 27, 2011)



- Spectrum measured in Chiba prefecture in the traversing plume caused by the Fukushima Dai-ichi

Nuclear Accident (March 15, 2011) (measurement taken by a fixed in-situ Ge detector installed outdoor in an upright position)



For measuring a plume, it is possible to calculate the radioactivity concentration and dose rate, assuming that radionuclides are evenly distributed in the air.

Explanation D Energy calibration in a nuclear disaster

In a nuclear accident, a large quantity of artificial radionuclides released during the accident is expected to increase the Compton continuum count. The radionuclides listed in Table D.1, especially those in the low-energy region, cannot be confirmed by their peaks; therefore, these may not be suitable for energy calibration (Figure D.1). If this is the case, it may be necessary to consider using the peaks of the artificial radionuclides emitted through the accident, as seen in Table D.2.

Table D.1 Naturally occurring radionuclides usable for energy calibration and their gamma-ray energies

Nuclides	Gamma-ray energy (keV)	Emission ratio*
²¹² Pb	239	0.434
²¹⁴ Pb	352	0.369
²⁰⁸ Tl	583	0.306
²¹⁴ Bi	609	0.469
²²⁸ Ac	911	0.290
⁴⁰ K	1461	0.107
²⁰⁸ Tl	2615	0.359

*For ²³⁸U and ²³²Th series, per-decay emission rates of the parent nuclides are shown (cited from ICRU Rep. 53, Table 3.4)

Table D.2 Artificial radionuclides usable for energy calibration in a nuclear accident and their gamma-ray energies

Nuclides	Gamma-ray energy (keV)	Emission ratio
¹³⁴ Cs	605	0.975
¹³⁷ Cs	662	0.849
¹³⁴ Cs	796	0.851
^{110m} Ag	885	0.729
^{110m} Ag	1384	0.243
^{110m} Ag	1505	0.131

(cited from ICRU Rep. 53, Table A.1)

Data measured in Fukushima prefecture (measured on December 27, 2011)

Real time: 4478.5 s. Live time: 3600 s. DT: 32.7%

Dose rate: 6 μ SV/h

^{134}Cs : $8.0 \times 10^5 \text{ Bq/m}^2$, ^{137}Cs : $9.3 \times 10^5 \text{ Bq/m}^2$, $^{110\text{m}}\text{Ag}$: $3.5 \times 10^3 \text{ Bq/m}^2$

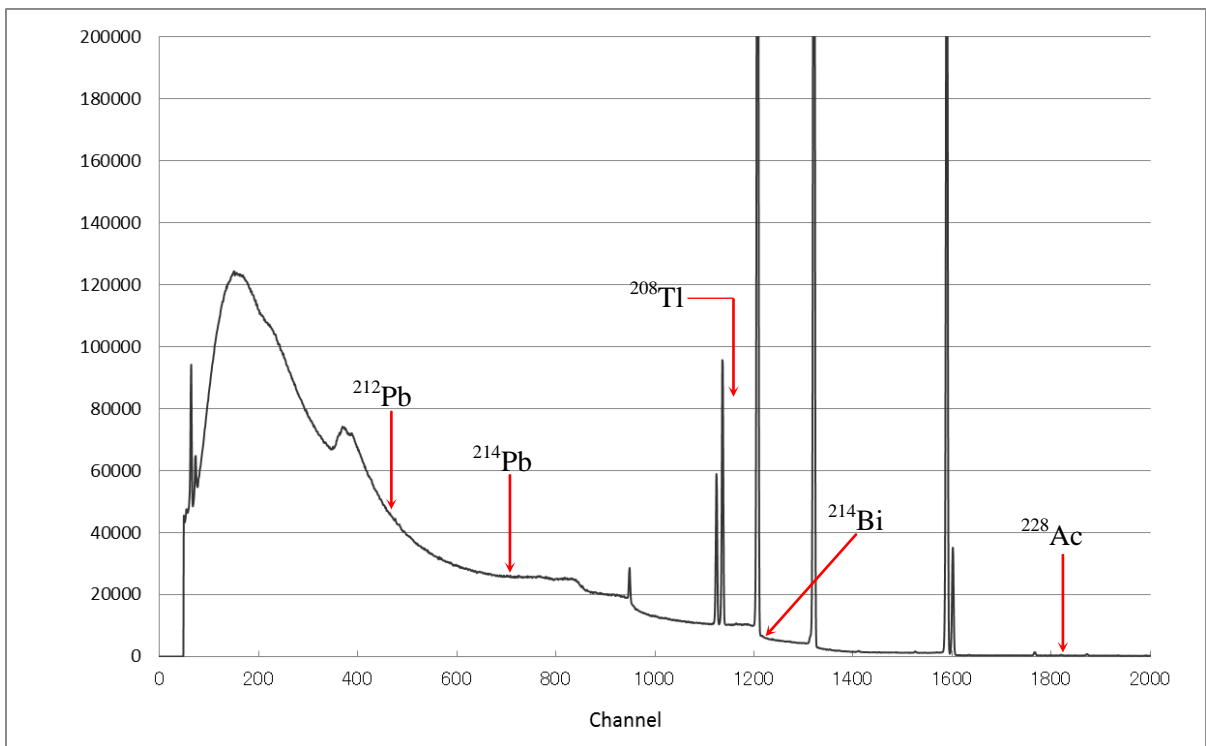
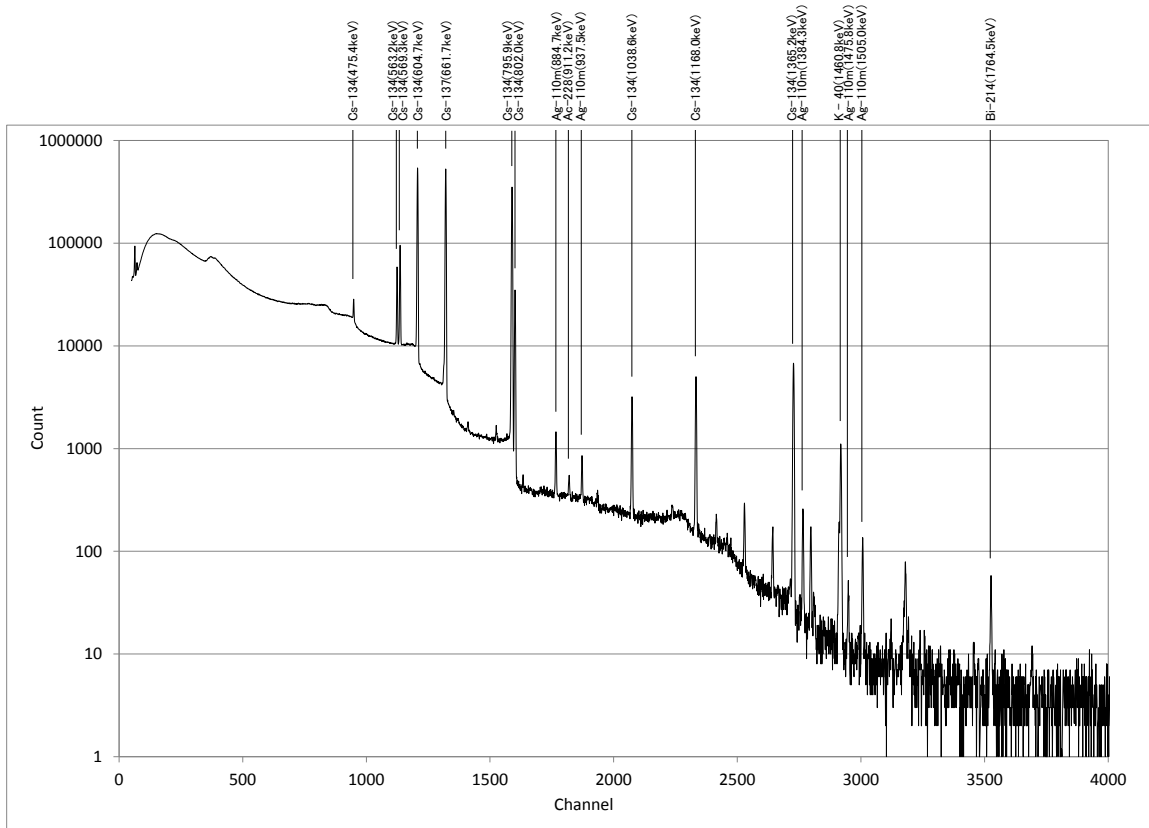


Figure D.1 Natural radionuclides not usable for energy calibration

Explanation E Vertical profile of radioactive materials in the ground

Explanation E.1 Evaluation of vertical profile parameter β

Although an accurate understanding of β , a parameter to indicate a vertical profile of radioactive materials in the ground, is the most effective way to improve the reliability of in-situ measurements, it is not easy to attain an accurate evaluation of β as it significantly fluctuates depending on the soil quality, weather conditions, and the elapsed time. It is also necessary to consider the land erosion and human activities on the ground following the deposition. For reference, Table E.1 lists various reports by different research groups on cesium and its β values.

Table E.1 Evaluations for vertical profile of radioactive materials (cesium) in the ground

Time elapsed after deposition	Fallout category	Location	β^a g/cm ²	Reference
3–4 weeks	Chernobyl	Western Russia	0.1–2.0 ^b	Golikov et al., 1993
5–6 weeks	Chernobyl	Germany	0.5–1.0 ^b	Jacob and Meckbach, 1992
<1 y	Chernobyl	Sweden	2.2	Karlberg, 1987
<1 y	Chernobyl	Germany	1.4	Winkelmann et al., 1988
<1 y	Chernobyl	Germany	0.5–4	Jacob et al., 1994a
1–3 y	Chernobyl	Germany	1.0–10	Jacob et al., 1994a
1–3 y	Chernobyl	Western Russia	1.4 ± 0.2	Golikov et al., 1993
4 y	Chernobyl	Western Russia	1–7	Miller et al., 1991
4 y	Chernobyl	Belarus, Ukraine	1.4–5.6	IAEA, 1991a
1–5 y	Weapons test	Eastern U.S.	4.2	Beck, 1966
5 y	Chernobyl	Western Russia	2–4.5	Jacob et al., 1994a
3–6 y	Chernobyl	Germany	2.5–15	Jacob et al., 1994a
3–6 y	Chernobyl	Ukraine	1–4	Jacob et al., 1994a
3–6y	Chernobyl	Western Russia	3.3 ± 0.7 ^b	Golikov et al., 1993
>15 y	Weapons test	Western U.S.	14 ± 4 ^c	Beck and Krey, 1980
>15 y	Weapons test	Western U.S.	2.9 ± 1.6 ^d	Miller and Helfer, 1985
>15 y	Weapons test	Southern U.S.	14–20	Faller, 1992
>15 y	Weapons test	Eastern U.S.	2–7 (forests) 8–19 (fields)	Miller et al., 1990

^a Symbol ± indicates a standard deviation.

^b Deposition through precipitation.

^c Dry area, irrigated turfs.

^d Dry area, uncultivated land.

(Cited from ICRU Rep.53)

E.1.1 Simplified evaluation method

The values given in Table E.2 (Table 5.3 in the main text) can be used according to the time elapsed and amount of precipitation after the radioactive deposition, provided that the land is not of a special type*¹ and not disturbed by human activities. The values for β in Table E.2 take into account the coarseness of the ground surface. Figure E.1 illustrates the chronological fluctuation of β following the Fukushima Dai-ichi Nuclear Accident.

Using a greater value of β in radioactivity concentration analysis yields higher results, leads to a safe-side evaluation. Therefore, if uncertainties are involved in terms of the post-deposition time flow and precipitation amounts, it is necessary to use a greater β within an assumed possible degree. To express the radioactive vertical profile in the ground, the soil density of that location considered; thus, either the parameter $\beta(\text{g}/\text{cm}^2)$ or $\alpha/\rho(\text{cm}^2/\text{g})$ should be used. However, some units of analytical software currently available on the market use $\alpha(\text{cm}^{-1})$ as a parameter for the in-soil vertical distribution of radioactive materials in the ground. Therefore, Table E.2 presents conversions for β , α , etc.

Table E.2 Conversion table of parameters for vertical profile of radioactive materials in the ground
(The soil density (ρ) is assumed to be $1.6 \text{ g}/\text{cm}^3$)

Time elapsed after deposition (years)	Precipitation (mm)	β (g/cm^2)	RL (cm)	α/ρ (cm^2/g)	α (cm^{-1})
0–1	<3	0.1	0.063	10	16
0–1	≥ 3	1.0	0.63	1.0	1.6
1–5	-	3.0	1.9	0.33	0.53
5–20	-	10	6.3	0.10	0.16
Workgroup Report		4.8	3.0	0.21	0.33^{*2}

Values are cited from ICRU Rep. 53, except for a few

RL is obtained by dividing β by the soil density (ρ), α/ρ is an inverse of β , and α is an inverse of RL.

*¹ In forested areas, β tends to be low owing to the humic soil.

*² “Evaluation of Public Radiation Dose in Safety Inspection Conducted at Light Water Reactor Power Stations” by the Nuclear Safety Commission (2001)

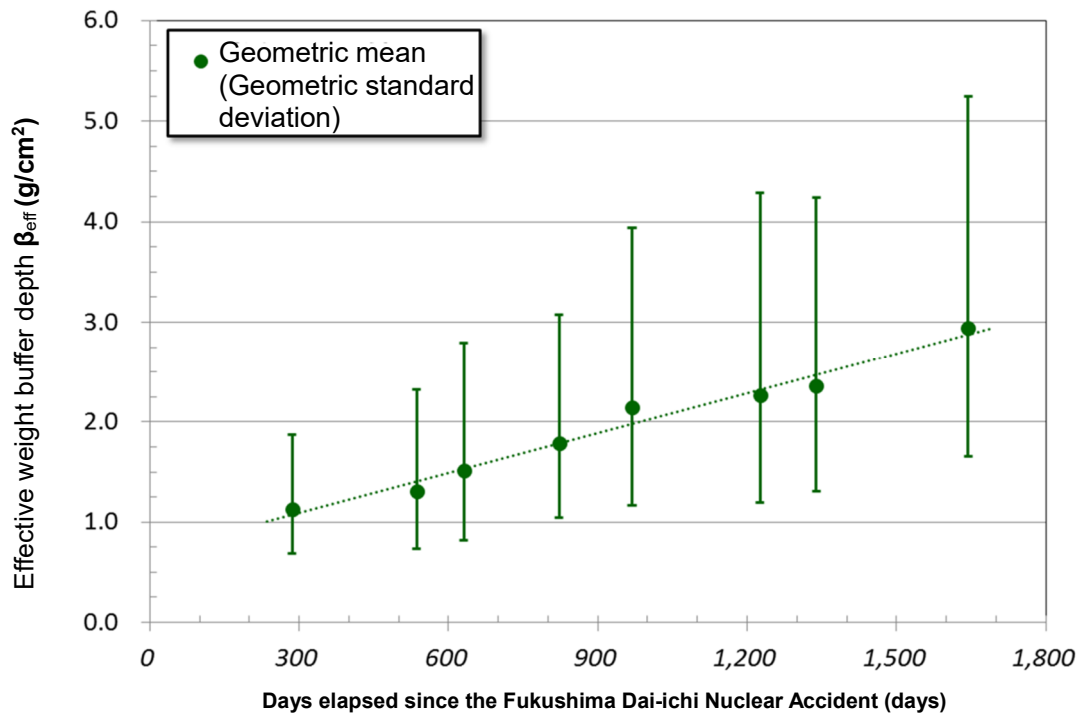


Figure E.1 Chronological fluctuation of β following the Fukushima Dai-ichi Nuclear Accident^{*3}

^{*3} Data source: Norihiro Matsuda, Japan Atomic Energy Agency

E.1.2 Evaluation by taking soil samples

To ensure higher accuracy of analysis based on in-situ measurement readings, it is necessary to sample the soil at the measurement site by soil layers to evaluate the distribution of artificial radioactive materials in the ground with respect to depth. The HASL manual suggests soil sampling at the layer depths of 0–2.5, 2.5–5, and 5–30 cm, or 0–5, 5–10, and 10–30 cm if the radioactive materials are considered to have penetrated the ground deeply. It has been reported^{*4} that the 90% penetration depth of radioactive cesium (the depth from the ground surface within which 90% of radioactive cesium deposition amount is contained) was 4.1 cm on average in Fukushima prefecture, measured 4.5 years after the Fukushima Dai-ichi Nuclear Accident (Figure E.2). Therefore, it is considered effective to take detailed samples near ground surface (within a depth of 10 cm) for several years following deposition.

The distribution of radioactive materials may be heterogeneous in a horizontal direction, but in a vertical direction it can be assumed to be reasonably homogeneous, provided that the soil quality is equally homogeneous. Therefore, it is not necessary to take many soil samples from the same location. For surveying radioactivity distribution over a wide area, it is more efficient to select several points in the area so that these points are not concentrated in one area, considering the environment of adjacent areas and the soil qualities, to obtain average depth-distribution evaluations. It is important to ensure that the mitigation of personnel exposure is considered to radiation when taking soil samples following a nuclear accident.

As for the methods of sampling, core samples may be taken with a soil auger, etc. and a scraper plate, etc. can be used to take layered samples. Taking core samples with an auger, etc. is more quickly executed than sampling with a scraper plate, which is useful for a simplified depth distribution analysis. For the method of sampling with an auger, see the Radioactivity Measurement Series No. 16 “Methods of environmental sampling.” In this section, the method of sampling with a scraper plate is explained, as it can adjust the sampling depths minutely and is useful for a detailed depth distribution evaluation.

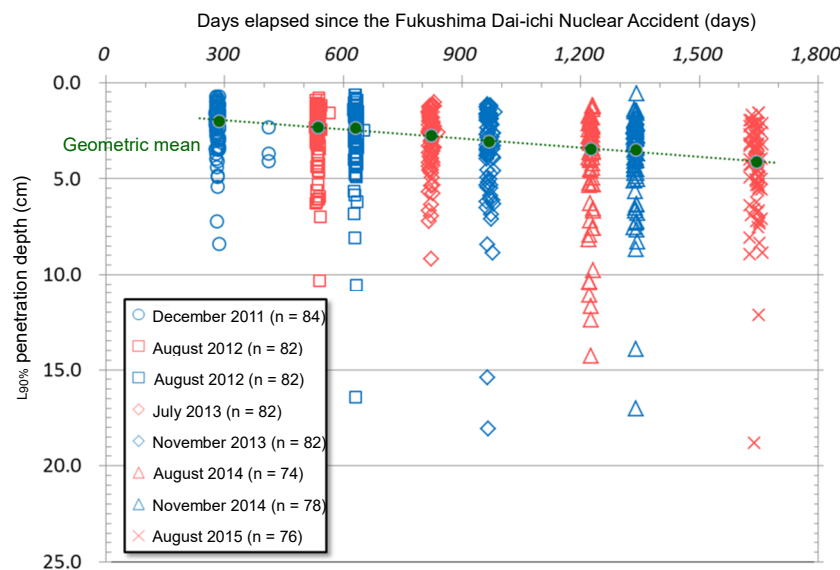


Figure E.2 Relationship between the days elapsed since the Fukushima Dai-ichi Nuclear Accident and 90% penetration depth of radioactive cesium^{*4}

^{*4} “FY 2015 Commissioned Investigation of Radioactive Materials (collection of data on the distribution of radioactive materials in relation to the accident at Tokyo Electric Power Company’s Fukushima Dai-ichi Nuclear Power Plant) Outcome Report: Research on Vertical Profile of Radioactive Cesium in the Ground” by Norihiro Matsuda and Kimiaki Saito (2016)

E.1.2.1 Soil sampling using a scraper plate

A scraper plate is a device designed to scrape a layer of soil at any given vertical interval (minimum 5 mm) (Figure E.3), comprising a metal frame to install the device on the ground and a metal plate for scraping the soil inside the frame. By attaching a metal bar on the metal plate, the depth is adjusted for sampling. Cross-contamination can be mitigated by taking the layered samples carefully.

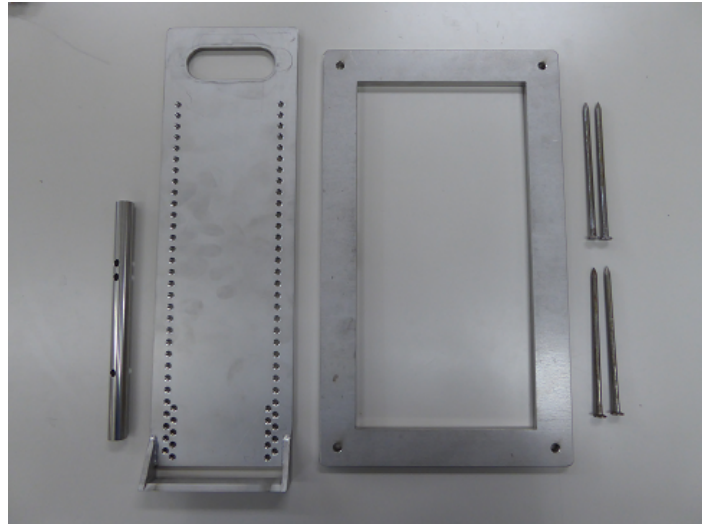


Figure E.3 Scraper plate

(1) Selection of sampling points

The sampling point is usually selected near the in-situ measurement location (see 4.1), where the topographic conditions are very close to those of the in-situ measurement site. Sampling normally takes several hours at a time, and for this reason it is unrealistic to sample from each in-situ measurement location if there are many. In this case, select several major sampling points so that they are spread evenly, in consideration of the environment of adjacent areas and the soil qualities to obtain average depth-distribution evaluations. It is important to ensure that the mitigation of personnel exposure to radiation is considered when taking soil samples following a nuclear accident.

(2) Determination of sampling layers

Determine the layer from which to take samples by considering the time elapsed since the deposition of radioactive materials. If it is immediately after the deposition has taken place, the radioactive materials are expected to be distributed close to the ground surface. Thus, samples are intensively taken from the near-surface segment at a small interval (every 5 mm). If the transfer of radioactive materials is evident over time, deeper sampling is necessary. Similarly, if decontamination has been evidently conducted, this must accordingly inform the decision regarding the depth of the sample.

- (3) Preparation of sampling tools
 - (1) Scraper plate
 - (2) Plastic bags to hold sampled soil (per sampled layer)
 - (3) Vat
 - (4) Hammer, a pair of shears, gardening shovel, spatula, forceps
 - (5) Disposable rubber gloves
 - (6) Pure water for cleansing measurement equipment (wet tissue papers are acceptable)
 - (7) Tarpaulin (this can be substituted with disposable paper sheets if sampling takes place in several locations to prevent contamination.)
 - (8) Scale (only if soil weighing takes place on site)
 - (9) U8 container (per sample layer; only if sample preparation takes place on site)
 - (10) Tent or parasol for rain cover and creating a shade (if necessary)
- (4) Sampling procedures
 - (1) Fix the scraper frame on the ground, using a hammer, etc. (see Figure E.4). Ensure that the frame is directly on the soil and stable.



Figure E.4 Fixing the frame

- (2) If vegetation grows in the ground, trim it with shears above ground and remove it carefully (see Figure E.5). If there are stones, remove those that are not buried in the soil. If these removed grass or stones should be measured for radioactivity concentration, keep them separately from the soil samples.

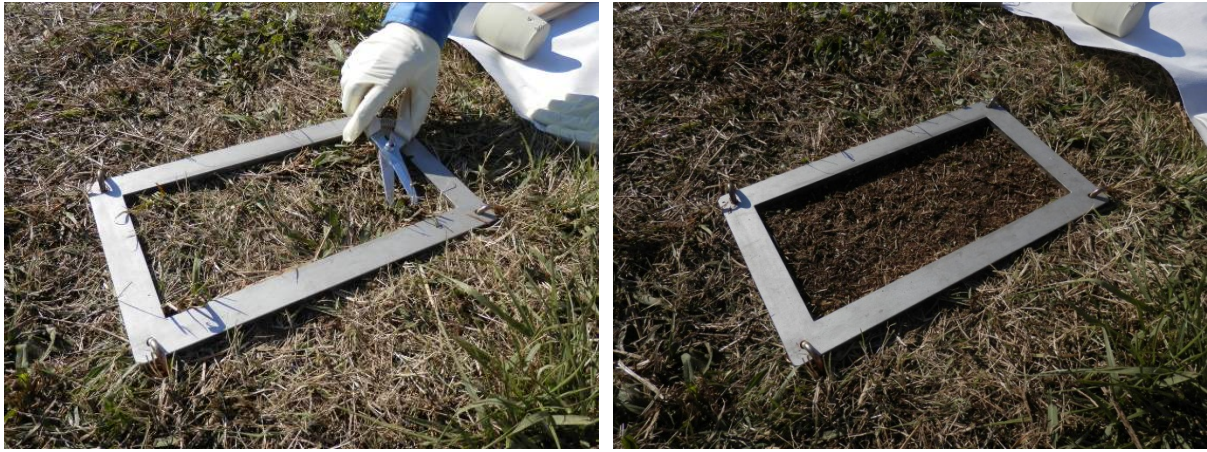


Figure E.5 Removing vegetation (Left: before, Right: after)

(3) Attach and fix the metal bar on the plate so that the sample will be of desired depth (see Figure E.6).

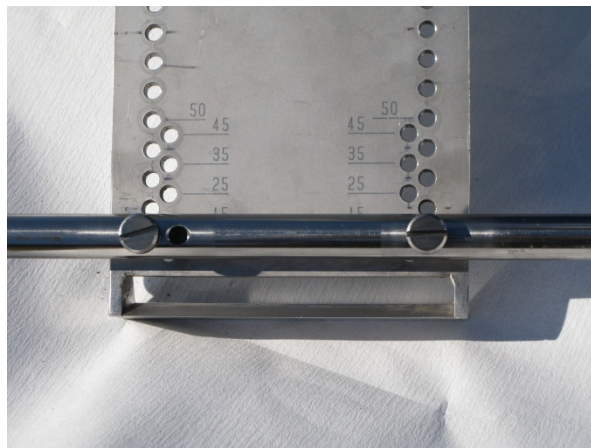


Figure E.6 Adjusting the plate

(4) Slide the plate horizontally in the frame to scrape the soil, then place the soil in a plastic bag (see Figure E.7). If the plate is held at an angle, the sample will be taken from a deeper section than intended. Keep the plate vertical at a right angle while scraping the soil. Take as much soil as possible for the sampled layer (see Figure E.8). Pay especially careful attention to the edges and corners inside the frame, and use a gardening shovel or spatula to ensure all the soil is taken for the sample. Any residual soil may contaminate the sample of subsequent layers, and may also contribute to errors when calculating the soil density.

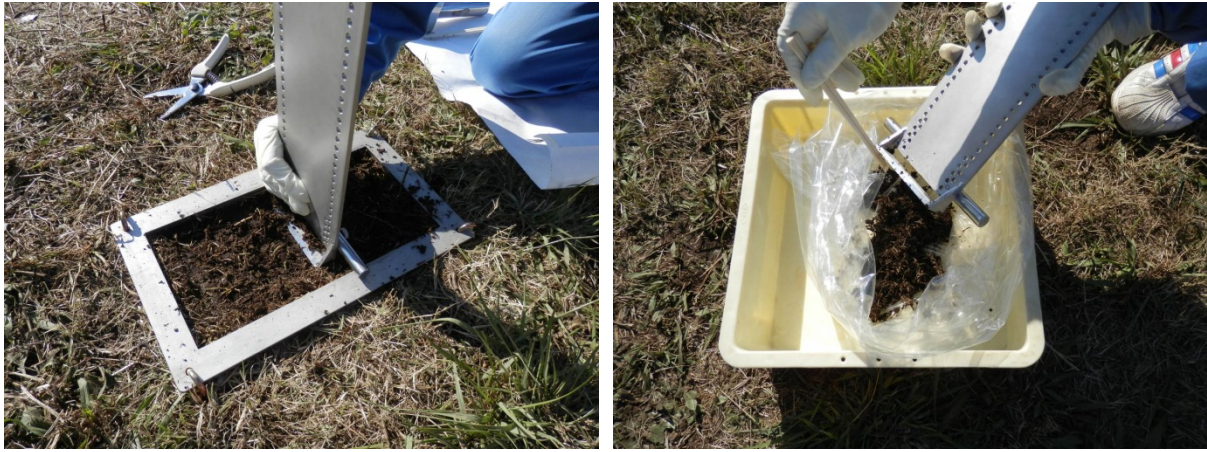


Figure E.7 Soil sampling using a scraper plate



Figure E.8 After the sampling is complete

- (5) Once a layer of soil sample is taken, clean the plate, etc. with pure water to wash off the remaining soil, and then wipe it dry (see Figure E.9). If pure water is not available on site, use wet tissue paper, etc. to wipe the soil off the plate. Change the rubber gloves used when sampling to a new pair, and discard the old pair.



Figure E.9 Cleaning sampling tools

- (6) Repeat procedures (3) to (5) for the number of layers to be sampled.
 - (7) When all the layers are sampled, fill the hole created by sampling with the soil from the surrounding areas, etc. (it is recommended to agree on how to refill the hole in advance).
- Procedures (8) to (10) below may be performed subsequently in the laboratory.
- (8) Weigh each sampled layer. Calculate the soil volume by the area inside the scraper frame and the thickness of the layer, and then obtain the density using these values.*⁵
 - (9) Mix each layer of soil well in a container, such as a bag, while it is still moist.
 - (10) Fill the U8 container with the sampled soil per layer while it is moist, and then measure the height and net weight. This will serve as a measurement sample for radioactivity concentration.

(5) Precautions for sampling exercises*⁶

- (1) As the sampling progresses, the internal wall of the dug hole may crumble and contaminate the lower layer samples. If this happens, remove the fallen segments of soil carefully to prevent contamination of the lower layers by the upper-layer soil. If the hole easily crumbles, spray water onto the walls to keep the soil in place.
- (2) If there are roots in the soil, nip them with scissors carefully and include in the soil of the applicable layer.
- (3) If a stone occupies several layers of soil, include it in the layer to which the major part of the stone belongs. If it is difficult to determine, include the stone in the upper layer (for it is usually the upper soil that has higher radioactivity concentration).
- (4) If the ground is frozen, either wait until it thaws or defreeze it with a gas burner, etc. before starting sampling.
- (5) If snow is on the ground, remove the snow carefully, so as not to disturb the ground surface before sampling.

(6) Recording

- (1) Sampling location
- (2) Sampling date
- (3) Weather condition at sampling
- (4) Land use category
- (5) Depth and weight of sampled soil
- (6) Photograph
Overall landscape and close up of the sampling point, sampling progress, sampled ground, etc.
- (7) Other remarks

*⁵ Alternatively, where the sample is taken with an auger, the density can be obtained from the weight of the soil sampled and the capacity of the equipment.

*⁶ “Handbook for the Assessment of Soil Erosion and Sedimentation Using Environmental Radionuclides”
F. Zapata (2010)

E.1.2.2 Calculation of β

- (1) When vertical distribution of radioactive materials in the ground can be exponentially approximated

Although the exponential model of vertical distribution of radioactive materials in the ground is simply an approximation, it suggests relatively realistic values after a certain time has elapsed since the radioactive fallout. If the exponential approximation is possible, a β value based on the measurement of sampled soil can be obtained by approximating the radioactivity concentration (Bq/g) against mass depth by an exponential function and obtaining $\beta(\text{g}/\text{cm}^2)$ from Equation (E.1). The conversion of depth (cm) to mass depth (g/cm^2) requires the soil density^{*7} of that location.

$$A(Z) = A_0 \cdot \exp\left(-\frac{Z}{\beta}\right) \quad (\text{E.1})$$

$A(Z)$: Radioactivity concentration (Bq/g) at mass depth Z

Z : Mass depth (g/cm^2)

The depth measured from the ground surface by per-unit-area mass of the soil.

A_0 : Radioactivity concentration (Bq/g) at ground surface

β : Weight buffer depth (g/cm^2)

A parameter to indicate vertical distribution of radioactive materials in the ground. It expresses the degree of penetration, where greater values indicate deeper penetration.

As parameters, in some cases, β divided by the soil density $\rho(\text{g}/\text{cm}^3)$ is $\text{RL}(\text{cm})$, the inverse of β is $\alpha/\rho(\text{cm}^2/\text{g})$, and the inverse of RL is $\alpha(\text{cm}^{-1})$.

Some of the analytical software packages presently available on the market are designed to use $\alpha(\text{cm}^{-1})$ as a parameter for the vertical distribution of radioactive materials in the ground, but this needs to be treated carefully.^{*8}

Example calculation of weight buffer depth β

- (1) Create a table such as Table E.3 based on the records and readings of the sampled soil.

Obtaining mass depth

The depth of each layer of sampled soil is between the ground surface (0 cm) to the middle of the layer. The mass of the soil is a sum of the soil mass from the ground surface to the layer immediately above the said layer and half of the mass of the said layer. For the area of the sampled soil, apply the area inside the auger or scraper plate used for sampling. The mass depth is calculated by dividing the soil mass by the soil sampling area.

^{*7} It is often the case that $1.6 \text{ g}/\text{cm}^3$ is used for soil density in general, but obtaining β after sampling soil requires the use of the actual soil density of that location.

^{*8} To express the radioactive vertical profile in the ground, the soil density of that location must be considered; thus, either the parameter $\beta(\text{g}/\text{cm}^2)$ or $\alpha/\rho(\text{cm}^2/\text{g})$ should be used. However, some of the analytical software presently available on the market uses $\alpha(\text{cm}^{-1})$. If this is the case, it is necessary to obtain α specifically by multiplying $\alpha/\rho(\text{cm}^2/\text{g})$ calculated from sampled soil by the soil density programmed in the software (e.g., $1.6 \text{ g}/\text{cm}^3$) instead of using the actual (apparent) α .

Table E.3 Example of a β calculation table

Sampled layer (cm)	Depth (cm)	Soil weight of sampled layer (g)	Soil weight to the depth (g)	Sampling area (cm ²)	Mass depth (g/cm ²)	Cesium-137 radioactivity concentration (Bq/g)
0.0–0.5	0.25	47.4	23.7	450	0.053	1.003
0.5–1.0	0.75	154.2	124.5	450	0.277	0.856
1.0–1.5	1.25	131.5	267.4	450	0.594	0.711
1.5–2.0	1.75	259.2	462.7	450	1.028	0.523
2.0–3.0	2.50	538.5	861.6	450	1.915	0.195
3.0–4.0	3.50	479.1	1370.4	450	3.045	0.065
4.0–5.0	4.50	560.9	1890.4	450	4.201	0.028
5.0–8.0	6.50	1718.2	3029.9	450	6.733	0.009

How to obtain mass density

Calculate the soil density of a segment from the ground surface (0 cm) to the depth by dividing the mass depth by the depth in Table E.3.

The soil density of the sampled layer is obtained by dividing the soil weight by the soil volume (thickness of sampled layer \times sampling area) of the layer.

(2) Calculation of β

Create a chart with the mass depth Z as the X-axis and cesium-137 radioactivity concentration $A(Z)$ as the Y-axis. Based on the plot yielded, apply an exponential function to approximate and obtain an approximation formula (Figure E. 10).

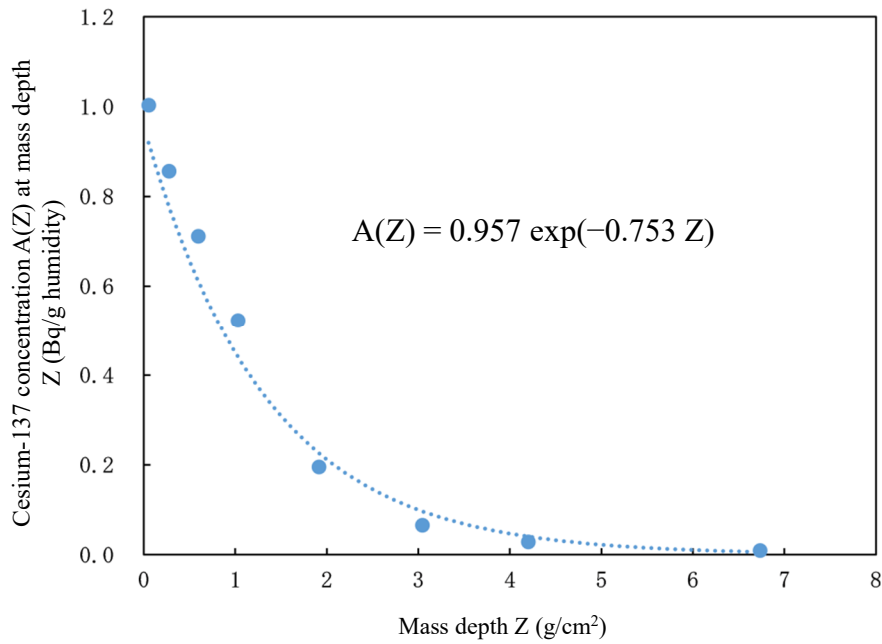


Figure E.10 Relationship between mass depth and cesium-137 concentration (when exponential approximation is possible)

Obtain β from the coefficients in the approximation formula. In Figure E.10, Equation (E.1) gives $-Z/\beta = -0.753 Z$, and therefore, $\beta = 1.33$.

(2) When vertical distribution of radioactive materials in the ground can be approximated by a hyperbolic secant function

As time elapses, the migration and diffusion of radioactive materials result in distributions that involve a peak at certain depth (Figure E.11).

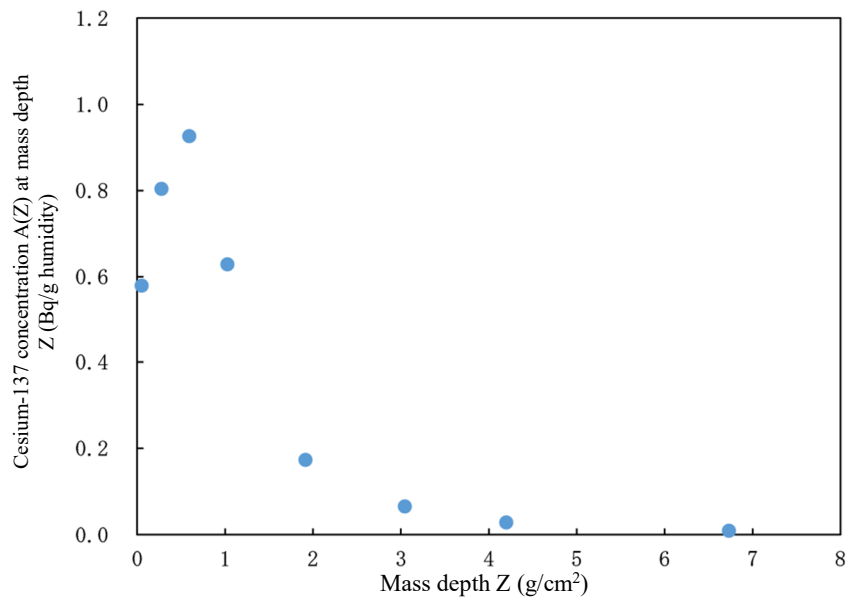


Figure E.11 Relationship between mass depth and cesium-137 concentration (when approximation by hyperbolic secant function is possible)

For this type of distribution, β can be calculated by an approximation formula (E.2) based on a hyperbolic secant function.*⁹ *¹⁰

$$A(Z) = A_0 \cosh(Z_0 / \beta) \operatorname{sech}\{(Z - Z_0) / \beta\} \quad (\text{E.2})$$

$$* \operatorname{sech}(x) = 1 / \cosh(x), \quad \cosh(x) = \{\exp(x) + \exp(-x)\} / 2$$

Z_0 : Mass depth (g/cm²) at which radioactivity concentration is maximum

A_0 , Z_0 , and β are calculated based on the depth profile and by the least square using an iterative algorithm. Equation (E.2) characteristically becomes the same function for deeper areas in soil as Equation (E.1).

In the case of a depth distribution approximated by an exponential function, there are two parameters (A_0 and β) in Equation (E.1), of which the weight buffer depth β , when given, will determine the depth profile pattern. Thus, this enables the quantification of the radioactive cesium deposition amount (Bq/cm²) from an in-situ measurement. However, if there are peaks of radioactivity concentrations at a certain depth over the profile, Equation (E.2), which has three parameters (A_0 , Z_0 , and β), cannot determine the depth distribution pattern with only β given. Therefore, in this case, it is practical for the purpose of analysis to evaluate the buffer depth that is equivalent to the exponential function (hereafter, “effective weight buffer depth β_{eff} ”). Given this, we propose Equation (E.3) for calculating dose rate and Equation (E.4) for calculating deposition amount, both using the conversion factor by Saito et al.,*¹¹ such that the relationship between the deposition amount and dose rate in the depth distribution analyzed through Equation (E.2) is equal to that in the exponential depth distribution. Then, the effective weight buffer depth β_{eff} can be obtained to satisfy both equations.*¹⁰

$$\int_0^{\infty} A_{0,\text{eff}} \exp(-Z / \beta_{\text{eff}}) I_{\gamma} C(Z) dZ = \int_0^{\infty} A_0 \cosh(Z_0 / \beta) \operatorname{sech}\{(Z - Z_0) / \beta\} I_{\gamma} C(Z) dZ \quad (\text{E.3})$$

$$\beta_{\text{eff}} A_{0,\text{eff}} = \beta A_{Z_0} \left[(\pi / 2) - \tan^{-1}\{-\sinh(Z_0 / \beta)\} \right] \quad (\text{E.4})$$

$A_{0,\text{eff}}$: Effective (tentative) radioactivity concentration (Bq/g) at ground surface

I_{γ} : Gamma-ray emission rate at radionuclide decay

$C(Z)$: Conversion factor proposed by Saito et al.*¹¹

A_{Z_0} : Radioactivity concentration (Bq/g) at the mass depth where the radioactivity concentration is at maximum

β_{eff} : Effective weight buffer depth (g/cm²)

*⁹ “Depth profiles of radioactive cesium in soil using a scraper plate over a wide area surrounding the Fukushima Dai-ichi Nuclear Power Plant” by N. Matsuda, S. Mikami, S. Shimoura, J. Takahashi, M. Nakano, K. Shimada, K. Uno, S. Hagiwara and K. Saito, Journal of Environmental Radioactivity 139, 427-434 (2015)

*¹⁰ “FY 2015 Commissioned Investigation of Radioactive Materials (collection of data on the distribution of radioactive materials in relation to the accident at Tokyo Electric Power Company’s Fukushima Dai-ichi Nuclear Power Plant) Outcome Report: Research on Vertical Profile of Radioactive Cesium in the Ground” by Norihiro Matsuda and Kimiaki Saito (2016)

*¹¹ K. Saito, P. Jacob, Fundamental data on environmental gamma-ray fields in the air due to source in the ground, JAERI-Data/Code 98-001 (1998)

In the case where the radioactivity against mass depth decreases exponentially as in Equation (E.1), the right side of Equation (E.3) becomes identical with the left side. Therefore, the weight buffer depth obtained by Equation (E.1) is the effective weight buffer depth as is.

By applying effective weight buffer depth β_{eff} in the exponential function model, the readings of ground surface measurements can be associated with the radiation source in the ground. Similarly, the coarseness of the ground surface can also be treated with the effective weight buffer depth β_{eff} .

Obtaining the average of β calculated from soil samples of different sampling spots can be done either by using the arithmetic mean or the geometric mean. Preferably, the average β is assumed to be the arithmetic mean when the created frequency distribution is similar to a normal distribution, and it is assumed to be the geometric mean when it is more similar to a log-normal distribution. However, β values taken from the locations where human activities such as decontamination has disturbed the natural vertical distribution must be excluded from the average calculation.

E.1.3 Use of gamma rays of different energies emitted from the same nuclide

If a nuclide emits gamma rays of different energies, the ratio of their fluence rates can be used to estimate β . The ratio of the fluence rates between the cesium-137 gamma ray of 662 keV and X ray of 32 keV (32 keV/662 keV) fluctuates by β , which is illustrated in Figure E.12. The difference in the decay of the 32 keV (X ray) and 662 keV (gamma ray) in soil is evident. This is used to estimate β . To apply this method, it is necessary to use an n-type Ge detector so that the low-energy area can be measured to detect 32 keV.

This method is also effective as it reduces the influence resulting from the coarseness of the ground. However, note that this method is not useful during the first month following a nuclear accident, as radiation from nuclides with short half-lives interferes with reading the energy region around 32 keV. It is equally difficult to apply this method when a long time has passed after an accident, for the X ray of 32 keV becomes difficult to detect as cesium penetrates deep into the ground. The method may be applied to lanthanum-140 or cesium-134, but it is not as effective as when it is applied to cesium-137.

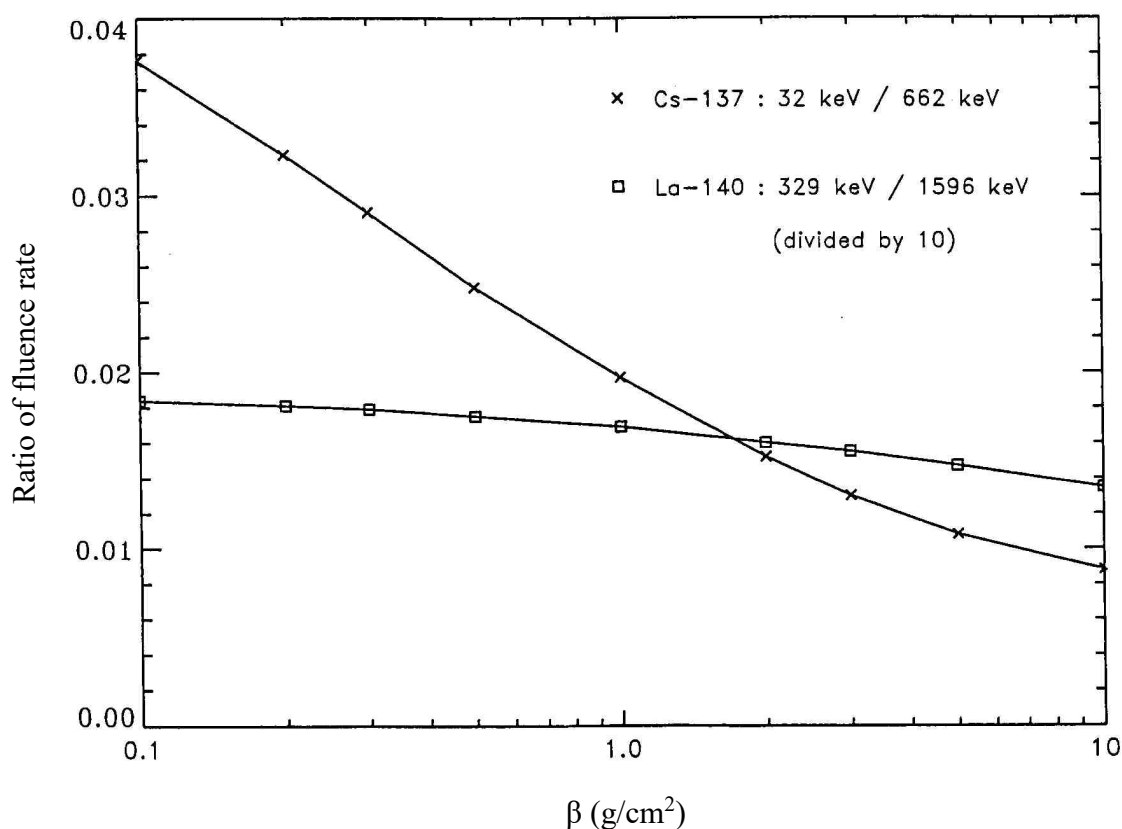


Figure E.12 Relationship between fluence rate ratio of gamma rays of different energies emitted by the same nuclide and vertical profile (β) of radioactive materials in the ground

(Cited from ICRU Rep.53)

Explanation E.2 Influence on analytical results

Figure E.13 illustrates the results from analyzing a spectrum taken at a certain location to obtain the dose rate and radioactivity concentration (per-unit-area radioactivity: Bq/cm²) by altering the parameter β for the vertical profile of radioactive materials in the ground. Although the dose rate does not significantly depend on β , the radioactivity concentration is considerably dependent on β .

Therefore, when calculating radioactivity concentration, understanding β correctly is most crucial for ensuring the credibility of the measurement. Currently, β is assumed to be 4.8 g/cm² (α : 0.33 cm⁻¹)*¹² for evaluating cesium-137 derived from atmospheric nuclear tests, but this value cannot be used for evaluating the post-accident ground surface distribution of radioactivity concentration, for it would overestimate the results by approximately three times.

Similarly, in the case where gamma rays of different energies are emitted by the same nuclide, if discrepancies are evident in the analytical results of radioactivity concentration between energies, it is possible that the assumptions of the vertical profile of radioactive materials in the ground, etc. are erroneous.

*¹² “Evaluation of Public Radiation Dose in Safety Inspection Conducted at Light Water Reactor Power Stations” by the Nuclear Safety Commission (2001)

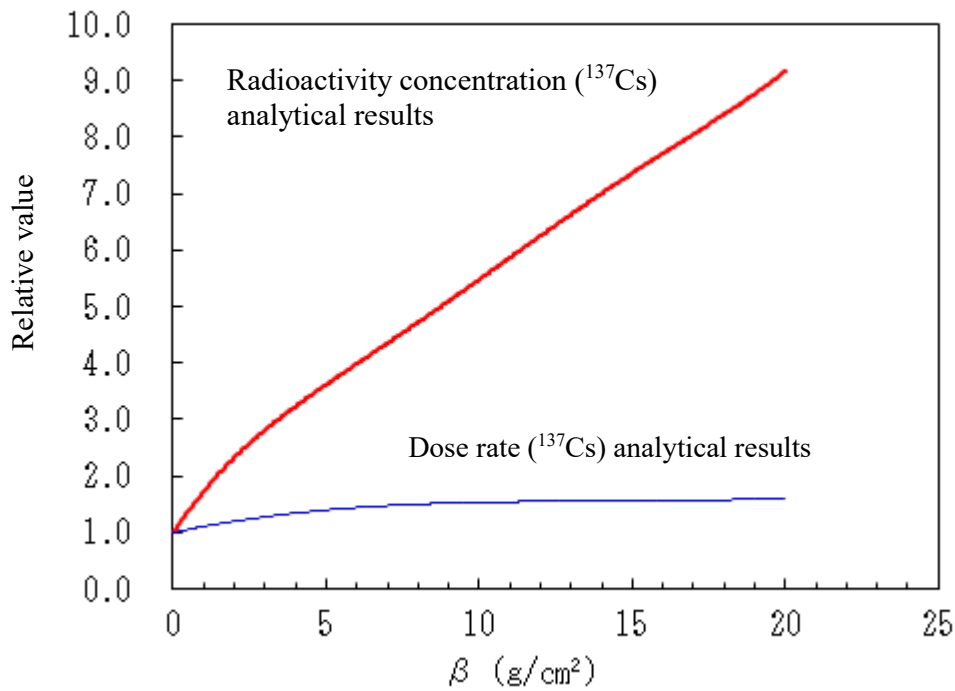


Figure E.13 Effects on the analytical results of vertical profile parameter β

This shows the results from analyzing cesium-137 (^{137}Cs) in a given spectrum from a measurement with β varied from 0 to 20, expressed as relative values by comparing with the ground surface distribution ($\beta = 0$).

The analytical results for radioactivity concentration increase as larger values are given for β . A greater value of β means that the radioactive material penetrates deep in the soil. Thus, dividing the measured peak count rate (constant in this case) by a diminished efficiency (N_f/A_a) yields a higher radioactivity concentration.

The dose rate is not considerably affected by β because the efficiency for the dose rate (N_f/I) does not change significantly, even when the radioactive materials penetrate deep in the soil.

Explanation F Implications of discrepancies between analytical and actual measurement conditions

Explanation F.1 Breadth of surrounding areas

The coefficients required for the calculation of radioactivity concentration from an in-situ measurement (ϕ/A in Equation 5.4 and values in Table-1 and Table 5.4) assume an infinitely open and flat landscape (infinite plane) with no obstacles that attenuate gamma rays, such as buildings and vehicles. However, in reality, it is impossible to expect such a perfect infinite plane; therefore, an analysis of radioactivity concentration based on this assumption of infinite plane will result in underestimation.

The impact of the breadths of surrounding areas on measurement readings is illustrated in Figures F.1 to F.6, by different vertical distributions (β) of radioactive materials in the ground. The values given in the charts indicate the efficiencies^{*1 *2} (peak count rate/radioactivity concentration) simulated by varying the breadth of the surrounding areas, which are expressed in relative values with respect to the values for a flat area of 150 m radius (considered as an infinite plane). These charts serve as a reference point to evaluate the extent of underestimation.

Given the acceptable margin of underestimation as -20% , a measurement of cesium-137 (approximately 600 keV) distributed on and near the ground surface ($\beta = 0.1 \text{ g/cm}^2$, Figure F.1) requires a breadth of at least 25 m radius. If $\beta = 4.8 \text{ g/cm}^2$ (Figure F.5), the radius becomes 10 m, with a radius of 5 m for an in-soil homogeneous distribution.

If it is difficult to secure a sufficiently open area, correction can be applied to the measurement readings using Figures F.1 to F.6. However, to minimize the uncertainties due to correction, it is desirable to secure at least a 10-m radius of open area if the distribution is found on and near the ground surface.

These results are based on a simulation^{*1 *2} using a p-type detector, which is a Ge detector with relatively less directional dependence. Figures F.7 and F.8 illustrate the results of calculating a near-surface distribution ($\beta = 0.1 \text{ g/cm}^2$) using a general p-type detector and an n-type detector, which can measure low energies. There are no major differences between the detectors in terms of the impact of the area breadths on their readings. As for the directional dependence of these detectors, see Explanation G.

Figures F.9 to F.11 show the extent of gamma ray contributions to in-situ measurements with respect to distance from the detector. Note that Figure 9 is based on the vertical distribution (β) of radioactive materials in the ground and Figures F.10 and F.11 are based on the difference in gamma-ray energies.

^{*1}For the simulation, peak efficiency simulation software (calculation code: MCNP Monte Carlo code^{*2}) was used.

^{*2}Briesmeister, J.F., "MCNP-A general Monte Carlo N particle Transport Code Version 4C", Los Alamos National Laboratory Report LA-13709-M (2000)

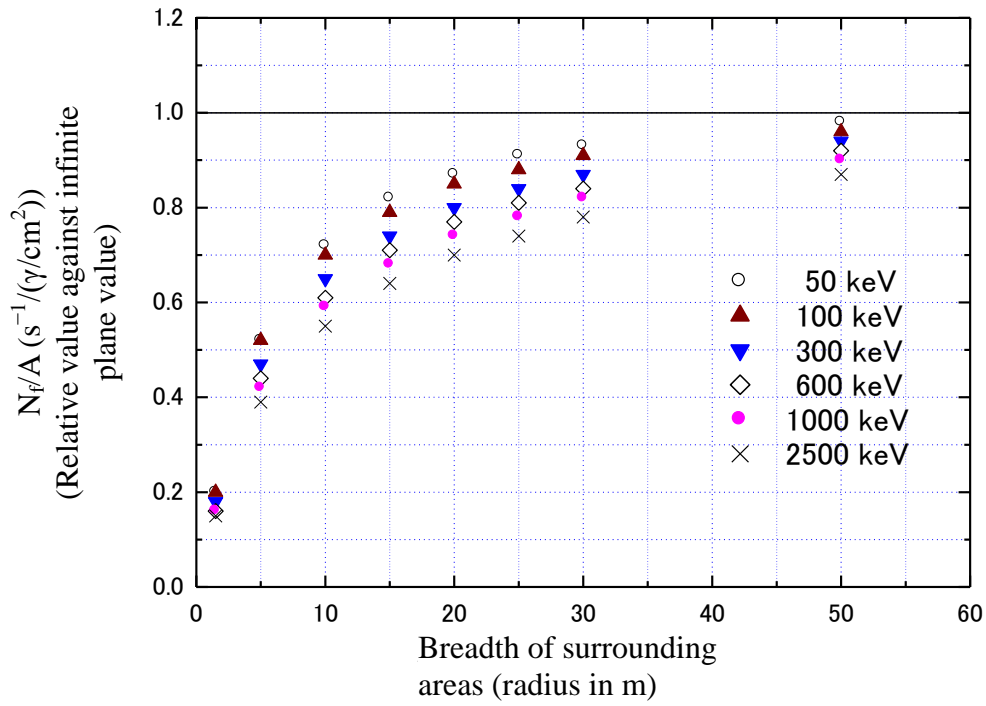


Figure F.1 Impact of breadth of surrounding areas on measurement readings (detector: p-type, β : 0.1 g/cm²)

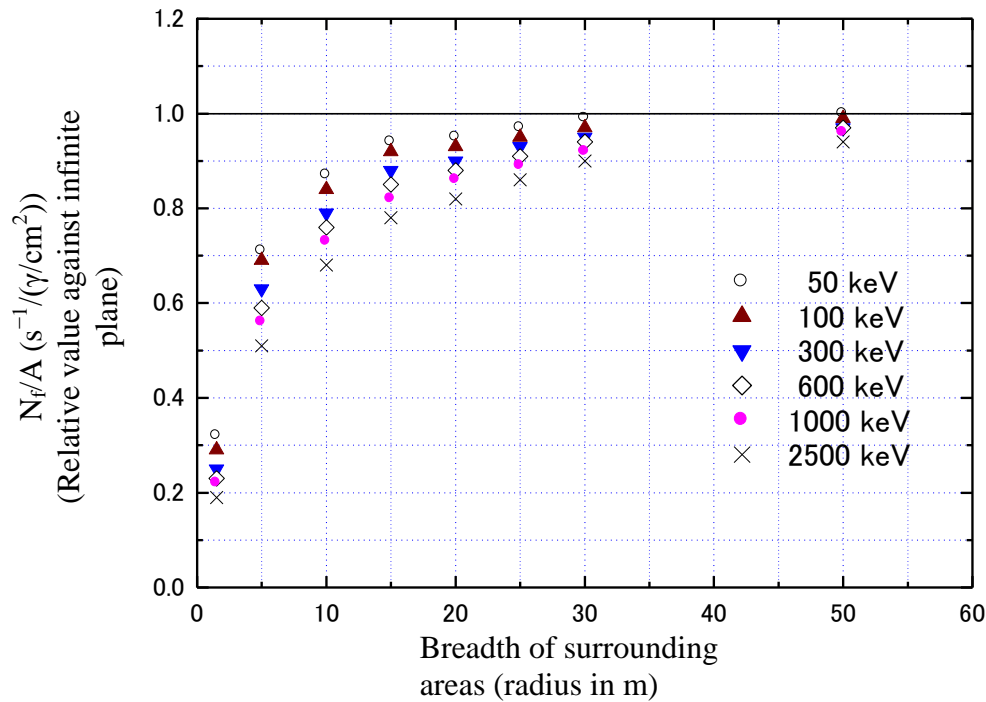


Figure F.2 Impact of breadth of surrounding areas on measurement readings (detector: p-type, β : 1.0 g/cm²)

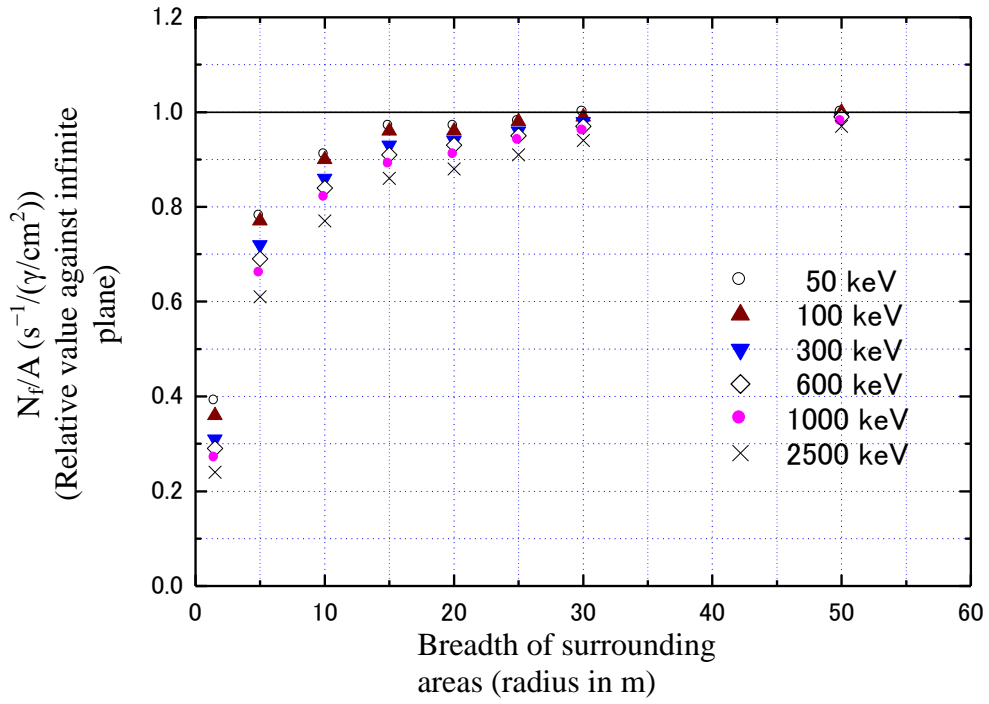


Figure F.3 Impact of breadth of surrounding areas on measurement readings (detector: p-type, β : 3.0 g/cm²)

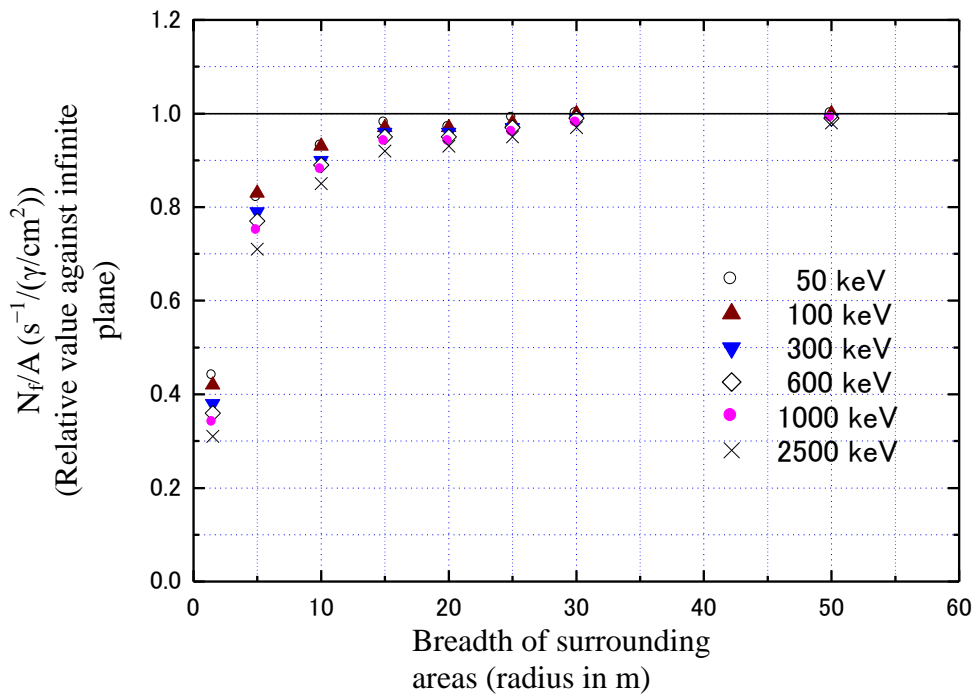


Figure F.4 Impact of breadth of surrounding areas on measurement readings (detector: p-type, β : 10 g/cm²)

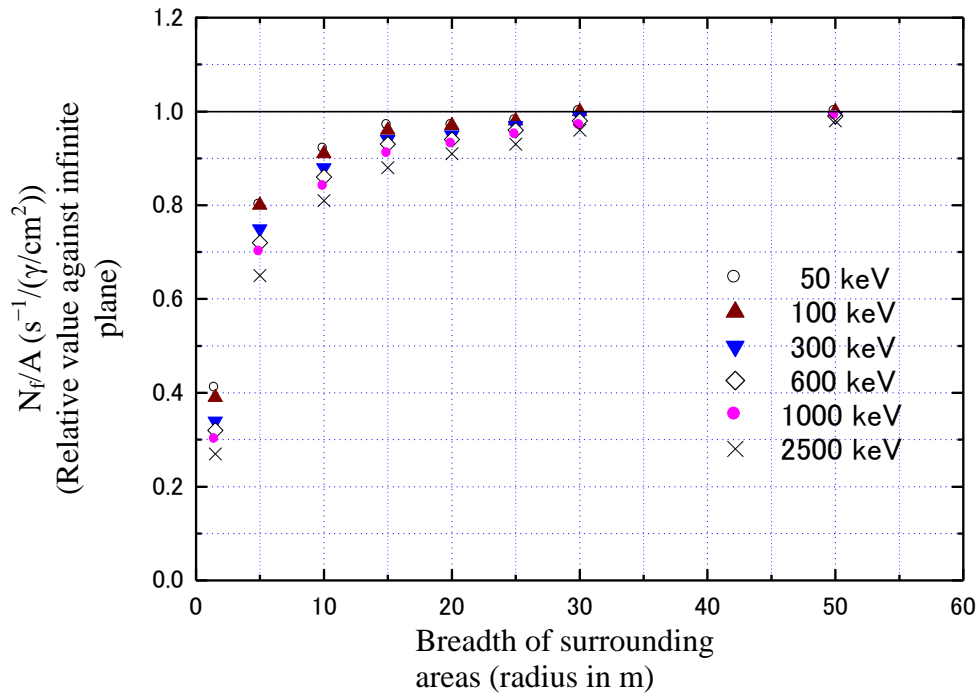


Figure F.5 Impact of breadth of surrounding areas on measurement readings (detector: p-type, β : 4.8 g/cm²)

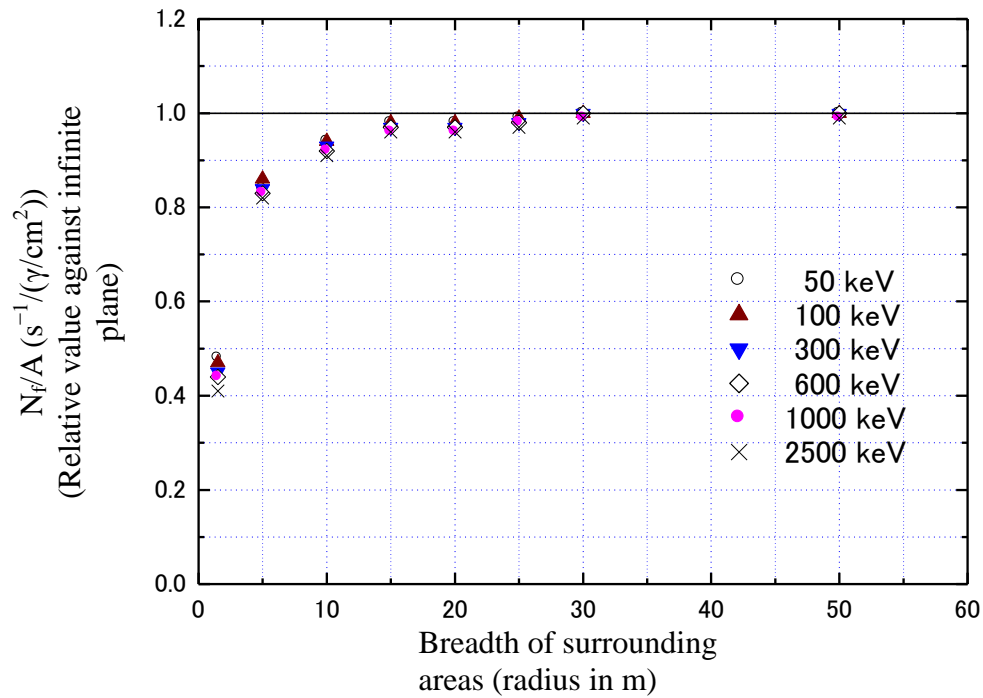


Figure F.6 Impact of breadth of surrounding areas on measurement readings (detector: p-type, homogeneous distribution)

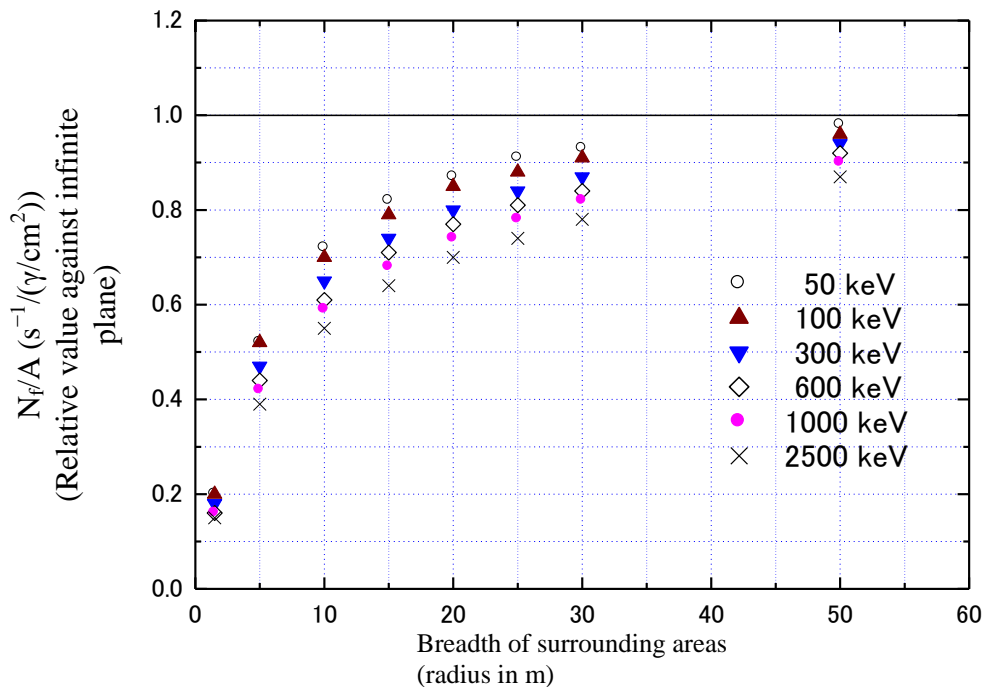


Figure F.7 Impact of breadth of surrounding areas on measurement readings (β : 0.1 g/cm^2) (detector: p-type, L/D; 0.9, dead layer; 1 mm, relative efficiency; 40%)

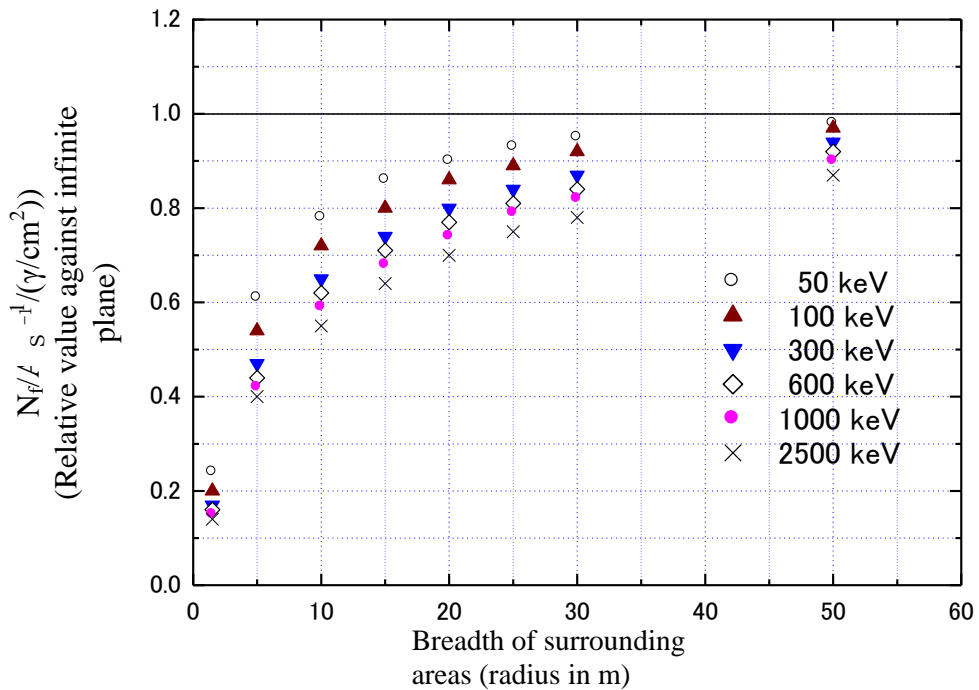


Figure F.8 Impact of breadth of surrounding areas on measurement readings (β : 0.1 g/cm^2) (detector: n-type, L/D; 1.0, dead layer; $0.1 \text{ }\mu\text{m}$, relative efficiency; 25%)

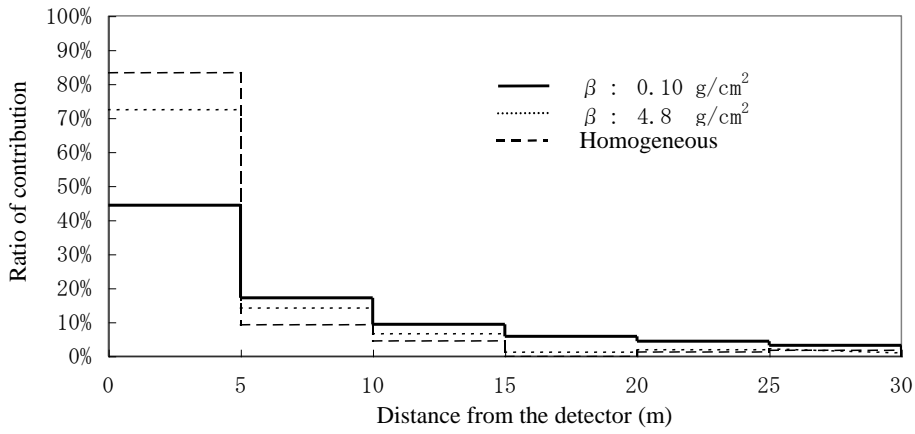


Figure F.9 Ratio of contribution from surrounding areas in in-situ measurement (gamma-ray energy: 600 keV)

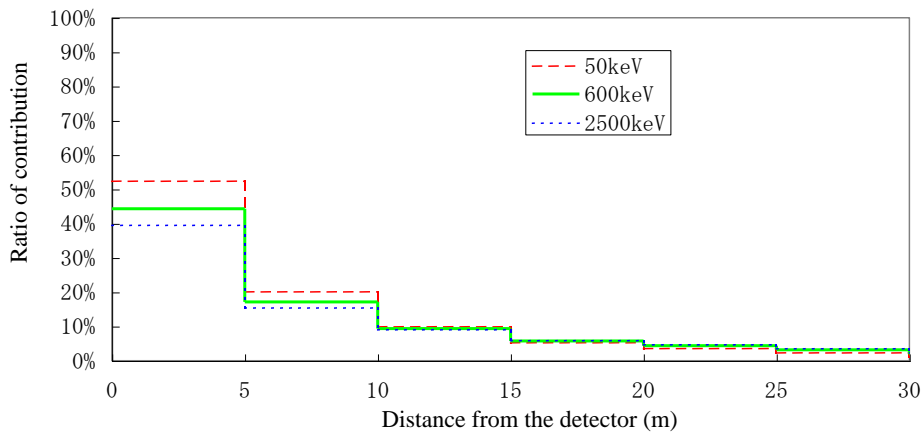


Figure F.10 Ratio of contribution from surrounding areas in in-situ measurement (β : 0.1 g/cm²)

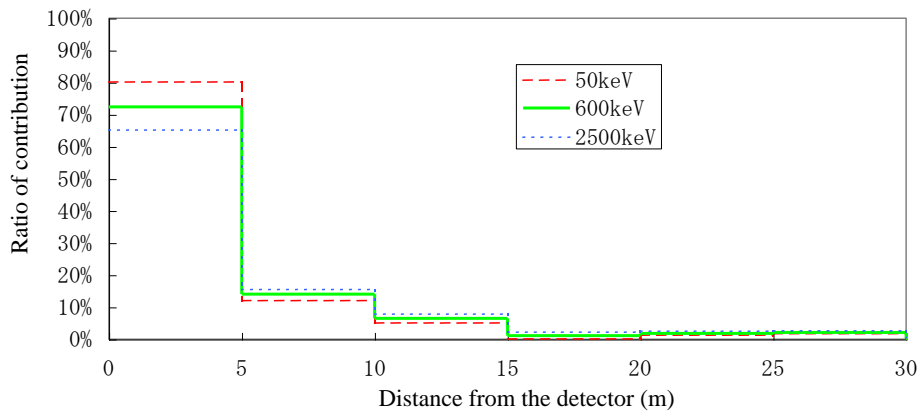


Figure F.11 Ratio of contribution from surrounding areas in in-situ measurement (β : 4.8 g/cm²)

Explanation F.2 Height of detector installation

The analysis for in-situ measurements assumes that the detector is installed at 1 m above the ground to take the measurement. Normally, there is no need for correction, as the detector is installed at 1 m above the ground. However, it is possible that, owing to topographical difficulties, etc., the detector may be installed at a different height. Therefore, the manner in which the height of the detector installation affects the measurement readings is described below.

Figures F.12 to F.14 illustrate the results of simulations^{*3} ^{*4} of in-situ measurement efficiencies (peak count rate/radioactivity concentration) at varied installation heights with respect to different vertical distributions (β) of radioactive materials in the ground. The values shown on the charts are relative to those of a 1-m installation. The higher the installation, the lower the efficiency. Therefore, if the detector is installed higher than 1 m, or if the surrounding areas are lower because, for example, there is a cliff, caution must be taken for possible underestimation.

A particular caution is required when radioactive materials are distributed near the ground surface (Figure F.12, $\beta = 0.1 \text{ g/cm}^2$), as the impact of installation height is greater.

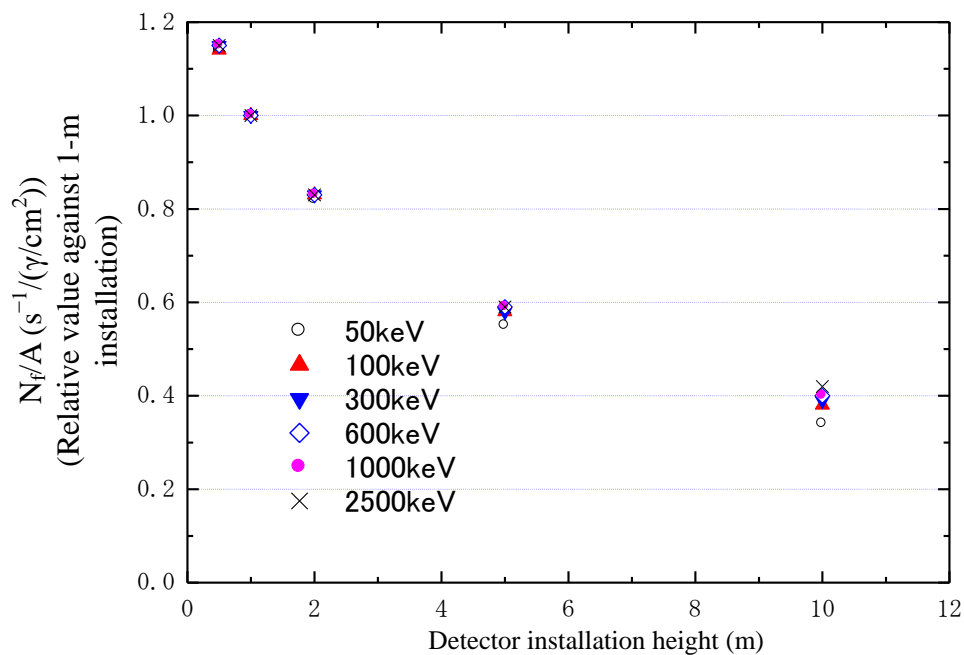


Figure F.12 Impact of detector installation height on measurement readings ($\beta: 0.1 \text{ g/cm}^2$)

^{*3} For the simulation, peak efficiency simulation software (calculation code: MCNP Monte Carlo code^{*4}) was used.

^{*4} Briesmeister, J.F., "MCNP-A general Monte Carlo N particle Transport Code Version 4C", Los Alamos National Laboratory Report LA-13709-M (2000)

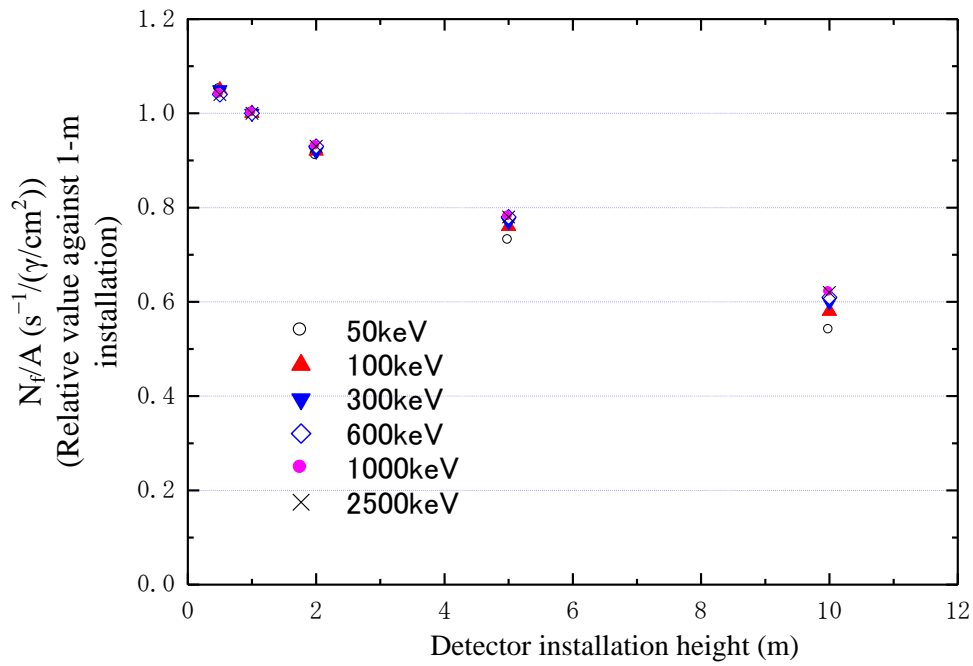


Figure F.13 Impact of detector installation height on measurement readings (β : 4.8 g/cm^2)

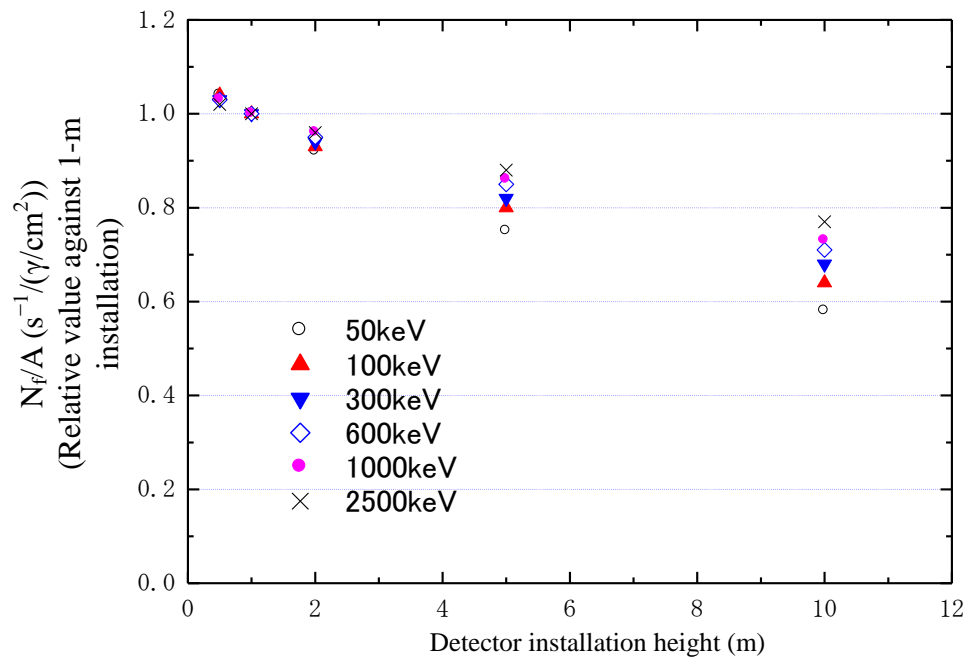


Figure F.14 Impact of detector installation height on measurement readings (homogeneous distribution)

Explanation F.3 Moisture in the ground

Moisture in the ground does not need correction, except in certain special cases, as it is included in the effects of vertical distribution of radioactive materials in the ground (Explanation E). However, in the case of a longitudinal measurement at the same point, it is conceivable that comparisons are made between in-situ measurements taken at different times, which may involve measurements taken under fine weather and others immediately after rain. Therefore, the manner in which the moisture in the ground can affect measurement readings is described below.

Figures F.15 to F.18 illustrate the results of simulations^{*5} ^{*6} of in-situ measurement efficiencies (peak count rate/radioactivity concentration) at varied moisture levels in the ground with respect to different vertical distributions (β) of radioactive materials in the ground. The values shown on the charts are relative to those with a moisture level of 10%.

Naturally, the impact of moisture in the ground is small if radioactive materials are distributed near the ground surface ($\beta = 0.1 \text{ g/cm}^2$) (Figure F.15). If radioactive materials penetrate the ground to some extent ($\beta = 4.8 \text{ g/cm}^2$), a greater amount of moisture in the ground will lower the efficiency more, owing to its shielding effect (Figure F.16). This means that the measurement reading will yield lower values. Immediately after the deposition of radioactive materials, the impact of moisture in the ground is negligible, but after some time has passed and radioactive materials have penetrated the ground deeply, caution must be taken as the measurement readings will be affected by the moisture in the ground at the time of the measurement. Therefore, it is recommended that moisture levels in the ground at the time of measurement be recorded if possible.

In the analysis of radioactive nuclides distributed homogeneously, there is hardly an effect of moisture in the ground (Figure F.17). This suggests that the efficiency ($\text{s}^{-1}/(\text{Bq/g moist soil})$) does not fluctuate significantly as the reduced count rate due to the shielding by water balances out the effect of diluting the radioactivity concentration.

However, the efficiency for radioactivity per dry soil ($\text{s}^{-1}/(\text{Bq/g dry soil})$) is not affected by dilution by water, whereas moisture shields radioactivity, which reduces the counting rate. Therefore, the efficiency is affected by the in-soil moisture (Figure F.18). The value obtained from the in-situ measurement is the radioactivity per the actual soil (moist). Normally, the in-soil radioactivity level measured in a laboratory is per dry-soil measurement; thus, caution must be taken when comparing such values.

^{*5} For the simulation, peak efficiency simulation software (calculation code: MCNP Monte Carlo code ^{*6}) was used.

^{*6} Briesmeister, J.F., "MCNP-A general Monte Carlo N particle Transport Code Version 4C", Los Alamos National Laboratory Report LA-13709-M (2000)

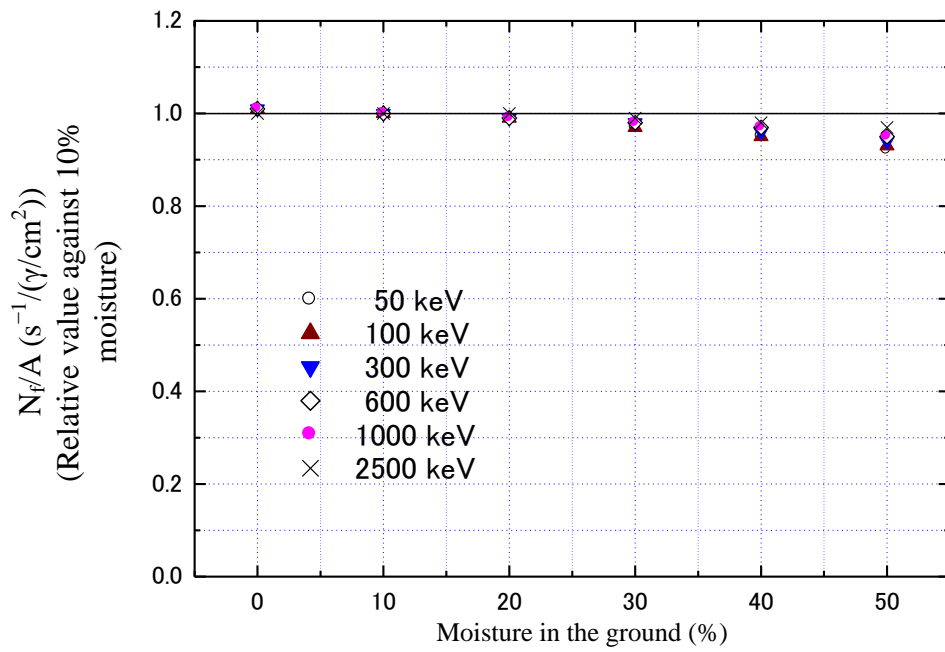


Figure F.15 Impact of moisture in the ground on measurement readings (when radioactive materials are distributed near the ground surface, β : 0.1 g/cm²)

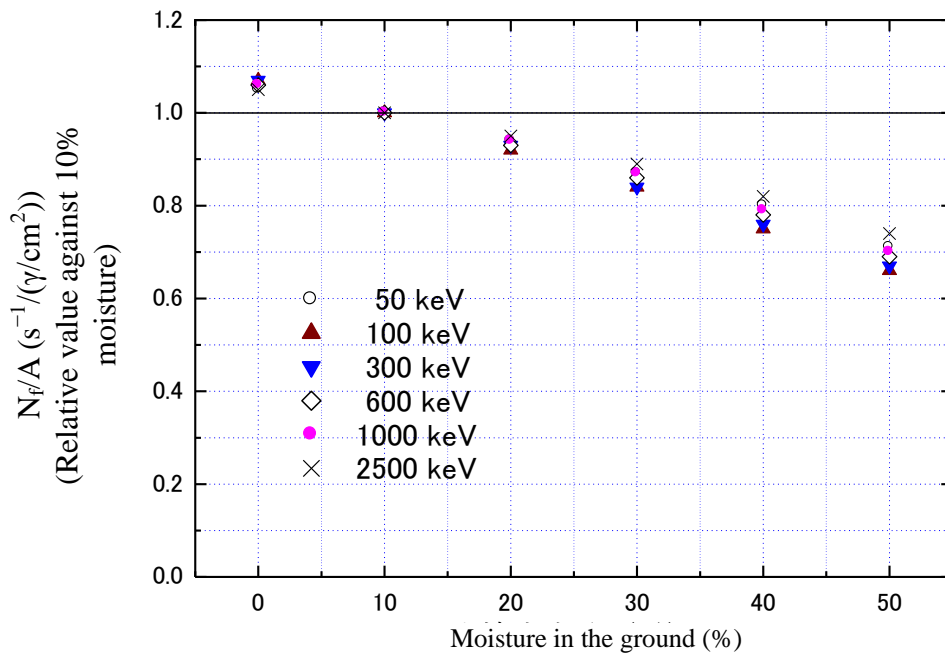


Figure F.16 Impact of moisture in the ground on measurement readings (when radioactive materials have penetrated into the ground, β : 4.8 g/cm²)

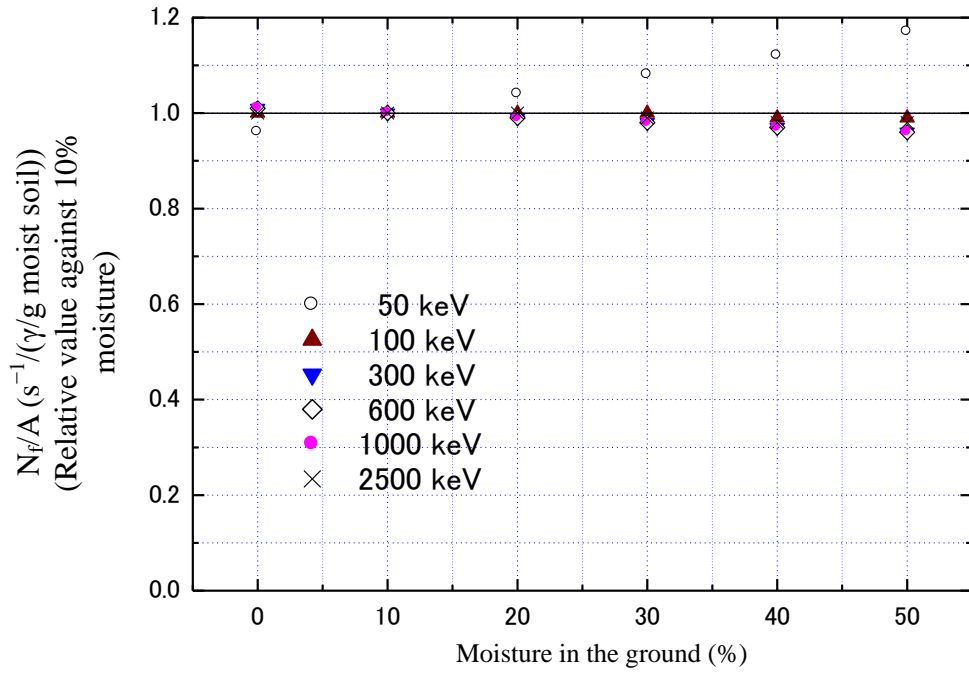


Figure F.17 Impact of moisture in the ground on measurement readings (when measuring radioactivity per moist soil, homogeneous distribution)

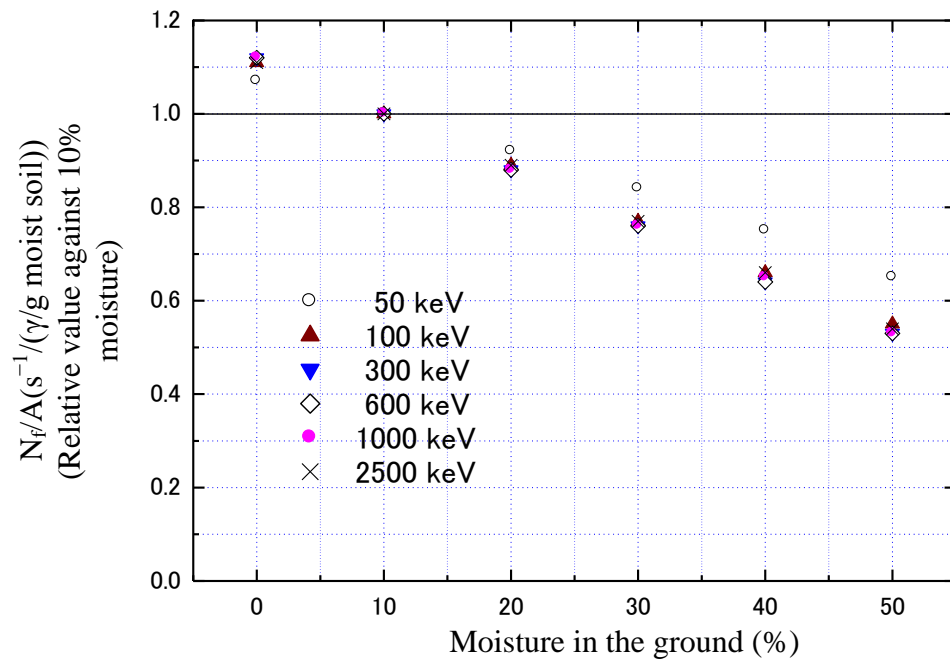


Figure F.18 Impact of soil moisture on measurement readings (when measuring radioactivity per dry soil, homogeneous distribution)

Explanation G Directional characteristics of detector (angular dependence of peak efficiency)

Examples of directional characteristics in terms of the p-type and n-type Ge detectors are shown in Figures G.1 and G.2, respectively. In in-situ measurements, the detector is normally installed facing downward. Given the right angle at the ground is zero degrees, the relative efficiencies are described below between the efficiency of a given degree against that of 0°. Note that these figures are simulation^{*1} ^{*2} results, assuming the distance between the radiation source and the detector to be 1 m. For the p-type detector, the parameters are as follows: relative efficiency 40%, diameter 61 mm, length 56 mm, and dead layer 1 mm. For the n-type: relative efficiency 25%, diameter 53 mm, length 53 mm, and dead layer 0.1 µm.

The p-type detector shows the tendency to yield low values in the low-energy region (50–60 keV) for gamma rays incident at an angle. This is considered to be because the angled incidence results in a longer passage through the dead layer, and therefore a greater attenuation. There is almost no directional dependence recognized at energies of 100 keV or more.

As to the n-type detector, the dead layer is extremely thin and angled incidence does not cause the lowering of peak efficiency in the low-energy region. On the contrary, there was a tendency that higher values were yielded. This is considered to be because the peak efficiency in the low-energy region depends more on the cross-sectional area than the volume. Overall, no significant directional dependence was recognized.

The detectors treated in this example those with the length–diameter ratio (L/D) of approximately 1.0. Detectors that fall outside the L/D range of 0.9 to 1.1, and special-purpose detectors for measuring low energy background, may have strong directional dependence. Therefore, it is necessary to understand the directional characteristics when using such detectors.

^{*1} For the simulation, peak efficiency simulation software (calculation code: MCNP Monte Carlo code) was used.

^{*2} Briesmeister, J.F., “MCNP-A general Monte Carlo N particle Transport Code Version 4C”, Los Alamos National Laboratory Report LA-13709-M (2000)

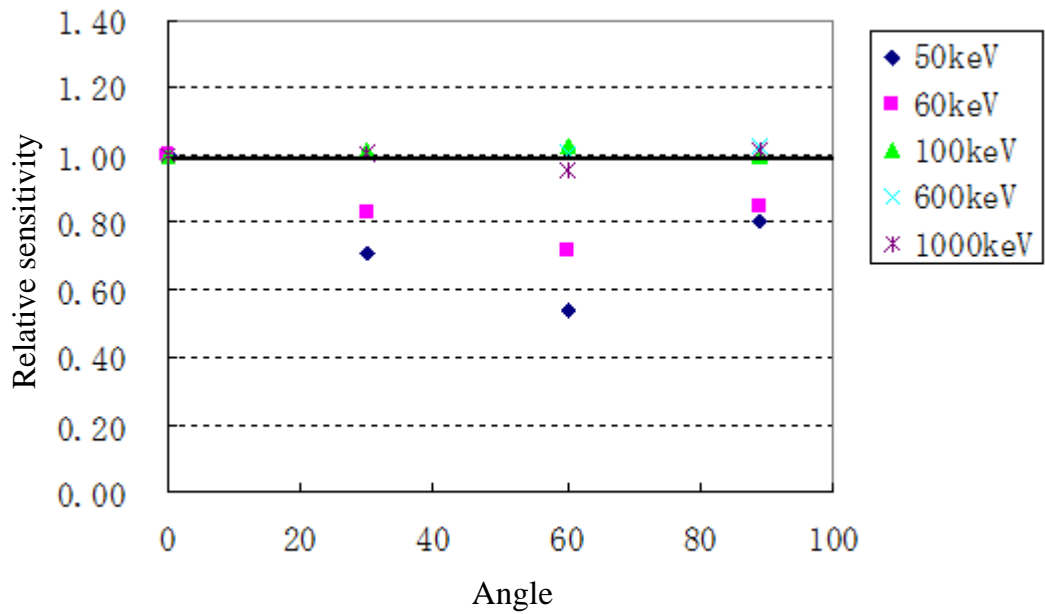


Figure G.1 Example of angular dependence of peak efficiency
(Detector: p-type, L/D: 0.9, dead layer: 1 mm, relative efficiency: 40%)

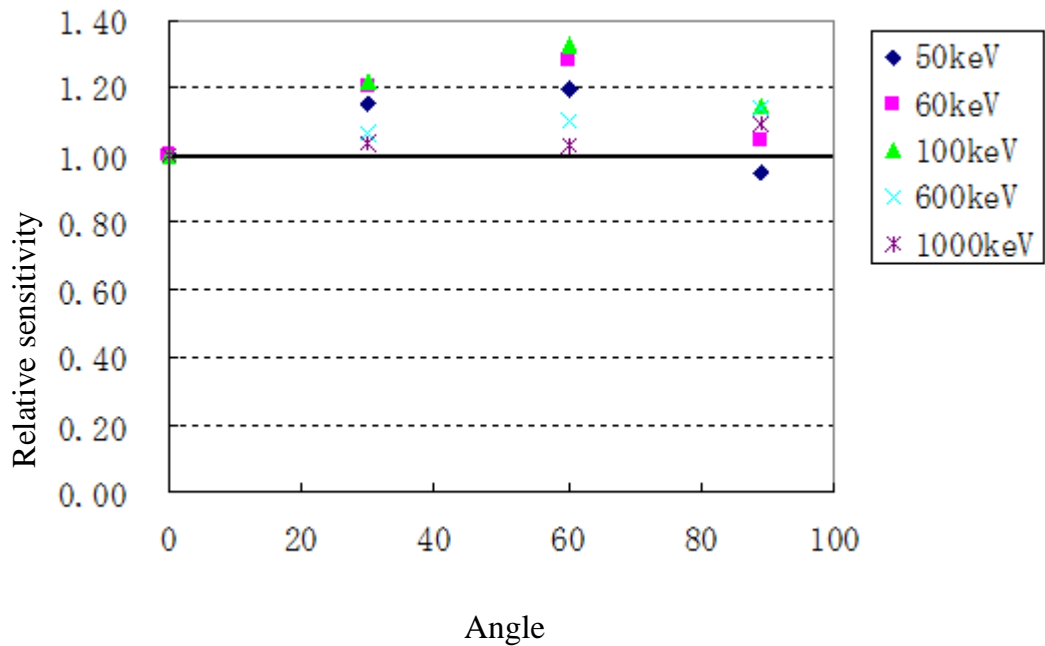


Figure G.2 Example of angular dependence of peak efficiency
(Detector: n-type, L/D: 1.0, dead layer: 0.1 μm , relative efficiency: 25%)

Explanation H Example of actual measurement

Explanation H.1 Artificial radioactive materials deposited on the ground

1. Purpose

To verify the validity of in-situ measurement for artificial radioactive materials deposited on the ground.

2. Methods considered

Both in-situ measurement and measurement of a gamma-ray spectrum for soil samples were conducted at the actual environmental site, and the results were compared. The measurement location was chosen near Mt. Fuji because it had a low concentration of naturally occurring radioactive materials, and it was possible to find unspoiled and uncultivated lands.

(1) In-situ measurement

The measurement was conducted at an open area of 10 m or more, devoid of trees. The Ge detector was installed at a height of 1 m, and the measurement was taken for 1 h. The analysis was performed using the HASL method to calculate the in-soil cesium-137 radioactivity concentration and gamma-ray dose rate at the location. Table H.1 lists the specifications of the detector used.

(2) Soil sampling and measuring

Soil samples were taken near the measurement point, using an auger of 5 cm diameter, and the 30-cm depth was divided into six layers, each of thickness 5 cm. The soil samples were not allowed to dry, and they were placed in measurement containers (U-8) after large stones, etc. were removed. In the laboratory, they were then measured for approximately 70000 s using a Ge detector, and the gamma-ray spectrum obtained was used to calculate the cesium-137 radioactivity concentration.

Table H.1 Specifications of the Ge detector used in the in-situ measurement

Detector	Relative efficiency (%)	Crystal diameter (D) (mm)	Crystal length (L) (mm)	(L/D)	End cap (mm)	Dead layer	Distance between end cap and crystal (mm)
A	25	53	53	1.00	0.5 (Al)	0.1 μ m	5.0
B	25	54.6	54.7	1.00	1.27(Al)	0.7 mm	3.0

3. Results and discussions

Table H.2 lists the cesium-137 radioactivity concentrations based on the in-situ measurement and sampling.

Calculating the radioactivity concentration from in-situ readings requires vertical distribution of radioactive materials in the ground; however, in this case, the analysis was conducted using both the general assumption of $\beta = 4.8 \text{ g/cm}^2$ and the actual values taken from the measurement.

Table H.2 radioactivity concentration measured at Mt. Fuji

Measurement location	Parameter of vertical distribution used in in-situ analysis $\beta \text{ (g/cm}^2\text{)}$	^{137}Cs radioactivity concentration (kBq/m ²)			Remarks
		in-situ (Detector A)	in-situ (Detector B)	Sampled soil	
Point A (Hitoana, Fujinomiya City)	4.8	1.6	1.6	1.7	Humic soil
	8.15 ¹⁾	-	2.1		
Point B (Fuji Skyline Drive)	4.8	2	2	4.0	
	15.4 ²⁾	-	4.2		

1)2) Values taken from the sampled soil

Concerning the analytical results using $\beta = 4.8 \text{ g/cm}^2$, the in-situ and sampling measurements yielded almost identical results at Point A, but at Point B there was a difference of almost double the value. A possible explanation for this is that the assumed vertical radioactive profile in the ground for analysis was discrepant from the actual profile.

We calculated β based on the vertical profiles of cesium-137 in the ground taken from each sampling point (see Figures H.1 and H.2) and the soil density of these points. ^{*1} The analysis of the in-situ reading using the β (Tables H.2 1) 2)) yielded a value close to the ^{137}Cs radioactivity of the sampled soil.

Figures H.3 and H.4 illustrate the in-situ spectra measured at the respective locations.

^{*1} The calculation was done by adapting the soil sampling depth $Z(\text{cm})$ and ^{137}Cs radioactivity concentration $A(Z)$ at depth Z (Bq/kg moist soil) to the exponential function $A(Z) = \exp(-\alpha Z)$ to obtain $\alpha(\text{cm}^{-1})$, and then obtain β by $\beta = \rho/\alpha$ (ρ : density of sampled soil).

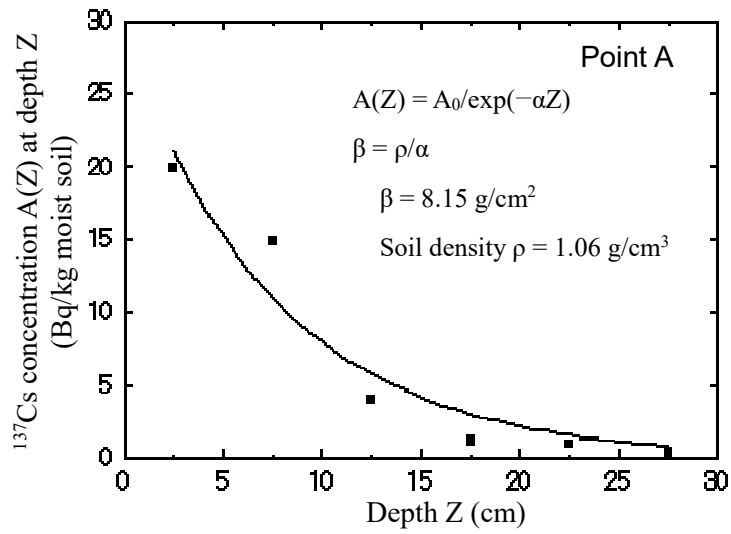


Figure H.1 Relationship between in-soil cesium-137 concentration and depth (Point A)

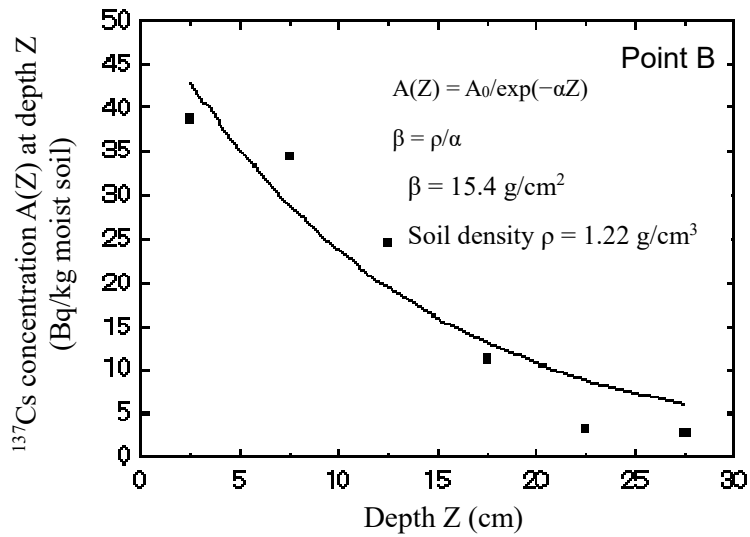
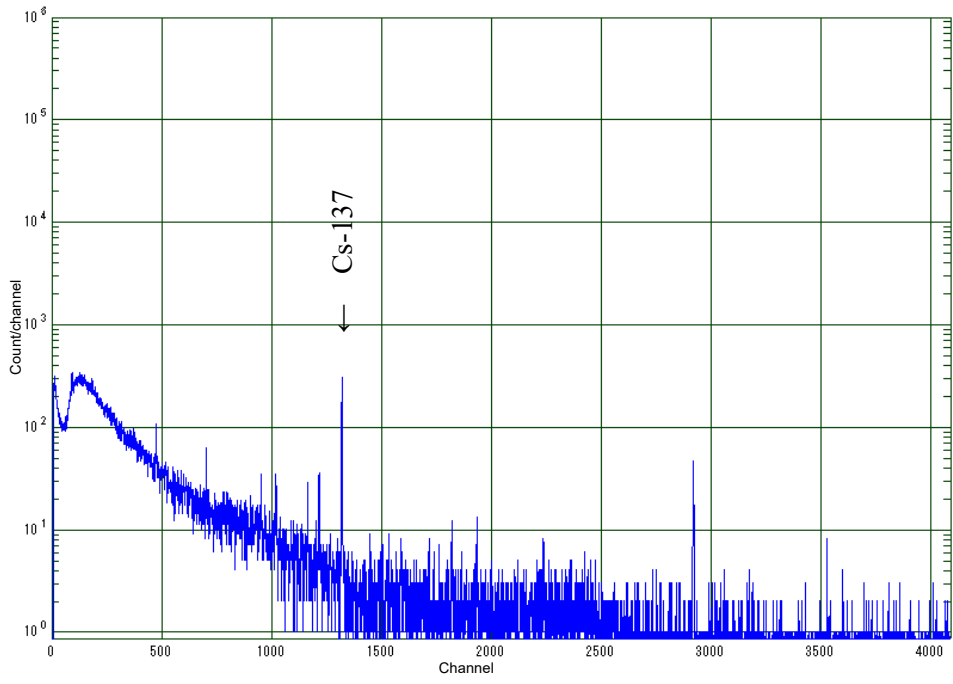
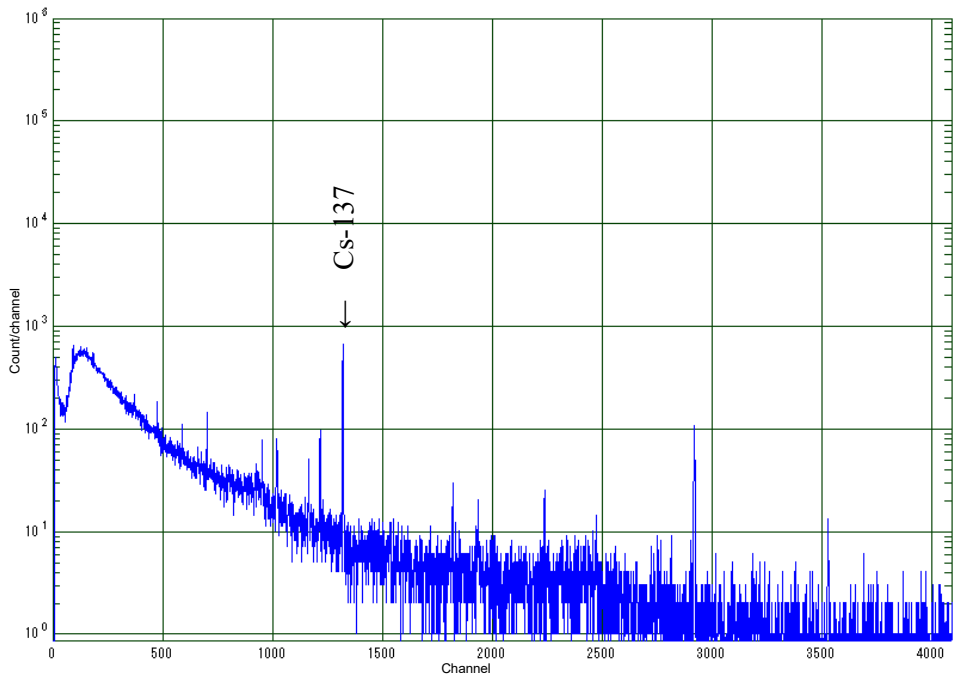


Figure H.2 Relationship between in-soil cesium-137 concentration and depth (Point B)



(Measuring time: 3600 s, 0.5 keV/channel)

Figure H.3 In-situ measurement spectrum using Ge detector
(Point A)



(Measuring time: 3600 s, 0.5 keV/channel)

Figure H.4 In-situ measurement spectrum using Ge detector
(Point B)

Explanation H.2 Naturally occurring radioactive materials

1. Purpose

To verify the validity of in-situ measurement for naturally occurring radioactive materials in the ground.

2. Methods considered

Both an in-situ measurement and measurement of a gamma-ray spectrum for a soil sample were conducted at the actual environmental site, and the results were compared.

(1) in-situ measurement

A location with an open area of at least 10 m around was selected. The Ge detector was installed at a height of 1 m from the ground, and the measurement was taken for 1 h. The resulting spectrum was analyzed using the HASL method to calculate the radioactivity concentration of naturally occurring radioactive materials in the ground.

(2) Soil sampling and measurement

Samples were taken near the measurement location using an auger. The soil samples were not allowed to dry, and they were placed in measurement containers (U-8) after large stones, etc. were removed. Then, the samples were measured in the laboratory for approximately 70000 s using a Ge detector, and the gamma-ray spectrum obtained was used to calculate radioactivity concentration.

3. Results and discussions

Table H.3 summarizes the results of the in-situ measurement and measured results of the soil sampled at every measurement location. The in-situ measurement and sampled soil measurement yielded very similar readings of naturally occurring radioactive nuclides. Note that the analysis of in-situ measurement was based on the assumption that the radioactive materials were distributed homogeneously in the ground.

Table H.5 indicates the relationship between the results of the in-situ measurement and measured results of the soil sampled at every measurement location. The results of the in-situ measurement and sampled soil measurement were well correlated.

Figure H.6 shows a view of the in-situ measurement, and Figure H.7 illustrates an example of a measured spectrum.

Table H.3 Comparison between in-situ measurement results and gamma-ray spectrometry of sampled soil

Unit: Bq/kg moist soil

Nuclides Sampling/measurement point	U series				Th series				K-40			
	²¹⁴ Pb (352.0keV)		²¹⁴ Bi (609.3keV)		²⁰⁸ Tl (583.1keV)		²¹² Pb (238.6keV)		²²⁸ Ac (911.1keV)		⁴⁰ K (1460.8keV)	
Point 1												
Composite sample	25 ±	1.0	23 ±	1.0	7.2 ±	0.47	24 ±	0.7	17 ±	1.6	380 ±	10
Core sample												
0~5cm	25 ±	0.8	22 ±	0.8	7.4 ±	0.32	23 ±	0.6	19 ±	1.1	370 ±	8
5~10cm	27 ±	0.8	23 ±	0.7	6.8 ±	0.29	23 ±	0.6	20 ±	0.9	350 ±	6
10~15cm	28 ±	1.2	25 ±	1.3	7.9 ±	0.58	25 ±	0.9	20 ±	2.0	360 ±	12
15~20cm	27 ±	0.8	23 ±	0.9	7.6 ±	0.34	22 ±	0.6	20 ±	1.2	370 ±	8
20~25cm	24 ±	1.2	20 ±	1.1	6.1 ±	0.44	24 ±	0.9	21 ±	1.4	320 ±	8
25~30cm	27 ±	1.1	24 ±	1.2	7.0 ±	0.53	23 ±	0.8	23 ±	2.0	360 ±	11
in-situ	19		21		7.6		17		22		430	
Point 2												
Composite sample	19 ±	0.6	16 ±	0.5	7.5 ±	0.26	26 ±	0.5	22 ±	0.8	470 ±	6
Core sample												
0~5cm	15 ±	0.9	16 ±	1.0	6.4 ±	0.48	24 ±	0.7	19 ±	1.7	410 ±	11
5~10cm	21 ±	0.6	17 ±	0.6	9.0 ±	0.31	28 ±	0.5	25 ±	1.0	470 ±	7
10~15cm	20 ±	0.6	16 ±	0.6	7.6 ±	0.26	26 ±	0.5	24 ±	0.8	470 ±	6
15~20cm	21 ±	1.0	20 ±	1.0	9.1 ±	0.50	31 ±	0.8	31 ±	1.8	510 ±	12
20~25cm	23 ±	0.7	20 ±	0.7	9.8 ±	0.31	29 ±	0.5	25 ±	1.1	500 ±	8
25~30cm	24 ±	0.8	21 ±	0.7	11 ±	0.3	37 ±	0.7	32 ±	1.1	530 ±	8
in-situ	16		18		9.3		23		24		490	
Point 3												
Composite sample	20 ±	0.7	20 ±	0.7	9.4 ±	0.33	29 ±	0.5	28 ±	1.1	500 ±	8
in-situ	17		18		11		26		29		530	

Composite sample: Mixed soil sampled from four corners of a 2-m square centering on the measurement point
 Core sample: Depth-layered soil sampled just under the measurement point
 The in-situ measurement results were analyzed assuming homogeneous distribution in the ground.

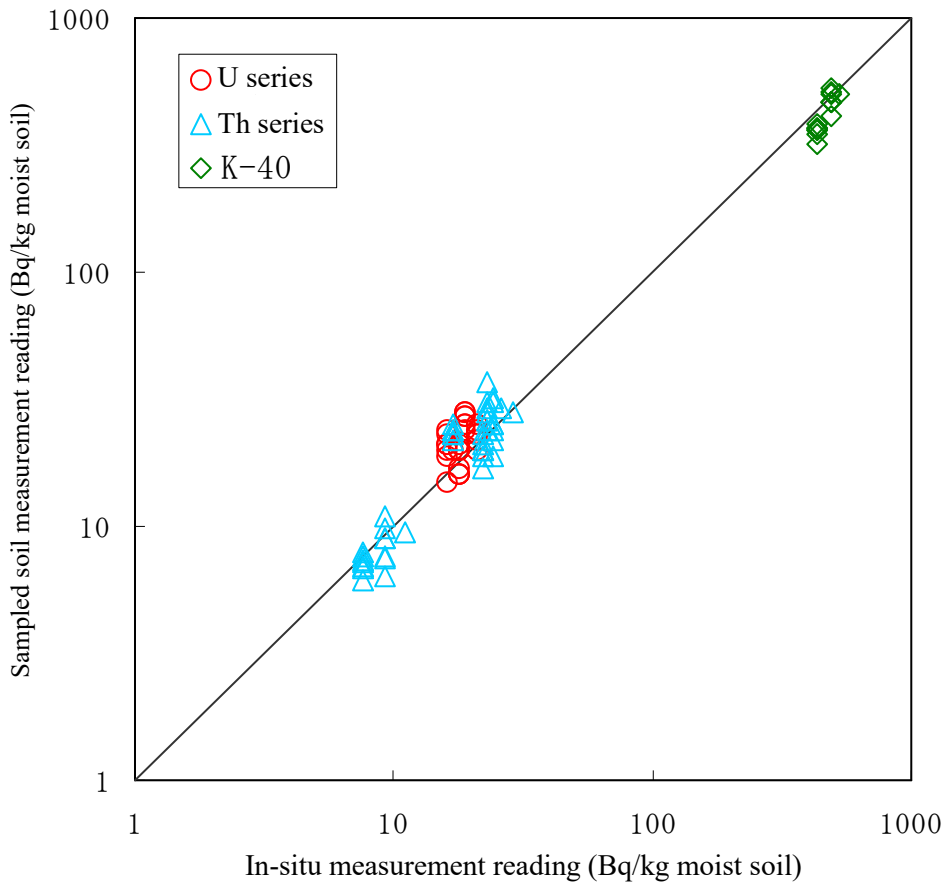
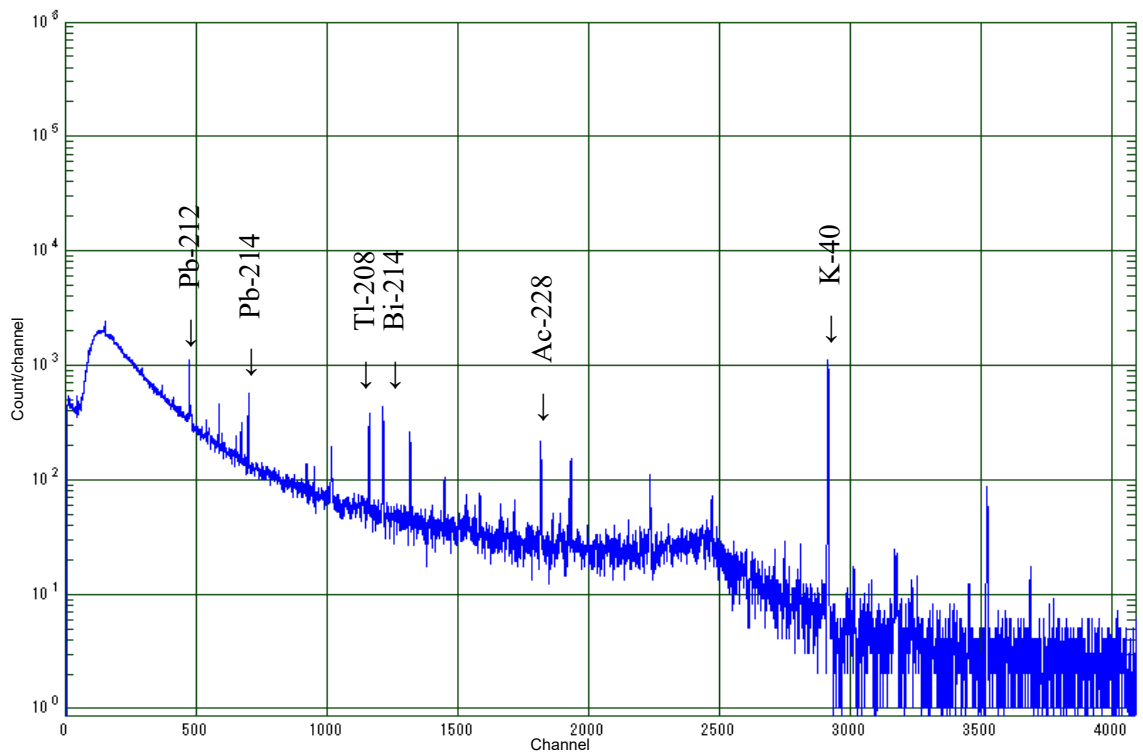


Figure H.5 Comparison between in-situ measured results and gamma-ray spectrometry of soil sampled at each location



Figure H.6 Performing an in-situ measurement



(Measuring time: 3600 s, 0.5 keV/channel)

Figure H.7 Example of in-situ measurement spectrum obtained by Ge detector

Explanation I Intercomparison measurement

The intercomparison of measurement equipment is an effective method to improve the reliability of in-situ measurement readings. Urgent in-situ measurement in a nuclear disaster is highly anticipated, and it is important to ascertain the equipment conditions regularly and routinely. If multiple pieces of measuring equipment are employed in surveying a wide area for the radioactivity distribution, it is advantageous to verify in advance that they are all equal in terms of measurement accuracy.

(1) Selection of location

See “4.1 Selection of the measurement site.”

(2) Verification of surrounding areas

Verify the areas near the location for the intercomparison measurement (ideally, an area of radius approximately 30 m), using a survey meter, etc., to ensure that there is a little difference in dose rate distribution in the areas.

(3) Measurement methods

The main measurement methods are the following two:

- (1) Simultaneous measurement using several detectors in a possibly small area (for example, on concentric circles), arranged such that they do not disrupt the measurements of one another (Figures I.1 and I.2)
- (2) Sequential measurement on the same point with alternating detectors

Owing to the possibility that circumstances may change with time at the measurement point, method (2) requires prompt execution of the measurement procedures.

To secure the validity of in-situ measurement readings, it is also recommended that the dose rate be measured at the same point simultaneously, using a survey meter.

(4) Evaluation of results

Compare the artificial and natural radionuclides detected separately. If correction is necessary owing to significant discrepancies between measurement points or changes in the environment, use the dose rates measured using a survey meter, which may help to mitigate the impact of such discrepancies on the comparisons (Figure I.3).



Figure I.1 Performing the intercomparison measurement (simultaneous measurement)^{*1}

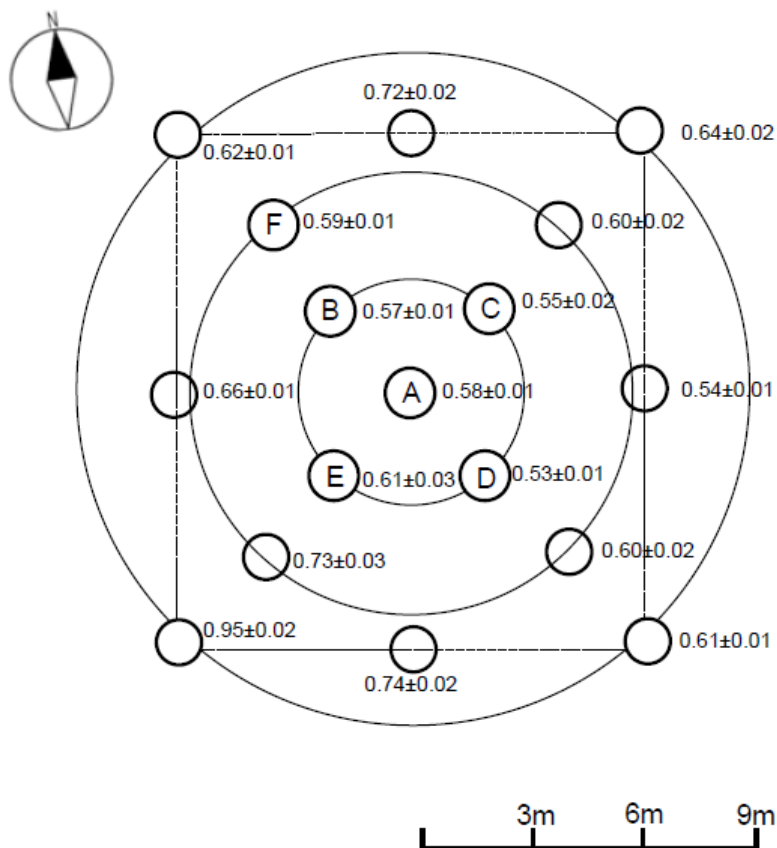


Figure I.2 Layout example of intercomparison measurement (simultaneous measurement)^{*1}
 (The smallest of the three concentric circles indicates the measurement points for dose rate using a survey meter. The figures indicated on the side are the dose rates (μSv/h) at 1 m above the ground in terms of the mean value and standard deviation (n = 5). Measurements were taken simultaneously with the Ge detectors installed at Points A to F for the intercomparison measurement.)

^{*1}“In Situ Gamma Spectrometry Intercomparison in Fukushima, Japan” S. Mikami, S. Sato, Y. Hoshide, R. Sakamoto, N. Okuda, K. Saito, Jpn. J. Health Phys., 50 (3), 182–188 (2015)

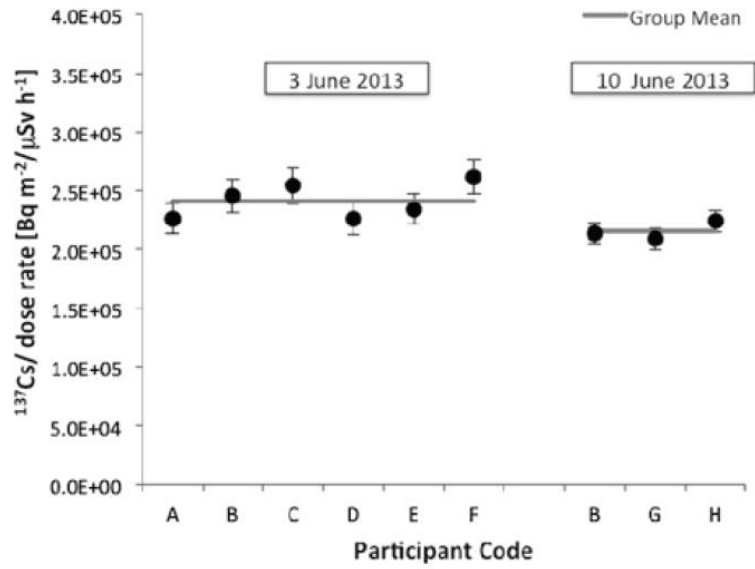


Figure I.3 Example of intercomparison measurement reading for cesium-137^{*1}
 (The vertical axis represents the dose rate (μSv/h) measured using a survey meter and cesium-137
 deposition amount (Bq/m²) measured using a Ge detector.)

Appendix

Appendix 1 Relationship between radionuclide activity and gamma-ray fluence rate 1 m
above ground

Appendix 2 Relationship between dose rate and gamma-ray fluence rate 1 m above
ground

Table-2-1 (continued)

Unit: (cm⁻²/s⁻¹) / (μGy/h)

Energy (keV)	Emission ratio (s ⁻¹ Bq ⁻¹)	Nuclides	Parameter β to indicate vertical distribution of radioactive materials in the ground (g/cm ⁻²)							
			0.0	0.1	0.2	0.3	0.5	1.0	2.0	
1030.1	0.126	Sb-129	4.43	4.32	4.23	4.19	4.08	3.93	3.73	
1038.8	0.080	I-135	2.70	2.64	2.58	2.56	2.48	2.39	2.27	
1048.1	0.798	Cs-136	1.89 1E+01	1.85 1E+01	1.82 1E+01	1.81 1E+01	1.76 1E+01	1.69 1E+01	1.61 1E+01	
1072.6	0.150	I-134	2.92	2.86	2.80	2.78	2.71	2.61	2.48	
1076.6	0.088	Rb-86	4.81 1E+01	4.69 1E+01	4.60 1E+01	4.56 1E+01	4.46 1E+01	4.28 1E+01	4.07 1E+01	
1085.9	0.099	Eu-152	4.54	4.43	4.33	4.30	4.19	4.05	3.85	
1099.2	0.565	Fe-59	2.53 1E+01	2.44 1E+01	2.41 1E+01	2.39 1E+01	2.33 1E+01	2.24 1E+01	2.13 1E+01	
1112.1	0.136	Eu-152	6.22	6.06	5.95	5.91	5.78	5.53	5.29	
1115.5	0.148	Ni-65	1.46 1E+01	1.43 1E+01	1.40 1E+01	1.39 1E+01	1.35 1E+01	1.30 1E+01	1.24 1E+01	
1115.5	0.507	Zn-65	4.20 1E+01	4.31 1E+01	4.28 1E+01	4.28 1E+01	4.19 1E+01	4.06 1E+01	3.85 1E+01	
1120.5	1.000	Sc-46	2.57 1E+01	2.50 1E+01	2.45 1E+01	2.43 1E+01	2.38 1E+01	2.29 1E+01	2.19 1E+01	
1121.3	0.349	Ta-182	1.38 1E+01	1.36 1E+01	1.35 1E+01	1.34 1E+01	1.31 1E+01	1.27 1E+01	1.21 1E+01	
1125.5	0.114	Te-131m	4.08	3.98	3.93	3.89	3.81	3.66	3.48	
1131.5	0.228	I-135	7.75	7.55	7.40	7.34	7.16	6.87	6.56	
1153.5	0.071	Eu-156	2.89	2.83	2.78	2.77	2.69	2.59	2.47	
1157.5	0.113	I-130	2.61	2.54	2.49	2.48	2.43	2.34	2.23	
1173.2	0.999	Co-60	2.14 1E+01	2.10 1E+01	2.06 1E+01	2.04 1E+01	1.99 1E+01	1.91 1E+01	1.83 1E+01	
1189.0	0.164	Ta-182	6.52	6.46	6.37	6.35	6.23	6.01	5.77	
1204.9	0.003	Y-91	4.44 1E+01	4.34 1E+01	4.27 1E+01	4.24 1E+01	4.15 1E+01	3.98 1E+01	3.80 1E+01	
1206.6	0.098	Te-131m	3.52	3.44	3.39	3.36	3.28	3.18	3.03	
1221.4	0.273	Ta-182	1.09 1E+01	1.08 1E+01	1.07 1E+01	1.06 1E+01	1.04 1E+01	1.01 1E+01	9.66	
1230.7	0.089	Eu-156	3.62	3.55	3.49	3.47	3.39	3.28	3.12	
1231.0	0.116	Ta-182	4.61	4.56	4.51	4.50	4.40	4.25	4.09	
1235.4	0.200	Cs-136	4.85	4.73	4.66	4.63	4.53	4.37	4.17	
1238.3	0.670	Co-56	1.11 1E+01	1.08 1E+01	1.07 1E+01	1.07 1E+01	1.03 1E+01	9.97	9.49	
1242.4	0.067	Eu-156	2.74	2.69	2.65	2.63	2.56	2.48	2.37	
1260.4	0.289	I-135	9.95	9.71	9.54	9.48	9.25	8.93	8.49	
1274.4	0.355	Eu-154	1.49 1E+01	1.47 1E+01	1.45 1E+01	1.44 1E+01	1.41 1E+01	1.37 1E+01	1.31 1E+01	
1274.5	0.999	Na-22	2.35 1E+01	2.30 1E+01	2.26 1E+01	2.24 1E+01	2.20 1E+01	2.12 1E+01	2.04 1E+01	
1291.6	0.432	Fe-59	1.96 1E+01	1.91 1E+01	1.88 1E+01	1.87 1E+01	1.82 1E+01	1.76 1E+01	1.68 1E+01	
1332.5	1.000	Co-60	2.17 1E+01	2.13 1E+01	2.09 1E+01	2.08 1E+01	2.03 1E+01	1.96 1E+01	1.88 1E+01	
1354.5	0.026	La-141	3.44 1E+01	3.35 1E+01	3.31 1E+01	3.28 1E+01	3.20 1E+01	3.10 1E+01	2.95 1E+01	
1368.6	1.000	Na-24	1.51 1E+01	1.47 1E+01	1.45 1E+01	1.44 1E+01	1.41 1E+01	1.35 1E+01	1.28 1E+01	
1383.9	0.900	Sr-92	3.73 1E+01	3.64 1E+01	3.58 1E+01	3.56 1E+01	3.49 1E+01	3.36 1E+01	3.22 1E+01	
1384.3	0.243	Ag-110m	4.59	4.52	4.44	4.42	4.33	4.19	4.01	
1408.0	0.209	Eu-152	9.81	9.58	9.43	9.42	9.21	8.90	8.53	
1435.9	0.763	Cs-138	1.84 1E+01	1.79 1E+01	1.76 1E+01	1.76 1E+01	1.71 1E+01	1.66 1E+01	1.58 1E+01	
1457.6	0.087	I-135	3.06	2.98	2.95	2.93	2.86	2.77	2.66	
1460.8	0.107	K-40	3.88 1E+01	3.79 1E+01	3.74 1E+01	3.72 1E+01	3.64 1E+01	3.51 1E+01	3.34 1E+01	
1465.1	0.222	Pm-148	2.09 1E+01	2.05 1E+01	2.01 1E+01	2.00 1E+01	1.96 1E+01	1.90 1E+01	1.83 1E+01	
1481.8	0.235	Ni-65	2.40 1E+01	2.33 1E+01	2.30 1E+01	2.29 1E+01	2.24 1E+01	2.17 1E+01	2.08 1E+01	
1505.0	0.131	Ag-110m	2.50	2.45	2.42	2.41	2.36	2.29	2.20	
1524.6	0.189	K-42	3.73 1E+01	3.65 1E+01	3.60 1E+01	3.59 1E+01	3.51 1E+01	3.39 1E+01	3.25 1E+01	
1596.2	0.954	La-140	2.33 1E+01	2.28 1E+01	2.24 1E+01	2.24 1E+01	2.19 1E+01	2.13 1E+01	2.04 1E+01	
1678.0	0.096	I-135	3.42	3.34	3.30	3.29	3.22	3.13	3.01	
1691.0	0.488	Sb-124	1.46 1E+01	1.43 1E+01	1.41 1E+01	1.41 1E+01	1.38 1E+01	1.34 1E+01	1.29 1E+01	
1736.5	0.060	Sb-129	2.21	2.18	2.15	2.15	2.10	2.05	1.97	
1771.4	0.155	Co-56	2.67	2.62	2.60	2.59	2.55	2.47	2.37	
1791.2	0.078	I-135	2.78	2.72	2.69	2.67	2.63	2.55	2.46	
1810.7	0.272	Mn-56	9.24	9.03	8.94	8.88	8.73	8.53	8.17	
1897.6	0.147	Br-84	5.18	5.08	5.02	4.99	4.90	4.77	4.57	
1901.3	0.072	La-142	1.89	1.84	1.83	1.82	1.78	1.73	1.66	
2091.0	0.056	Sb-124	1.72	1.69	1.66	1.67	1.63	1.60	1.54	
2113.0	0.143	Mn-56	4.96	4.86	4.82	4.79	4.71	4.63	4.45	
2218.0	0.152	Cs-138	3.83	3.75	3.72	3.70	3.65	3.56	3.43	
2397.8	0.133	La-142	3.58	3.52	3.48	3.47	3.41	3.33	3.23	
2484.1	0.067	Br-84	2.43	2.39	2.37	2.36	2.33	2.27	2.20	
2542.7	0.100	La-142	2.71	2.67	2.65	2.62	2.59	2.53	2.45	
2598.6	0.167	Co-56	2.99	2.97	2.96	2.95	2.90	2.84	2.76	
2639.6	0.076	Cs-138	1.96	1.93	1.91	1.90	1.88	1.84	1.79	
2754.0	0.999	Na-24	1.63 1E+01	1.61 1E+01	1.59 1E+01	1.58 1E+01	1.56 1E+01	1.53 1E+01	1.48 1E+01	
3253.5	0.074	Co-56	1.35	1.35	1.35	1.34	1.33	1.30	1.28	
3927.5	0.068	Br-84	2.61	2.58	2.55	2.55	2.53	2.49	2.44	

Table-2-1 (continued)

Unit: (cm⁻²/s⁻¹) / (μGy/h)

Energy (keV)	Emission ratio (s ⁻¹ Bq ⁻¹)	Nuclides	Parameter β to indicate vertical distribution of radioactive materials in the ground (g/cm ⁻²)							
			3.0	5.0	10	20	30	50	100	
1030.1	0.126	Sb-129	3.58	3.42	3.16	2.92	2.82	2.70	2.61	
1038.8	0.080	I-135	2.18	2.06	1.89	1.73	1.67	1.59	1.52	
1048.1	0.798	Cs-136	1.55 1E+01	1.48 1E+01	1.37 1E+01	1.27 1E+01	1.23 1E+01	1.19 1E+01	1.15 1E+01	
1072.6	0.150	I-134	2.38	2.29	2.11	1.96	1.90	1.82	1.77	
1076.6	0.088	Rb-86	3.94 1E+01	3.73 1E+01	3.45 1E+01	3.18 1E+01	3.06 1E+01	2.95 1E+01	2.84 1E+01	
1085.9	0.099	Eu-152	3.71	3.53	3.28	3.05	2.94	2.84	2.76	
1099.2	0.565	Fe-59	2.05 1E+01	1.94 1E+01	1.80 1E+01	1.66 1E+01	1.59 1E+01	1.52 1E+01	1.47 1E+01	
1112.1	0.136	Eu-152	5.09	4.86	4.53	4.21	4.07	3.92	3.82	
1115.5	0.148	Ni-65	1.19 1E+01	1.12 1E+01	1.04 1E+01	9.55	9.14	8.78	8.45	
1115.5	0.507	Zn-65	3.72 1E+01	3.55 1E+01	3.28 1E+01	3.03 1E+01	2.93 1E+01	2.80 1E+01	2.72 1E+01	
1120.5	1.000	Sc-46	2.11 1E+01	2.01 1E+01	1.86 1E+01	1.73 1E+01	1.67 1E+01	1.60 1E+01	1.56 1E+01	
1121.3	0.349	Ta-182	1.17 1E+01	1.12 1E+01	1.05 1E+01	9.65	9.35	9.02	8.71	
1125.5	0.114	Te-131m	3.39	3.23	3.01	2.81	2.73	2.64	2.56	
1131.5	0.228	I-135	6.30	5.98	5.53	5.09	4.88	4.68	4.49	
1153.5	0.071	Eu-156	2.37	2.26	2.08	1.92	1.84	1.76	1.69	
1157.5	0.113	I-130	2.16	2.07	1.94	1.84	1.80	1.74	1.70	
1173.2	0.999	Co-60	1.76 1E+01	1.67 1E+01	1.55 1E+01	1.43 1E+01	1.37 1E+01	1.32 1E+01	1.27 1E+01	
1189.0	0.164	Ta-182	5.59	5.36	5.00	4.64	4.49	4.34	4.22	
1204.9	0.003	Y-91	3.66 1E+01	3.48 1E+01	3.24 1E+01	3.00 1E+01	2.88 1E+01	2.78 1E+01	2.68 1E+01	
1206.6	0.098	Te-131m	2.94	2.81	2.63	2.47	2.39	2.31	2.26	
1221.4	0.273	Ta-182	9.34	9.00	8.43	7.82	7.57	7.33	7.11	
1230.7	0.089	Eu-156	3.00	2.87	2.65	2.45	2.36	2.26	2.18	
1231.0	0.116	Ta-182	3.95	3.81	3.56	3.31	3.21	3.11	3.01	
1235.4	0.200	Cs-136	4.05	3.86	3.62	3.41	3.30	3.20	3.12	
1238.3	0.670	Co-56	9.14	8.69	8.00	7.39	7.07	6.76	6.52	
1242.4	0.067	Eu-156	2.27	2.17	2.01	1.86	1.79	1.71	1.65	
1260.4	0.289	I-135	8.20	7.80	7.26	6.75	6.47	6.22	5.99	
1274.4	0.355	Eu-154	1.27 1E+01	1.22 1E+01	1.14 1E+01	1.07 1E+01	1.04 1E+01	1.01 1E+01	9.86	
1274.5	0.999	Na-22	1.96 1E+01	1.88 1E+01	1.77 1E+01	1.67 1E+01	1.62 1E+01	1.56 1E+01	1.52 1E+01	
1291.6	0.432	Fe-59	1.62 1E+01	1.55 1E+01	1.45 1E+01	1.35 1E+01	1.30 1E+01	1.25 1E+01	1.21 1E+01	
1332.5	1.000	Co-60	1.81 1E+01	1.73 1E+01	1.61 1E+01	1.50 1E+01	1.45 1E+01	1.40 1E+01	1.35 1E+01	
1354.5	0.026	La-141	2.85 1E+01	2.72 1E+01	2.52 1E+01	2.35 1E+01	2.25 1E+01	2.17 1E+01	2.09 1E+01	
1368.6	1.000	Na-24	1.24 1E+01	1.17 1E+01	1.08 1E+01	9.87	9.34	8.92	8.50	
1383.9	0.900	Sr-92	3.11 1E+01	2.98 1E+01	2.77 1E+01	2.58 1E+01	2.49 1E+01	2.40 1E+01	2.32 1E+01	
1384.3	0.243	Ag-110m	3.89	3.74	3.50	3.35	3.24	3.15	3.08	
1408.0	0.209	Eu-152	8.29	7.99	7.52	7.13	6.90	6.72	6.58	
1435.9	0.763	Cs-138	1.53 1E+01	1.47 1E+01	1.37 1E+01	1.28 1E+01	1.22 1E+01	1.19 1E+01	1.15 1E+01	
1457.6	0.087	I-135	2.57	2.46	2.30	2.17	2.08	2.01	1.95	
1460.8	0.107	K-40	3.26 1E+01	3.11 1E+01	2.91 1E+01	2.72 1E+01	2.60 1E+01	2.52 1E+01	2.43 1E+01	
1465.1	0.222	Pm-148	1.77 1E+01	1.70 1E+01	1.59 1E+01	1.51 1E+01	1.46 1E+01	1.42 1E+01	1.39 1E+01	
1481.8	0.235	Ni-65	2.02 1E+01	1.93 1E+01	1.80 1E+01	1.70 1E+01	1.63 1E+01	1.58 1E+01	1.53 1E+01	
1505.0	0.131	Ag-110m	2.14	2.06	1.94	1.86	1.81	1.76	1.73	
1524.6	0.189	K-42	3.14 1E+01	3.00 1E+01	2.80 1E+01	2.63 1E+01	2.52 1E+01	2.43 1E+01	2.35 1E+01	
1596.2	0.954	La-140	1.98 1E+01	1.90 1E+01	1.78 1E+01	1.69 1E+01	1.63 1E+01	1.58 1E+01	1.54 1E+01	
1678.0	0.096	I-135	2.93	2.81	2.65	2.52	2.42	2.35	2.29	
1691.0	0.488	Sb-124	1.25 1E+01	1.21 1E+01	1.14 1E+01	1.09 1E+01	1.05 1E+01	1.03 1E+01	1.00 1E+01	
1736.5	0.060	Sb-129	1.92	1.86	1.78	1.70	1.65	1.61	1.58	
1771.4	0.155	Co-56	2.30	2.22	2.09	1.97	1.91	1.84	1.80	
1791.2	0.078	I-135	2.40	2.31	2.18	2.08	2.01	1.96	1.91	
1810.7	0.272	Mn-56	7.96	7.69	7.30	6.91	6.72	6.50	6.34	
1897.6	0.147	Br-84	4.44	4.28	4.02	3.78	3.64	3.51	3.40	
1901.3	0.072	La-142	1.62	1.55	1.46	1.37	1.33	1.28	1.24	
2091.0	0.056	Sb-124	1.51	1.47	1.40	1.35	1.32	1.30	1.27	
2113.0	0.143	Mn-56	4.35	4.21	4.04	3.86	3.78	3.67	3.59	
2218.0	0.152	Cs-138	3.37	3.25	3.13	2.98	2.91	2.85	2.79	
2397.8	0.133	La-142	3.16	3.05	2.90	2.77	2.70	2.62	2.54	
2484.1	0.067	Br-84	2.16	2.09	1.99	1.90	1.85	1.80	1.75	
2542.7	0.100	La-142	2.41	2.33	2.23	2.13	2.09	2.02	1.97	
2598.6	0.167	Co-56	2.72	2.65	2.53	2.44	2.40	2.34	2.30	
2639.6	0.076	Cs-138	1.76	1.71	1.66	1.60	1.57	1.55	1.52	
2754.0	0.999	Na-24	1.46 1E+01	1.41 1E+01	1.34 1E+01	1.28 1E+01	1.24 1E+01	1.22 1E+01	1.18 1E+01	
3253.5	0.074	Co-56	1.26	1.24	1.20	1.17	1.16	1.13	1.13	
3927.5	0.068	Br-84	2.41	2.37	2.32	2.26	2.23	2.20	2.18	

Table-2-2 Relationship between dose rate and gamma-ray fluence rate at 1 m above ground

Unit: (cm⁻²/s⁻¹) / (μSv/h)

Energy (keV)	Conversion ratio (s ⁻¹ Bq ⁻¹)	Nuclides	Parameter β to indicate vertical distribution of radioactive materials in the ground (g/cm ⁻²)							
			0.0	0.1	0.2	0.3	0.5	1.0	2.0	

Table-2-2 (continued)

Unit: (cm⁻²/s⁻¹) / (μSv/h)

Energy (keV)	Emission ratio (s ⁻¹ Bq ⁻¹)	Nuclides	Parameter β to indicate vertical distribution of radioactive materials in the ground (g/cm ⁻²)							
			0.0	0.1	0.2	0.3	0.5	1.0	2.0	
1030.1	0.126	Sb-129	3.65	3.57	3.49	3.44	3.36	3.22	3.04	
1038.8	0.080	I-135	2.26	2.22	2.17	2.14	2.08	1.99	1.89	
1048.1	0.798	Cs-136	1.54 1E+01	1.52 1E+01	1.49 1E+01	1.47 1E+01	1.43 1E+01	1.37 1E+01	1.30 1E+01	
1072.6	0.150	I-134	2.42	2.36	2.33	2.30	2.24	2.14	2.03	
1076.6	0.088	Rb-86	4.09 1E+01	4.01 1E+01	3.92 1E+01	3.86 1E+01	3.74 1E+01	3.59 1E+01	3.42 1E+01	
1085.9	0.099	Eu-152	3.45	3.41	3.35	3.31	3.24	3.14	2.99	
1099.2	0.565	Fe-59	2.11 1E+01	2.06 1E+01	2.02 1E+01	2.00 1E+01	1.94 1E+01	1.86 1E+01	1.77 1E+01	
1112.1	0.136	Eu-152	4.74	4.67	4.60	4.55	4.46	4.30	4.11	
1115.5	0.148	Ni-65	1.21 1E+01	1.18 1E+01	1.15 1E+01	1.15 1E+01	1.12 1E+01	1.07 1E+01	1.01 1E+01	
1115.5	0.507	Zn-65	3.82 1E+01	3.75 1E+01	3.66 1E+01	3.62 1E+01	3.51 1E+01	3.37 1E+01	3.22 1E+01	
1120.5	1.000	Sc-46	2.13 1E+01	2.09 1E+01	2.05 1E+01	2.02 1E+01	1.96 1E+01	1.89 1E+01	1.80 1E+01	
1121.3	0.349	Ta-182	1.15 1E+01	1.13 1E+01	1.11 1E+01	1.10 1E+01	1.07 1E+01	1.03 1E+01	9.86	
1125.5	0.114	Te-131m	3.22	3.17	3.12	3.08	3.01	2.89	2.74	
1131.5	0.228	I-135	6.49	6.35	6.22	6.15	6.00	5.74	5.46	
1153.5	0.071	Eu-156	2.65	2.60	2.56	2.53	2.45	2.37	2.25	
1157.5	0.113	I-130	2.09	2.04	2.00	1.99	1.94	1.86	1.77	
1173.2	0.999	Co-60	1.80 1E+01	1.77 1E+01	1.74 1E+01	1.71 1E+01	1.67 1E+01	1.60 1E+01	1.52 1E+01	
1189.0	0.164	Ta-182	5.46	5.35	5.25	5.21	5.08	4.89	4.69	
1204.9	0.003	Y-91	3.73 1E+01	3.65 1E+01	3.58 1E+01	3.55 1E+01	3.45 1E+01	3.31 1E+01	3.16 1E+01	
1206.6	0.098	Te-131m	2.78	2.74	2.69	2.66	2.59	2.51	2.39	
1221.4	0.273	Ta-182	9.10	8.95	8.79	8.71	8.49	8.22	7.85	
1230.7	0.089	Eu-156	3.32	3.27	3.20	3.17	3.10	2.99	2.84	
1231.0	0.116	Ta-182	3.86	3.78	3.72	3.69	3.59	3.47	3.32	
1235.4	0.200	Cs-136	3.93	3.89	3.80	3.76	3.66	3.53	3.36	
1238.3	0.670	Co-56	8.80	8.61	8.51	8.37	8.16	7.83	7.47	
1242.4	0.067	Eu-156	2.52	2.47	2.43	2.40	2.34	2.26	2.15	
1260.4	0.289	I-135	8.34	8.16	8.02	7.94	7.74	7.45	7.07	
1274.4	0.355	Eu-154	1.33 1E+01	1.31 1E+01	1.29 1E+01	1.28 1E+01	1.25 1E+01	1.21 1E+01	1.16 1E+01	
1274.5	0.999	Na-22	1.91 1E+01	1.89 1E+01	1.85 1E+01	1.83 1E+01	1.79 1E+01	1.72 1E+01	1.65 1E+01	
1291.6	0.432	Fe-59	1.63 1E+01	1.61 1E+01	1.58 1E+01	1.56 1E+01	1.52 1E+01	1.46 1E+01	1.39 1E+01	
1332.5	1.000	Co-60	1.83 1E+01	1.80 1E+01	1.76 1E+01	1.74 1E+01	1.70 1E+01	1.64 1E+01	1.57 1E+01	
1354.5	0.026	La-141	4.63 1E+01	4.57 1E+01	4.49 1E+01	4.46 1E+01	4.34 1E+01	4.17 1E+01	3.97 1E+01	
1368.6	1.000	Na-24	1.29 1E+01	1.26 1E+01	1.25 1E+01	1.24 1E+01	1.21 1E+01	1.16 1E+01	1.10 1E+01	
1383.9	0.900	Sr-92	3.14 1E+01	3.08 1E+01	3.02 1E+01	3.01 1E+01	2.95 1E+01	2.82 1E+01	2.69 1E+01	
1384.3	0.243	Ag-110m	3.82	3.74	3.68	3.67	3.58	3.45	3.29	
1408.0	0.209	Eu-152	7.46	7.38	7.29	7.25	7.11	6.91	6.64	
1435.9	0.763	Cs-138	1.54 1E+01	1.51 1E+01	1.48 1E+01	1.47 1E+01	1.43 1E+01	1.39 1E+01	1.32 1E+01	
1457.6	0.087	I-135	2.57	2.51	2.48	2.45	2.40	2.31	2.21	
1460.8	0.107	K-40	3.30 1E+01	3.22 1E+01	3.18 1E+01	3.16 1E+01	3.09 1E+01	2.98 1E+01	2.82 1E+01	
1465.1	0.222	Pm-148	1.73 1E+01	1.70 1E+01	1.67 1E+01	1.66 1E+01	1.63 1E+01	1.57 1E+01	1.50 1E+01	
1481.8	0.235	Ni-65	1.97 1E+01	1.93 1E+01	1.91 1E+01	1.89 1E+01	1.85 1E+01	1.79 1E+01	1.70 1E+01	
1505.0	0.131	Ag-110m	2.08	2.03	2.01	2.00	1.95	1.89	1.81	
1524.6	0.189	K-42	3.29 1E+01	3.24 1E+01	3.19 1E+01	3.19 1E+01	3.12 1E+01	3.00 1E+01	2.86 1E+01	
1596.2	0.954	La-140	1.95 1E+01	1.91 1E+01	1.87 1E+01	1.87 1E+01	1.83 1E+01	1.77 1E+01	1.69 1E+01	
1678.0	0.096	I-135	2.87	2.81	2.77	2.76	2.69	2.61	2.51	
1691.0	0.488	Sb-124	1.21 1E+01	1.19 1E+01	1.17 1E+01	1.17 1E+01	1.14 1E+01	1.11 1E+01	1.06 1E+01	
1736.5	0.060	Sb-129	1.82	1.80	1.78	1.76	1.73	1.68	1.61	
1771.4	0.155	Co-56	2.13	2.08	2.06	2.04	2.01	1.94	1.86	
1791.2	0.078	I-135	2.33	2.29	2.26	2.24	2.20	2.13	2.05	
1810.7	0.272	Mn-56	7.73	7.59	7.52	7.43	7.31	7.12	6.81	
1901.3	0.072	La-142	1.59	1.56	1.55	1.54	1.51	1.46	1.40	
2091.0	0.056	Sb-124	1.42	1.40	1.38	1.38	1.36	1.32	1.27	
2113.0	0.143	Mn-56	4.14	4.09	4.05	4.01	3.95	3.86	3.71	
2218.0	0.152	Cs-138	3.21	3.16	3.13	3.11	3.06	2.98	2.86	
2397.8	0.133	La-142	3.01	2.98	2.95	2.94	2.89	2.82	2.73	
2542.7	0.100	La-142	2.28	2.26	2.24	2.22	2.19	2.14	2.07	
2598.6	0.167	Co-56	2.38	2.36	2.35	2.32	2.29	2.23	2.18	
2639.6	0.076	Cs-138	1.64	1.63	1.61	1.60	1.58	1.54	1.49	
2754.0	0.999	Na-24	1.39 1E+01	1.38 1E+01	1.37 1E+01	1.36 1E+01	1.34 1E+01	1.31 1E+01	1.26 1E+01	
3253.5	0.074	Co-56	1.08	1.07	1.07	1.05	1.05	1.02	1.00	

Table-2-2 (continued)

Unit: (cm⁻²/s⁻¹) / (µSv/h)

Energy (keV)	Emission ratio (s ⁻¹ Bq ⁻¹)	Nuclides	Parameter β to indicate vertical distribution of radioactive materials in the ground (g/cm ⁻²)							
			3.0	5.0	10	20	30	50	100	
345.9	0.120	Hf-181	5.16	4.77	4.27	3.87	3.75	3.58	3.44	
364.5	0.812	I-131	4.84 1E+01	4.47 1E+01	3.98 1E+01	3.62 1E+01	3.46 1E+01	3.33 1E+01	3.18 1E+01	
400.7	0.116	Se-75	6.79	6.33	5.80	5.39	5.23	5.10	4.96	
402.5	0.690	Cm-247	5.12 1E+01	4.72 1E+01	4.22 1E+01	3.84 1E+01	3.71 1E+01	3.56 1E+01	3.42 1E+01	
414.8	0.833	Sb-126	7.63	7.05	6.22	5.57	5.34	5.05	4.78	
417.9	0.010	Te-127	4.79 1E+01	4.42 1E+01	3.96 1E+01	3.62 1E+01	3.48 1E+01	3.36 1E+01	3.21 1E+01	
418.0	0.341	I-130	4.05	3.74	3.30	2.96	2.84	2.69	2.55	
427.9	0.294	Sb-125	1.68 1E+01	1.57 1E+01	1.40 1E+01	1.27 1E+01	1.22 1E+01	1.16 1E+01	1.11 1E+01	
435.1	0.186	Te-134	5.33	4.97	4.43	4.03	3.88	3.69	3.53	
438.6	0.949	Zn-69m	5.47 1E+01	5.07 1E+01	4.54 1E+01	4.12 1E+01	3.97 1E+01	3.81 1E+01	3.67 1E+01	
459.6	0.074	Te-129	3.08 1E+01	2.88 1E+01	2.59 1E+01	2.37 1E+01	2.29 1E+01	2.18 1E+01	2.09 1E+01	
461.0	0.099	Te-134	2.88	2.69	2.40	2.19	2.11	2.01	1.93	
462.8	0.307	Cs-138	3.94	3.63	3.15	2.79	2.61	2.44	2.28	
463.4	0.105	Sb-125	6.10	5.69	5.10	4.64	4.49	4.27	4.08	
469.4	0.175	Ru-105	6.09	5.68	5.05	4.56	4.38	4.15	3.95	
473.0	0.247	Sb-127	9.26	8.59	7.65	6.91	6.65	6.31	6.04	
477.6	0.103	Be-7	5.10 1E+01	4.76 1E+01	4.25 1E+01	3.86 1E+01	3.74 1E+01	3.57 1E+01	3.44 1E+01	
479.5	0.253	W-187	1.47 1E+01	1.38 1E+01	1.23 1E+01	1.12 1E+01	1.08 1E+01	1.03 1E+01	9.85	
479.5	0.900	Y-90m	3.44 1E+01	3.22 1E+01	2.90 1E+01	2.67 1E+01	2.59 1E+01	2.49 1E+01	2.41 1E+01	
482.0	0.830	Hf-181	3.87 1E+01	3.62 1E+01	3.29 1E+01	3.02 1E+01	2.95 1E+01	2.83 1E+01	2.74 1E+01	
487.0	0.459	La-140	5.99	5.54	4.84	4.28	4.03	3.75	3.53	
497.1	0.889	Ru-103	4.54 1E+01	4.22 1E+01	3.79 1E+01	3.44 1E+01	3.34 1E+01	3.18 1E+01	3.05 1E+01	
507.7	0.053	Zr-97	1.66	1.54	1.38	1.24	1.18	1.11	1.06	
511.0	0.301	Co-58	8.47	7.91	7.01	6.33	6.04	5.70	5.43	
511.0	1.810	Na-22	2.33 1E+01	2.16 1E+01	1.91 1E+01	1.71 1E+01	1.64 1E+01	1.53 1E+01	1.46 1E+01	
511.9	0.207	Rh-106	2.67 1E+01	2.49 1E+01	2.21 1E+01	2.00 1E+01	1.93 1E+01	1.84 1E+01	1.75 1E+01	
526.5	0.450	Sb-128	3.95	3.69	3.27	2.97	2.85	2.69	2.57	
529.9	0.863	I-133	3.74 1E+01	3.49 1E+01	3.12 1E+01	2.82 1E+01	2.74 1E+01	2.59 1E+01	2.48 1E+01	
531.0	0.131	Nd-147	2.50 1E+01	2.40 1E+01	2.25 1E+01	2.10 1E+01	2.06 1E+01	2.00 1E+01	1.94 1E+01	
536.1	0.990	I-130	1.25 1E+01	1.16 1E+01	1.04 1E+01	9.43	9.06	8.62	8.20	
537.3	0.244	Ba-140	3.49 1E+01	3.28 1E+01	2.96 1E+01	2.71 1E+01	2.63 1E+01	2.52 1E+01	2.42 1E+01	
544.7	0.179	Sb-129	3.57	3.34	2.95	2.65	2.52	2.38	2.24	
550.3	0.220	Pm-148	1.14 1E+01	1.06 1E+01	9.37	8.37	7.98	7.45	7.07	
550.3	0.944	Pm-148m	1.28 1E+01	1.20 1E+01	1.07 1E+01	9.72	9.37	8.92	8.52	
551.5	0.059	W-187	3.52	3.32	2.99	2.73	2.65	2.53	2.43	
555.6	0.949	Y-91m	4.75 1E+01	4.42 1E+01	3.98 1E+01	3.62 1E+01	3.50 1E+01	3.34 1E+01	3.21 1E+01	
566.0	0.183	Te-134	5.58	5.23	4.74	4.36	4.21	4.04	3.87	
569.3	0.150	Cs-134	2.67	2.50	2.23	2.02	1.95	1.84	1.75	
600.6	0.178	Sb-125	1.10 1E+01	1.03 1E+01	9.38	8.63	8.41	8.05	7.69	
602.7	0.979	Sb-124	1.62 1E+01	1.51 1E+01	1.34 1E+01	1.20 1E+01	1.14 1E+01	1.08 1E+01	1.01 1E+01	
604.6	0.975	Cs-134	1.76 1E+01	1.65 1E+01	1.48 1E+01	1.34 1E+01	1.29 1E+01	1.22 1E+01	1.17 1E+01	
606.6	0.050	Sb-125	3.11	2.93	2.66	2.45	2.38	2.28	2.18	
610.3	0.056	Ru-103	2.98	2.78	2.53	2.31	2.26	2.17	2.08	
618.4	0.073	W-187	4.45	4.21	3.82	3.51	3.42	3.26	3.13	
621.8	0.098	Rh-106	1.32 1E+01	1.23 1E+01	1.11 1E+01	1.01 1E+01	9.82	9.37	8.92	
628.7	0.310	Sb-128	2.82	2.64	2.38	2.17	2.09	1.99	1.90	
630.0	0.886	Pm-148m	1.24 1E+01	1.16 1E+01	1.05 1E+01	9.58	9.25	8.84	8.43	
635.9	0.113	Sb-125	7.09	6.68	6.07	5.60	5.45	5.24	5.01	
636.2	0.360	Sb-128	3.30	3.08	2.77	2.53	2.43	2.33	2.21	
637.0	0.073	I-131	4.93	4.63	4.23	3.94	3.84	3.71	3.58	
641.3	0.474	La-142	6.96	6.44	5.66	5.02	4.71	4.40	4.09	
647.5	0.194	Te-133m	3.13	2.95	2.63	2.38	2.27	2.16	2.06	
657.7	0.947	Ag-110m	1.04 1E+01	9.74	8.71	7.89	7.58	7.20	6.80	
657.9	0.983	Nb-97	4.19 1E+01	3.91 1E+01	3.54 1E+01	3.23 1E+01	3.13 1E+01	2.98 1E+01	2.83 1E+01	
661.6	0.899	Ba-137m	4.26 1E+01	4.02 1E+01	3.61 1E+01	3.30 1E+01	3.20 1E+01	3.05 1E+01	2.89 1E+01	
664.5	0.053	Ce-143	5.18	4.94	4.59	4.30	4.19	4.06	3.93	
666.3	0.997	Sb-126	1.02 1E+01	9.55	8.64	7.91	7.65	7.32	6.95	
667.7	0.987	I-132	1.28 1E+01	1.20 1E+01	1.08 1E+01	9.83	9.44	9.00	8.52	
668.5	0.961	I-130	1.27 1E+01	1.19 1E+01	1.08 1E+01	9.87	9.53	9.13	8.69	
676.4	0.157	Ru-105	5.89	5.55	5.02	4.62	4.48	4.28	4.08	
685.7	0.353	Sb-127	1.44 1E+01	1.35 1E+01	1.22 1E+01	1.12 1E+01	1.09 1E+01	1.04 1E+01	9.95	
685.8	0.316	W-187	1.98 1E+01	1.88 1E+01	1.71 1E+01	1.58 1E+01	1.54 1E+01	1.48 1E+01	1.42 1E+01	
695.0	0.997	Sb-126	1.03 1E+01	8.91	8.72	8.01	7.78	7.45	7.07	
697.0	0.289	Sb-126	2.98	2.79	2.53	2.32	2.25	2.15	2.05	

Table-2-2 (continued)

Unit: (cm⁻²/s⁻¹) / (μSv/h)

Energy (keV)	Emission ratio (s ⁻¹ Bq ⁻¹)	Nuclides	Parameter β to indicate vertical distribution of radioactive materials in the ground (g/cm ⁻²)							
			3.0	5.0	10	20	30	50	100	
1030.1	0.126	Sb-129	2.91	2.77	2.55	2.35	2.28	2.18	2.09	
1038.8	0.080	I-135	1.81	1.71	1.56	1.42	1.38	1.31	1.25	
1048.1	0.798	Cs-136	1.25 1E+01	1.19 1E+01	1.09 1E+01	1.01 1E+01	9.82	9.46	9.15	
1072.6	0.150	I-134	1.94	1.86	1.71	1.58	1.54	1.47	1.42	
1076.6	0.088	Rb-86	3.30 1E+01	3.14 1E+01	2.86 1E+01	2.64 1E+01	2.54 1E+01	2.44 1E+01	2.34 1E+01	
1085.9	0.099	Eu-152	2.89	2.77	2.56	2.38	2.32	2.22	2.15	
1099.2	0.565	Fe-59	1.69 1E+01	1.61 1E+01	1.47 1E+01	1.36 1E+01	1.31 1E+01	1.25 1E+01	1.20 1E+01	
1112.1	0.136	Eu-152	3.96	3.81	3.52	3.29	3.20	3.08	2.97	
1115.5	0.148	Ni-65	9.69	9.17	8.41	7.74	7.46	7.09	6.81	
1115.5	0.507	Zn-65	3.09 1E+01	2.94 1E+01	2.69 1E+01	2.49 1E+01	2.41 1E+01	2.30 1E+01	2.21 1E+01	
1120.5	1.000	Sc-46	1.73 1E+01	1.65 1E+01	1.51 1E+01	1.40 1E+01	1.36 1E+01	1.30 1E+01	1.25 1E+01	
1121.3	0.349	Ta-182	9.52	9.15	8.47	7.89	7.62	7.31	7.05	
1125.5	0.114	Te-131m	2.65	2.53	2.35	2.19	2.13	2.05	1.99	
1131.5	0.228	I-135	5.24	4.97	4.57	4.17	4.04	3.84	3.68	
1153.5	0.071	Eu-156	2.16	2.05	1.87	1.74	1.66	1.59	1.52	
1157.5	0.113	I-130	1.70	1.63	1.52	1.42	1.40	1.36	1.32	
1173.2	0.999	Co-60	1.46 1E+01	1.39 1E+01	1.27 1E+01	1.18 1E+01	1.13 1E+01	1.09 1E+01	1.04 1E+01	
1189.0	0.164	Ta-182	4.54	4.36	4.05	3.79	3.66	3.52	3.42	
1204.9	0.003	Y-91	3.04 1E+01	2.89 1E+01	2.67 1E+01	2.46 1E+01	2.38 1E+01	2.27 1E+01	2.19 1E+01	
1206.6	0.098	Te-131m	2.30	2.20	2.05	1.92	1.87	1.80	1.75	
1221.4	0.273	Ta-182	7.59	7.34	6.83	6.39	6.18	5.94	5.76	
1230.7	0.089	Eu-156	2.74	2.60	2.39	2.22	2.13	2.04	1.96	
1231.0	0.116	Ta-182	3.21	3.10	2.88	2.71	2.62	2.52	2.44	
1235.4	0.200	Cs-136	3.25	3.10	2.89	2.72	2.64	2.54	2.48	
1238.3	0.670	Co-56	7.17	6.81	6.25	5.76	5.53	5.29	5.10	
1242.4	0.067	Eu-156	2.07	1.97	1.81	1.69	1.62	1.55	1.49	
1260.4	0.289	I-135	6.82	6.47	6.00	5.54	5.36	5.11	4.90	
1274.4	0.355	Eu-154	1.12 1E+01	1.08 1E+01	1.00 1E+01	9.38	9.18	8.86	8.58	
1274.5	0.999	Na-22	1.58 1E+01	1.51 1E+01	1.41 1E+01	1.32 1E+01	1.29 1E+01	1.24 1E+01	1.21 1E+01	
1291.6	0.432	Fe-59	1.34 1E+01	1.29 1E+01	1.18 1E+01	1.10 1E+01	1.07 1E+01	1.02 1E+01	9.88	
1332.5	1.000	Co-60	1.51 1E+01	1.44 1E+01	1.33 1E+01	1.24 1E+01	1.20 1E+01	1.15 1E+01	1.10 1E+01	
1354.5	0.026	La-141	3.83 1E+01	3.66 1E+01	3.36 1E+01	3.14 1E+01	3.01 1E+01	2.87 1E+01	2.75 1E+01	
1368.6	1.000	Na-24	1.06 1E+01	1.00 1E+01	9.12	8.35	7.93	7.53	7.15	
1383.9	0.900	Sr-92	2.61 1E+01	2.48 1E+01	2.30 1E+01	2.15 1E+01	2.07 1E+01	1.98 1E+01	1.90 1E+01	
1384.3	0.243	Ag-110m	3.19	3.06	2.84	2.70	2.63	2.55	2.48	
1408.0	0.209	Eu-152	6.45	6.27	5.85	5.57	5.43	5.27	5.12	
1435.9	0.763	Cs-138	1.28 1E+01	1.22 1E+01	1.13 1E+01	1.06 1E+01	1.01 1E+01	9.83	9.39	
1457.6	0.087	I-135	2.14	2.04	1.90	1.78	1.72	1.65	1.60	
1460.8	0.107	K-40	2.75 1E+01	2.63 1E+01	2.42 1E+01	2.27 1E+01	2.18 1E+01	2.09 1E+01	2.00 1E+01	
1465.1	0.222	Pm-148	1.45 1E+01	1.38 1E+01	1.29 1E+01	1.23 1E+01	1.19 1E+01	1.15 1E+01	1.11 1E+01	
1481.8	0.235	Ni-65	1.65 1E+01	1.58 1E+01	1.46 1E+01	1.38 1E+01	1.33 1E+01	1.28 1E+01	1.23 1E+01	
1505.0	0.131	Ag-110m	1.75	1.69	1.58	1.50	1.46	1.43	1.39	
1524.6	0.189	K-42	2.78 1E+01	2.64 1E+01	2.45 1E+01	2.29 1E+01	2.21 1E+01	2.11 1E+01	2.03 1E+01	
1596.2	0.954	La-140	1.64 1E+01	1.57 1E+01	1.46 1E+01	1.38 1E+01	1.34 1E+01	1.29 1E+01	1.25 1E+01	
1678.0	0.096	I-135	2.43	2.33	2.19	2.06	2.01	1.93	1.88	
1691.0	0.488	Sb-124	1.03 1E+01	9.89	9.31	8.81	8.57	8.36	8.12	
1736.5	0.060	Sb-129	1.56	1.51	1.43	1.36	1.33	1.30	1.27	
1771.4	0.155	Co-56	1.80	1.74	1.63	1.53	1.49	1.44	1.41	
1791.2	0.078	I-135	2.00	1.92	1.80	1.71	1.67	1.61	1.56	
1810.7	0.272	Mn-56	6.63	6.38	6.01	5.65	5.54	5.34	5.20	
1901.3	0.072	La-142	1.36	1.30	1.22	1.14	1.11	1.07	1.03	
2091.0	0.056	Sb-124	1.24	1.20	1.14	1.09	1.08	1.06	1.03	
2113.0	0.143	Mn-56	3.62	3.50	3.32	3.16	3.11	3.01	2.94	
2218.0	0.152	Cs-138	2.81	2.71	2.58	2.46	2.41	2.35	2.29	
2397.8	0.133	La-142	2.65	2.56	2.42	2.30	2.25	2.18	2.11	
2542.7	0.100	La-142	2.03	1.96	1.86	1.77	1.74	1.68	1.64	
2598.6	0.167	Co-56	2.13	2.08	1.98	1.90	1.88	1.83	1.80	
2639.6	0.076	Cs-138	1.46	1.43	1.37	1.32	1.30	1.28	1.25	
2754.0	0.999	Na-24	1.25 1E+01	1.20 1E+01	1.14 1E+01	1.08 1E+01	1.06 1E+01	1.03 1E+01	9.91	
3253.5	0.074	Co-56	9.88 1E-01	9.68 1E-01	9.35 1E-01	9.10 1E-01	9.05 1E-01	8.89 1E-01	8.83 1E-01	

Appendix 3 Relationship between radionuclide activity and dose rate 1 m above ground

Table 3-2 (continued)

Unit: ($\mu\text{Sv/h}$) / (kBq/m^2)

Nuclides	Parameter β to indicate vertical distribution of radioactive materials in the ground (g/cm^{-2})													
	0.0		0.1		0.2		0.3		0.5		1.0		2.0	
Bi-212	5.34	1E-04	4.79	1E-04	4.48	1E-04	4.26	1E-04	3.95	1E-04	3.46	1E-04	2.91	1E-04
Bi-214	7.13	1E-03	6.43	1E-03	6.03	1E-03	5.74	1E-03	5.32	1E-03	4.67	1E-03	3.94	1E-03
Po-216	8.15	1E-08	7.33	1E-08	6.87	1E-08	6.56	1E-08	6.08	1E-08	5.32	1E-08	4.48	1E-08
Ra-224	6.50	1E-05	5.88	1E-05	5.51	1E-05	5.24	1E-05	4.86	1E-05	4.27	1E-05	3.57	1E-05
Ra-226	4.74	1E-05	4.24	1E-05	3.96	1E-05	3.77	1E-05	3.49	1E-05	3.06	1E-05	2.54	1E-05
Ac-228	4.56	1E-03	4.07	1E-03	3.80	1E-03	3.63	1E-03	3.36	1E-03	2.94	1E-03	2.47	1E-03
Th-228	2.99	1E-05	1.82	1E-05	1.52	1E-05	1.36	1E-05	1.17	1E-05	9.50	1E-06	7.43	1E-06
Th-231	3.10	1E-04	1.75	1E-04	1.38	1E-04	1.18	1E-04	9.54	1E-05	7.03	1E-05	5.01	1E-05
Th-232	1.47	1E-05	6.25	1E-06	4.40	1E-06	3.50	1E-06	2.58	1E-06	1.69	1E-06	1.09	1E-06
Th-234	8.80	1E-05	6.53	1E-05	5.76	1E-05	5.29	1E-05	4.68	1E-05	3.84	1E-05	2.98	1E-05
Pa-233	1.45	1E-03	1.25	1E-03	1.16	1E-03	1.09	1E-03	1.01	1E-03	8.73	1E-04	7.28	1E-04
U-232	2.83	1E-05	1.20	1E-05	8.27	1E-06	6.44	1E-06	4.62	1E-06	2.88	1E-06	1.77	1E-06
U-234	2.51	1E-05	1.03	1E-05	6.99	1E-06	5.36	1E-06	3.74	1E-06	2.23	1E-06	1.29	1E-06
U-235	1.09	1E-03	9.58	1E-04	8.90	1E-04	8.45	1E-04	7.81	1E-04	6.82	1E-04	5.67	1E-04
U-236	2.24	1E-05	9.04	1E-06	6.05	1E-06	4.59	1E-06	3.15	1E-06	1.81	1E-06	1.01	1E-06
U-237	1.06	1E-03	8.62	1E-04	7.82	1E-04	7.30	1E-04	6.59	1E-04	5.59	1E-04	4.50	1E-04
U-238	1.81	1E-05	7.28	1E-06	4.87	1E-06	3.70	1E-06	2.54	1E-06	1.47	1E-06	8.20	1E-07
Np-237	3.44	1E-04	2.24	1E-04	1.88	1E-04	1.67	1E-04	1.42	1E-04	1.12	1E-04	8.40	1E-05
Np-238	3.36	1E-03	2.98	1E-03	2.78	1E-03	2.65	1E-03	2.46	1E-03	2.15	1E-03	1.80	1E-03
Np-239	1.27	1E-03	1.06	1E-03	9.78	1E-04	9.20	1E-04	8.40	1E-04	7.26	1E-04	5.98	1E-04
Pu-236	3.19	1E-05	1.33	1E-05	8.96	1E-06	6.81	1E-06	4.65	1E-06	2.65	1E-06	1.44	1E-06
Pu-238	2.92	1E-05	1.21	1E-05	8.13	1E-06	6.16	1E-06	4.18	1E-06	2.35	1E-06	1.26	1E-06
Pu-239	1.29	1E-05	5.54	1E-06	3.81	1E-06	2.95	1E-06	2.08	1E-06	1.25	1E-06	7.39	1E-07
Pu-240	2.76	1E-05	1.15	1E-05	7.69	1E-06	5.83	1E-06	3.97	1E-06	2.24	1E-06	1.21	1E-06
Pu-241	1.33	1E-08	1.03	1E-08	9.25	1E-09	8.60	1E-09	7.74	1E-09	6.56	1E-09	5.29	1E-09
Pu-242	2.33	1E-05	9.90	1E-06	6.75	1E-06	5.19	1E-06	3.63	1E-06	2.15	1E-06	1.25	1E-06
Am-241	3.60	1E-04	2.30	1E-04	1.91	1E-04	1.68	1E-04	1.40	1E-04	1.06	1E-04	7.53	1E-05
Am-242m	8.47	1E-05	3.80	1E-05	2.63	1E-05	2.04	1E-05	1.43	1E-05	8.41	1E-06	4.75	1E-06
Am-242	1.80	1E-04	1.19	1E-04	1.00	1E-04	8.99	1E-05	7.75	1E-05	6.27	1E-05	4.89	1E-05
Am-243	4.59	1E-04	3.75	1E-04	3.39	1E-04	3.16	1E-04	2.83	1E-04	2.33	1E-04	1.80	1E-04
Cm-242	3.10	1E-05	1.34	1E-05	9.07	1E-06	6.92	1E-06	4.73	1E-06	2.68	1E-06	1.44	1E-06
Cm-243	9.33	1E-04	7.76	1E-04	7.11	1E-04	6.67	1E-04	6.09	1E-04	5.26	1E-04	4.33	1E-04
Cm-244	2.67	1E-05	1.15	1E-05	7.84	1E-06	5.99	1E-06	4.11	1E-06	2.35	1E-06	1.28	1E-06
Cm-245	7.92	1E-04	6.37	1E-04	5.78	1E-04	5.40	1E-04	4.88	1E-04	4.17	1E-04	3.39	1E-04
Cm-246	4.09	1E-05	2.69	1E-05	2.28	1E-05	2.06	1E-05	1.80	1E-05	1.47	1E-05	1.18	1E-05
Cm-247	1.88	1E-03	1.70	1E-03	1.60	1E-03	1.52	1E-03	1.41	1E-03	1.24	1E-03	1.04	1E-03
Cm-248	7.09	1E-03	6.37	1E-03	5.97	1E-03	5.71	1E-03	5.30	1E-03	4.64	1E-03	3.90	1E-03

Table 3-2 (continued)

Unit: ($\mu\text{Sv/h}$) / (kBq/m^2)

Nuclides	Parameter β to indicate vertical distribution of radioactive materials in the ground (g/cm^{-2})													
	3.0		5.0		10		20		30		50		100	
Bi-212	2.57	1E-04	2.13	1E-04	1.56	1E-04	1.05	1E-04	7.88	1E-05	5.36	1E-05	3.00	1E-05
Bi-214	3.49	1E-03	2.91	1E-03	2.15	1E-03	1.45	1E-03	1.10	1E-03	7.55	1E-04	4.24	1E-04
Po-216	3.96	1E-08	3.28	1E-08	2.39	1E-08	1.60	1E-08	1.20	1E-08	8.13	1E-09	4.53	1E-09
Ra-224	3.15	1E-05	2.57	1E-05	1.80	1E-05	1.15	1E-05	8.47	1E-06	5.56	1E-06	3.00	1E-06
Ra-226	2.23	1E-05	1.80	1E-05	1.25	1E-05	7.85	1E-06	5.75	1E-06	3.74	1E-06	1.99	1E-06
Ac-228	2.18	1E-03	1.81	1E-03	1.32	1E-03	8.80	1E-04	6.64	1E-04	4.50	1E-04	2.51	1E-04
Th-228	6.26	1E-06	4.89	1E-06	3.22	1E-06	1.96	1E-06	1.41	1E-06	9.06	1E-07	4.78	1E-07
Th-231	4.03	1E-05	2.99	1E-05	1.86	1E-05	1.07	1E-05	7.61	1E-06	4.80	1E-06	2.50	1E-06
Th-232	8.37	1E-07	5.84	1E-07	3.41	1E-07	1.90	1E-07	1.31	1E-07	8.19	1E-08	4.23	1E-08
Th-234	2.47	1E-05	1.89	1E-05	1.19	1E-05	6.97	1E-06	4.94	1E-06	3.12	1E-06	1.63	1E-06
Pa-233	6.33	1E-04	5.17	1E-04	3.62	1E-04	2.31	1E-04	1.70	1E-04	1.12	1E-04	6.07	1E-05
U-232	1.32	1E-06	9.11	1E-07	5.27	1E-07	2.96	1E-07	2.05	1E-07	1.28	1E-07	6.67	1E-08
U-234	9.34	1E-07	6.19	1E-07	3.41	1E-07	1.85	1E-07	1.26	1E-07	7.80	1E-08	4.02	1E-08
U-235	4.95	1E-04	4.01	1E-04	2.77	1E-04	1.74	1E-04	1.27	1E-04	8.28	1E-05	4.40	1E-05
U-236	7.12	1E-07	4.57	1E-07	2.42	1E-07	1.28	1E-07	8.63	1E-08	5.27	1E-08	2.70	1E-08
U-237	3.84	1E-04	3.03	1E-04	2.03	1E-04	1.24	1E-04	8.98	1E-05	5.78	1E-05	3.06	1E-05
U-238	5.79	1E-07	3.73	1E-07	1.99	1E-07	1.07	1E-07	7.23	1E-08	4.45	1E-08	2.30	1E-08
Np-237	6.92	1E-05	5.26	1E-05	3.35	1E-05	1.97	1E-05	1.41	1E-05	8.96	1E-06	4.67	1E-06
Np-238	1.59	1E-03	1.32	1E-03	9.68	1E-04	6.49	1E-04	4.92	1E-04	3.35	1E-04	1.86	1E-04
Np-239	5.16	1E-04	4.16	1E-04	2.84	1E-04	1.77	1E-04	1.29	1E-04	8.39	1E-05	4.49	1E-05
Pu-236	9.96	1E-07	6.26	1E-07	3.24	1E-07	1.68	1E-07	1.12	1E-07	6.79	1E-08	3.48	1E-08
Pu-238	8.68	1E-07	5.39	1E-07	2.75	1E-07	1.41	1E-07	9.35	1E-08	5.63	1E-08	2.88	1E-08
Pu-239	5.40	1E-07	3.65	1E-07	2.08	1E-07	1.17	1E-07	8.09	1E-08	5.07	1E-08	2.66	1E-08
Pu-240	8.28	1E-07	5.16	1E-07	2.64	1E-07	1.36	1E-07	9.00	1E-08	5.42	1E-08	2.77	1E-08
Pu-241	4.48	1E-09	3.54	1E-09	2.33	1E-09	1.40	1E-09	1.01	1E-09	6.48	1E-10	3.40	1E-10
Pu-242	9.06	1E-07	6.09	1E-07	3.52	1E-07	2.02	1E-07	1.42	1E-07	9.06	1E-08	4.84	1E-08
Am-241	5.98	1E-05	4.27	1E-05	2.52	1E-05	1.40	1E-05	9.64	1E-06	5.98	1E-06	3.08	1E-06
Am-242m	3.37	1E-06	2.17	1E-06	1.17	1E-06	6.17	1E-07	4.19	1E-07	2.55	1E-07	1.31	1E-07
Am-242	4.08	1E-05	3.19	1E-05	2.08	1E-05	1.24	1E-05	8.93	1E-06	5.69	1E-06	2.98	1E-06
Am-243	1.48	1E-04	1.12	1E-04	6.97	1E-05	4.02	1E-05	2.82	1E-05	1.78	1E-05	9.23	1E-06
Cm-242	9.89	1E-07	6.12	1E-07	3.14	1E-07	1.60	1E-07	1.06	1E-07	6.37	1E-08	3.25	1E-08
Cm-243	3.75	1E-04	3.03	1E-04	2.07	1E-04	1.30	1E-04	9.48	1E-05	6.17	1E-05	3.30	1E-05
Cm-244	8.85	1E-07	5.57	1E-07	2.93	1E-07	1.53	1E-07	1.03	1E-07	6.29	1E-08	3.25	1E-08
Cm-245	2.89	1E-04	2.30	1E-04	1.53	1E-04	9.26	1E-05	6.71	1E-05	4.30	1E-05	2.26	1E-05
Cm-246	1.03	1E-05	8.36	1E-06	6.04	1E-06	4.01	1E-06	3.02	1E-06	2.05	1E-06	1.14	1E-06
Cm-247	9.13	1E-04	7.54	1E-04	5.40	1E-04	3.52	1E-04	2.60	1E-04	1.73	1E-04	9.48	1E-05
Cm-248	3.45	1E-03	2.85	1E-03	2.09	1E-03	1.40	1E-03	1.06	1E-03	7.19	1E-04	4.00	1E-04

Appendix 4 References

- (1) “放射性セシウム沈着量の面的調査”
三上智、斎藤公明：平成 26 年度放射性物質測定調査委託費（東京電力株式会社福島第一原子力発電所事故に伴う放射性物質の分布データの集約及び移行モデルの開発）事業成果報告書(2015)
- (2) “In Situ Ge(Li) and NaI(Tl) Gamma-ray Spectrometry”
H.L. Beck, J. DeCampo and C. Gogolak: Report HASL-258 (1972)
- (3) “Gamma-Ray Spectrometry in the Environment”
International Commission on Radiation Units and Measurements: ICRU Report 53 (1994)
- (4) “ゲルマニウム半導体検出器によるガンマ線スペクトロメトリー”
：放射能測定法シリーズ No.7 (1992)
- (5) “Radiation protection instrumentation – Measurement of discrete radionuclides in the environment – In situ photon spectrometry system using a germanium detector”
：IEC 61275 Ed.2 (2013)
- (6) “ENSDF (Evaluated Nuclear Structure Data File)”
：National Nuclear Data Center, Brookhaven (2016)
- (7) “Field Gamma-Ray Spectrometry”
K.M. Miller：EML Procedures Manual, HASL-300, Section 3.3 (1997)
- (8) “環境試料採取法”
：放射能測定法シリーズ No.16(1983)
- (9) “Generic procedures for monitoring in a nuclear or radiological emergency” International Atomic Energy Agency: IAEA-TECDOC-1092 (1999)
- (10) “PHOTX データベース”
- (11) “可搬型 Ge(Li)検出器を用いた環境ガンマ線の in-situ 測定”
阪井英次、寺田博海、片桐政樹：JAERI-M6498 (1976)
- (12) “MCNP-A General Monte Carlo N-particle Transport Code Version 4C”
Briesmeister, J.F.: Los Alamos National Laboratory Report LA-13709-M (2000)
- (13) “Performance of Digital Signal Processors for Gamma Spectrometry”
Canberra Industries, Inc.: Application Note (2008)
- (14) “Comparisons of the Portable Digital Spectrometer Systems”
Duc T. Vo, Phyllis A. Russo, Los Alamos NATIONAL LABORATORY: LA-13895-MS, (2002)
- (15) “発電用軽水型原子炉施設の安全審査における一般公衆の線量評価について”
原子力安全委員会：(2001)
- (16) “土壌中の放射性セシウムの深度分布調査”
松田規宏、斎藤公明：平成 27 年度放射性物質測定調査委託費（東京電力株式会社福島第一原子力発電所事故に伴う放射性物質の分布データの集約）事業成果報告書(2016)

- (17) “Handbook for the Assessment of Soil Erosion and Sedimentation Using Environmental Radionuclides”
F. Zapata: (2010)
- (18) “Depth profiles of radioactive cesium in soil using a scraper plate over a wide area surrounding the Fukushima Dai-ichi Nuclear Power Plant”
N. Matsuda, S. Mikami, S. Shimoura, J. Takahashi, M. Nakano, K. Shimada, K. Uno, S. Hagiwara, K. Saito: *Journal of Environmental Radioactivity* 139, 427–434 (2015)
- (19) “Fundamental data on environmental gamma-ray fields in the air due to source in the ground”
K. Saito, P.JACOB : JAERI-Data/Code 98-001 (1998)
- (20) “In Situ Gamma Spectrometry Intercomparison in Fukushima, Japan”
S. Mikami, S. Sato, Y. Hoshide, R. Sakamoto, N. Okuda, K. Saito: *J. Health Phys.*, 50 (3), 182–188 (2015)
- (21) “Ambient dose equivalent conversion coefficients for radionuclides exponentially distributed in the ground”
K. Saito, N. Petoussi-Hens: *Journal of Nuclear Science and Technology* (2014)

Revision history
Established in March 2008
Revised March 2017